Transmit Precoded Spatial Modulation: Maximizing the Minimum Euclidean Distance Versus Minimizing the Bit Error Ratio

Ping Yang, Yong Liang Guan, *Member, IEEE*, Yue Xiao, Marco Di Renzo, *Senior Member, IEEE*, Shaoqian Li, *Senior Member, IEEE*, and Lajos Hanzo, *Fellow, IEEE*

***Abstract*—In this paper, we investigate a pair of transmit precoding (TPC) algorithms conceived for spatial modulation (SM) systems communicating over flat-fading multiple-input multiple-output (MIMO) channels. In order to retain all the benefits of conventional SM, we design the TPC matrix to be diagonal and introduce two design criteria for optimizing the elements of the TPC matrix. Specifically, we first investigate a TPC design based on maximizing the minimum Euclidean distance $d_{\min}$ (max-$d_{\min}$) between the SM signal points at the receiver side. A closed-form solution of the optimal max-$d_{\min}$-based TPC matrix is derived. Then, another TPC design algorithm is proposed for directly minimizing the bit error ratio (BER) upper bound of SM, which is capable of jointly optimizing the overall Euclidean distance between all received signal points. In the minimum BER (min-BER)-based TPC algorithm, the theoretical gradient of the BER with respect to the diagonal TPC matrix is derived and a simplified iterative conjugate gradient (SCG) algorithm is invoked for TPC optimization. Our simulation results demonstrate that the proposed max-$d_{\min}$-based TPC algorithm is optimal in terms of the minimum distance. However, increasing $d_{\min}$ does not achieve a further BER improvement. We also confirm that the min-BER-based TPC outperforms the max-$d_{\min}$-based TPC schemes in terms of the achievable BER performance.**

Manuscript received March 23, 2015; revised November 2, 2015; accepted November 2, 2015. This work was supported in part by the National Science Foundation of China under Grant 61471090, in part by the National Basic Research Program of China under Grant 2013CB329001, in part by the National High-Tech R&D Program of China ("863" Project under Grant 2014AA01A707), in part by the Foundation Project of National Key Laboratory of Science and Technology on Communications under Grant 9140C020108140C02005, and in part by the European Research Council's Advanced Fellow Grant are gratefully acknowledged. The work of M. D. Renzo was supported by the European Commission under the auspices of the FP7-PEOPLE MITN-CROSSFIRE project (grant 317126). The associate editor coordinating the review of this paper and approving it for publication was Z. Wang.

P. Yang is with the National Key Laboratory of Science and Technology on Communications, University of Electronic Science and Technology of China, Sichuan 611731, China, and also with the School of Electrical and Electronic Engineering, Nanyang Technological University, Singapore (e-mail: yang.ping@uestc.edu.cn).

Y. L. Guan is with the School of Electrical and Electronic Engineering, Nanyang Technological University, Singapore (e-mail: eylguan@ntu.edu.sg).

Y. Xiao and S. Li are with the National Key Laboratory of Science and Technology on Communications, University of Electronic Science and Technology of China, Sichuan 611731, China (e-mail: xiaoyue@uestc.edu.cn; lsq@yeste.edu.cn).

M. D. Renzo is with the Laboratory of Signals and Systems (L2S), University of Paris-Sud XI, Orsay, France (e-mail: marco.direnzo@lss.supelec.fr).

L. Hanzo is with the School of Electronics and Computer Science, University of Southampton, Southampton SO17 1BJ, U.K. (e-mail: lh@ecs.soton.ac.uk).

Color versions of one or more of the figures in this paper are available online at http://ieeexplore.ieee.org.

Digital Object Identifier 10.1109/TWC.2015.2497692

***Index Terms*—Minimum Euclidean distance, minimum BER, multiple-input multiple-output, pre-coding technique, spatial modulation.**

I. Introduction

RECENTLY, spatial modulation (SM) has been proposed as a new class of low-complexity energy-efficient multiple-input multiple-output (MIMO) approach, whilst relying on a single-radio frequency (RF) chain [1]–[3]. SM scheme relies on the unique encoding philosophy of activating one out of N_t transmit antennas (TAs) during each transmission slot [4]. The activated TA then transmits classic complex-valued symbols of amplitude and phase modulation (APM). The potential benefits of SM over the conventional MIMO techniques have been validated not only via numerical simulations [5], [6] but also by laboratory experiments [7], [8].

Early work has been focused on low-complexity receiver designs conceived for minimizing the bit error ratio (BER) of SM [9]–[12]. It was shown in [9] that a low-complexity single-stream maximum likelihood (ML) detector or an even lower-complexity near-ML detector [10]–[12] is capable of striking a beneficial trade-off amongst the potentially conflicting factors of energy-efficiency, multiplexing gain and diversity gain compared to other MIMO transmission techniques [13]. In addition to a plethora of receivers, preprocessing at the transmitter has also been conceived for achieving a further performance improvement. Specifically, several antenna selection (AS) methods [14], [15] originally designed for conventional MIMO systems have also been generalized for employment in SM systems with the goal of enhancing its capacity or BER performance [16]–[18]. In [19]–[21], an adaptive SM (ASM) scheme was proposed for improving the achievable BER, while maintaining the target throughput with the aid of adaptive modulation (AM) techniques. In [22], the power allocation between the pilot and data was optimized for maximizing the capacity of SM transmission. In [23] and [24], a specific constellation design was proposed for space shift keying (SSK) systems in order to improve their BER. The constellation design was further developed in [25] for SM by finding the optimal combination of the number of TAs and the APM size that minimizes the BER.

Among the promising design alternatives, linear transmit pre-coding (TPC) techniques constitute an attractive transmit preprocessing regime, since they use a simple matrix $\mathbf{U}$ for

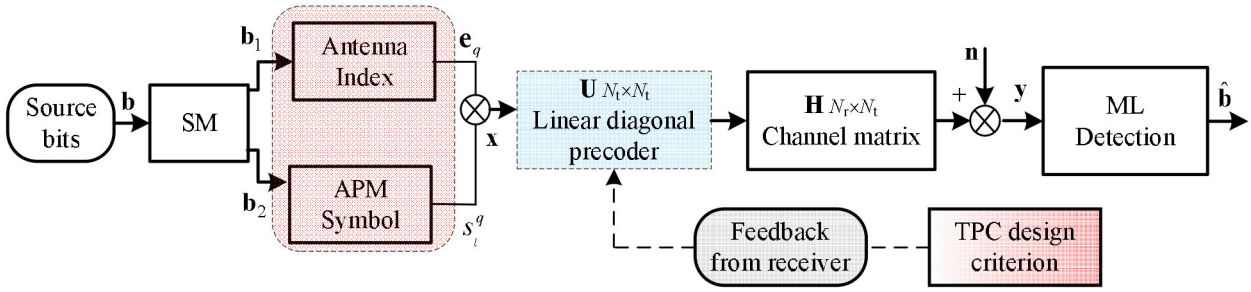

Fig. 1. The diagonal TPC based SM transmission system.

weighting the channel matrix in order to enhance the attainable performance [26]. Indeed, TPC has been widely researched in the context of classic spatial multiplexing systems [27]. However, since only a single TA is activated in each time slot in SM, these TPC approaches are not directly suitable for SM systems.

In [28] the effect of power imbalance has been researched in the context of SSK associated with TPC algorithms. More recently, the research efforts have been focused on the TPC design of SM based on maximizing the minimum Euclidean distance $d_{\min}$ (max-$d_{\min}$) in the received SM constellation. In [29], the phase alignment technique has also been extended to SM systems for constellation shaping in order to provide BER benefit in multiple-input single-output (MISO) channels. In [30], the max-$d_{\min}$ based TPC is designed by using an iterative concave-convex process, where the TPC parameters are calculated for each transmit constellation points. In [31], [32], a diagonal TPC was proposed for maximizing $d_{\min}$ in SM systems. However, an exhaustive numerical search method was used for identifying the specific TPC parameters. On the other hand, in [33], a special case of the diagonal TPC, namely an adaptive power allocation (PA) method, was investigated, where a simple real-valued diagonal TPC matrix was considered. As shown in [33], closed-form solutions of the optimal max-$d_{\min}$ aided PA were derived in the case of two TAs. In [34], another diagonal TPC method, namely phase rotation precoding (PRP), was proposed for energy-efficient transmission, where only the phases of the SM symbols were optimized based on the max-$d_{\min}$ criterion. The corresponding closed-form solutions were derived for two TAs and for PSK-modulated SM schemes in [35].

Against this background, the novel contributions of this paper are as follows.

1) We first investigate a general TPC matrix design algorithm based on the max-$d_{\min}$ criterion, where a complex-valued TPC matrix is considered instead of the real-valued PA matrix of [33] and the constant-modulus PRP matrix of [34], [35]. Compared to the heuristic method of computing the TPC matrix of [31], in this paper we derive closed-form solutions of the max-$d_{\min}$ TPC for a $(2 \times N_r)$-element BPSK-modulated SM scheme as well as for the more general cases of M-PSK modulated $(2 \times N_r)$-element SM. Moreover, we extend this method to the case of $N_t > 2$.
2) It is shown that the max-$d_{\min}$ based TPC-aided SM scheme is capable of achieving a larger $d_{\min}$ than other max-$d_{\min}$ aided adaptive SM schemes, such as the PA based TPC-aided SM scheme of [33] and the ASM scheme of [21]. However an increase of $d_{\min}$ does not achieve a further BER improvement. We find the reason that the max-$d_{\min}$ TPC only has a higher the minimum received distance $d_{\min}$ and may result in reduced Euclidean distances between the non-adjacent received constellation points.
3) To alleviate this shortcoming, we propose a new minimum-BER (min-BER) based TPC method, which is capable of jointly optimizing the overall Euclidean distance between the received signal points. Specifically, the theoretical gradient of the BER upper bound of SM with respect to the diagonal TPC matrix $\mathbf{U}$ is derived, and the simplified conjugate gradient (SCG) algorithm [36], [37] is invoked for efficient TPC optimization. We demonstrate that the overall BER gain of the proposed method is significantly improved compared to both that of conventional SM and to the other existing TPC schemes of [29]–[35]. We also extend the proposed algorithm to cope with channel state information (CSI) inaccuracies.

The organization of the paper is as follows. Section II introduces the concept as well as the system model of the TPC-based SM. In Section III and Section IV, we present a pair of TPC designs conceived for enhancing the BER performance of SM. The complexity analysis results are provided in Section V. Our Simulation results and performance comparisons are presented in Section VI. Finally, Section VII concludes the paper.

Notation: $(\cdot)^*$, $(\cdot)^T$ and $(\cdot)^H$ denote conjugate, transpose, and Hermitian transpose, respectively. The probability of an event is represented by $P(\cdot)$. Furthermore, $\|\cdot\|$ stands for the Frobenius norm and all logarithms are base of 2. $Tr(\cdot)$ denotes the trace of a square matrix, $E(\cdot)$ represents expectation, while $Re\{\mathbf{x}\}$ and $Im\{\mathbf{x}\}$ represent the real and imaginary parts of $\mathbf{x}$, respectively. $\mathbf{I}_b$ denotes a $(b \times b)$-element identity matrix and the operator diag$\{\cdot\}$ to be applied to a length i vector returns an $i \times i$ square matrix with the vector elements along the diagonal.

II. System Model

A. Signal Model of the Diagonal TPC Aided SM-MIMO

Consider a MIMO system having N_t transmit and N_r receive antennas. In this paper, N_t is assumed to be a power of two. Let $\mathbf{b} = [b_1, \ldots, b_L]$ be the transmit bit vector of each time slot, which contains $L = \log_2(N_t M)$ bits. As shown in Fig. 1, the input vector $\mathbf{b}$ is divided into two sub-vectors of $\log_2(N_t)$

and $\log_2(M)$ bits, denoted as $\mathbf{b}_1$ and $\mathbf{b}_2$, respectively. The bits in the sub-vector $\mathbf{b}_1$ are used for selecting a unique TA index q for activation, which is mapped to a N_t-dimensional standard basis vector $\mathbf{e}_q$ $(1 \le q \le N_t)$. The bits in the sub-vector $\mathbf{b}_2$ are mapped to a Gray-coded APM symbol $s_m^q \in \Im$ $(m \in \{1, \ldots, M\})$ [38]. Then, the resultant SM symbol $\mathbf{x} \in \mathbb{C}^{N_t \times 1}$ can be formulated as [1]

$$\mathbf{x} = s_m^q \mathbf{e}_q = [0, \ldots, \underset{\downarrow\, qth \text{ term}}{s_m^q}, \ldots, 0]^{\cdot}. \tag{1}$$

As shown in Fig. 1, after TPC relying on the linear diagonal matrix $\mathbf{U}$, the signal observed at the N_r receive antennas is given by

$$\mathbf{y} = \mathbf{HUx} + \mathbf{n}, \tag{2}$$

where $\mathbf{H}$ is the $(N_r \times N_t)$-element channel matrix, $\mathbf{U}$ is the $(N_t \times N_t)$-element TPC matrix, and $\mathbf{n}$ is the $(N_r \times 1)$-element noise vector. We assume $E[\mathbf{nn}^H] = N_0 \mathbf{I}_{N_r}$ and $E[\mathbf{xn}^H] = \mathbf{0}_{N_t \times N_t}$. The elements of the noise vector $\mathbf{n}$ are complex Gaussian random variables obeying $\mathcal{CN}(0, N_0)$. Furthermore, the diagonal TPC matrix $\mathbf{U}$ is given by

$$\mathbf{U} = \text{diag}\{u_1, \ldots, u_q, \ldots, u_{N_t}\}, \tag{3}$$

where u_q is a complex-valued TPC parameter, which controls the channel gain associated with x_q. We enforce the constraint $\sum_{q=1}^{N_t} |u_q|^2 = P_T$ for the sake of normalizing the transmit power. The diagonal structure of $\mathbf{U}$ guarantees that the transmit vector $\mathbf{Ux}$ has a single non-zero component, hence the single-RF-chain benefits (such as the avoidance of both the inter antenna interference (IAI) and of the multiple RFs) of SM are preserved. The matrix $\mathbf{U}$ can be decomposed as follows [31]

$$\mathbf{U} = \mathbf{P\Theta} = \text{diag}\{p_1, p_2 e^{j\theta_1}, \ldots, p_q e^{j\theta_{q-1}}, \ldots, p_{N_t} e^{j\theta_{N_t-1}}\}, \tag{4}$$

where $u_q = p_q e^{j\theta_{q-1}}$ and p_q represents the complex modulus of u_q, while θ_{q-1} represents the phase angle of u_q. In (4), the TPC matrix $\mathbf{U}$ is decomposed into two matrices related to the modulus and phase, which correspond to the real-valued PA matrix $\mathbf{P} = \text{diag}\{p_1, p_2, \ldots, p_q, \ldots, p_{N_t}\}$ and to the complex-valued PRP matrix $\mathbf{\Theta} = \text{diag}\{1, e^{j\theta_1}, \ldots, e^{j\theta_{q-1}}, \ldots, e^{j\theta_{N_t-1}}\}$, respectively.

Remark: The max-$d_{\min}$ based PA-aided SM schemes of [33] and the PRP-aided SM schemes of [34], [35] constitute special cases of the proposed TPC schemes, which can be obtained by setting $\mathbf{\Theta} = \mathbf{I}_{N_t}$ and $\mathbf{P} = \mathbf{I}_{N_t}$, respectively.

B. Maximum Likelihood Receiver

The receiver performs ML detection over all possible SM symbols $\mathbf{x} \in \mathbb{C}^{N_t \times 1}$ for retrieving the transmit symbols, which can be formulated as [9], [10]:

$$\begin{aligned}\hat{\mathbf{x}} &= \arg\min_{\mathbf{x}\in\mathbb{X}} \|\mathbf{y} - \mathbf{HUx}\|^2 \\ &= \arg\min_{\mathbf{x}\in\mathbb{X}} \left\|\mathbf{y} - \tilde{\mathbf{H}}\mathbf{x}\right\|^2 = \arg\min_{q\in\{1,\ldots,N_t\}} \left\|\mathbf{y} - \tilde{\mathbf{h}}_q s_m^q\right\|^2 \\ &\Leftrightarrow \arg\min_{q\in\{1,\ldots,N_t\}} \left\|\tilde{\mathbf{h}}_q^H \mathbf{y}/\left\|\tilde{\mathbf{h}}_q\right\|^2 - s_m^q\right\|^2,\end{aligned} \tag{5}$$

where $\mathbb{X}$ is the set of all legitimate transmit symbols and $\tilde{\mathbf{h}}_q$ is the $q-th$ column of the equivalent channel matrix $\tilde{\mathbf{H}} = \mathbf{HU}$. As shown in Eq. (5), a low-complexity single-stream ML detector is obtained [10], [22]. Moreover, it is shown in Proposition 1 of [22] that for a square- or for a rectangular-QAM constellation, the complexity imposed is independent of the constellation size, and that it increases only with N_t.

The conditional error performance of a ML receiver for a given channel $\mathbf{H}$ can be approximated by the sum of the pairwise error probability (PEP) [39], which is given by

$$P(\mathbf{H}) \le \frac{1}{L} \sum_{i=1}^{L} \sum_{\substack{j=1,\\ i\neq j}}^{L} Q\left(\sqrt{\frac{1}{2N_0} d_{ij}(\mathbf{H})}\right), \tag{6}$$

where $Q(x) = (1/\sqrt{2\pi}) \int_x^\infty e^{-y^2/2} dy$ denotes the Gaussian tail probability, while the distance $d_{ij}(\mathbf{H})$ at the receiver is defined as

$$\begin{aligned} d_{ij}(\mathbf{H}) &= \left\|\mathbf{HU}(\mathbf{x}_i - \mathbf{x}_j)\right\|^2 \\ &= \left\|\mathbf{HUe}_{ij}\right\|^2, \end{aligned} \tag{7}$$

where $\mathbf{e}_{ij} = \mathbf{x}_i - \mathbf{x}_j$, $i \neq j$ denotes the error vector. The PEP depends on the specific SM symbol pair $(\mathbf{x}_i, \mathbf{x}_j)$, on the instantaneous channel realization $\mathbf{H}$ and the TPC matrix $\mathbf{U}$.

III. Minimum Euclidean Distance Based TPC

It follows by direct inspection of the PEP expression of Eq. (6) that the performance of the ML receiver is predominantly affected by the distances $d_{ij}(\mathbf{H})$. Motivated by this observation, TPC design methods based on maximizing the minimum value of $d_{ij}(\mathbf{H})$ (the distance $d_{\min}$) have been introduced in [31] and [32]. However, only a high-complexity numerical approach was proposed for optimizing the TPC matrix. In this section, we first briefly introduce the max-$d_{\min}$ based TPC method. Then, we derive the related solutions.

A. Design Criterion

At high SNR, Eq. (6) can be further simplified as follows [39]

$$P(\mathbf{H}) \le \lambda \cdot Q\left(\sqrt{\frac{1}{2N_0} d_{\min}}\right), \tag{8}$$

where λ is the number of neighbor points [39] and $d_{\min}$ is defined as

$$d_{\min} = \min_{\substack{i,j\\ i\neq j}} d_{ij}(\mathbf{H}) = \min_{\mathbf{e}_{ij}\in\mathbb{E}} \left\|\mathbf{HUe}_{ij}\right\|^2. \tag{9}$$

In Eq. (8), $P(\mathbf{H})$ is a monotonically decreasing function of $d_{\min}$. Hence, the system's BER performance may be improved by maximizing the distance $d_{\min}$ of the received constellation upon carefully adapting the TPC matrix $\mathbf{U}$ under the power

constraint P_{T}.[1] Based on this principle, the max-$d_{\min}$ based TPC matrix $\mathbf{U}$ design rule can be formulated as follows

$$\mathbf{U}_{\mathrm{opt}} = \arg\max_{\mathbf{U}} d_{\min} \quad \text{s.t.} \quad tr\left(\mathbf{U}\mathbf{U}^T\right) \le P_{\mathrm{T}}. \tag{10}$$

Note that in [33] and [35] the closed-form solutions for two special cases of Eq. (10), namely for the max-$d_{\min}$ based PA matrix and for the max-$d_{\min}$ based PRP matrix, have been derived. However, to the best of our knowledge, the closed-form solution for the joint design of the PA and PRP of Eq. (10) has not been reported in the existing literature. In the following subsections, we derive a closed-form solution for the TPC matrix of the BPSK-modulated $(2 \times N_r)$-element SM and extend the method to the more general M-PSK modulated $(2 \times N_r)$-element SM arrangements. Additionally, as shown in [2] and [6], PSK schemes are preferred over QAM schemes in SM. Hence, PSK is adopted in this paper.

B. Optimal TPC Matrix for BPSK-modulated $2 \times N_r$ SM

Let us consider a BPSK-modulated SM systems associated with $N_t = 2$, where the BPSK symbols belong to the set $\Im = \{1, -1\}$, and all possible error vectors $\mathbf{e}_{ij} = \mathbf{x}_i - \mathbf{x}_j$, $i \neq j$ are listed as follows: $\{[-2, 0]^T, [2, 0]^T, [0, -2]^T, [0, 2]^T, [-1, 1]^T, [-1, -1]^T, [1, -1]^T, [1, 1]^T\}$. Similar to the method of [33], since some vectors are collinear, the set to be studied is reduced to $\tilde{\mathbb{E}}_{BPSK} = \{\mathbf{e}_1, \mathbf{e}_2, \mathbf{e}_3, \mathbf{e}_4\} = \{[2, 0]^T, [0, 2]^T, [1, -1]^T, [1, 1]^T\}$. Given the channel matrix $\mathbf{H} = [\mathbf{h}_1, \mathbf{h}_2]$ and the corresponding TPC matrix $\mathbf{U} = \mathrm{diag}\{p_1, p_2 e^{j\theta_1}\}$, the distances at the receiver based on Eq. (7) are given by

$$\begin{cases} d_1 = \|\mathbf{H}\mathbf{U}\mathbf{e}_1\|^2 = 4\,\|p_1\mathbf{h}_1\|^2 \\ d_2 = \|\mathbf{H}\mathbf{U}\mathbf{e}_2\|^2 = 4\,\|p_2\mathbf{h}_2\|^2 \\ d_3 = \|\mathbf{H}\mathbf{U}\mathbf{e}_3\|^2 = \left\|p_1\mathbf{h}_1 - p_2 e^{j\theta_1}\mathbf{h}_2\right\|^2 \\ d_4 = \|\mathbf{H}\mathbf{U}\mathbf{e}_4\|^2 = \left\|p_1\mathbf{h}_1 + p_2 e^{j\theta_1}\mathbf{h}_2\right\|^2 \end{cases}. \tag{11}$$

Based on the distances in Eq. (11), the optimization problem of Eq. (10) can be modified as follows

$$\mathbf{U}_{\mathrm{opt}} = \arg\max_{\mathbf{U}} \{\min\{d_1, d_2, d_3, d_4\}\} \quad \text{s.t.} \quad tr(\mathbf{U}\mathbf{U}^T) \le P_{\mathrm{T}}. \tag{12}$$

To obtain the specific TPC matrix $\mathbf{U}_{\mathrm{opt}}$, which maximizes the distance $d_{\min}$, the parameters p_1, p_2 and θ_1 in Eq. (12) have to be computed. As indicated in Eq. (11) and shown in Fig. 2, for a fixed PA matrix $\mathbf{P} = \mathrm{diag}\{p_1, p_2\}$, d_1 and d_2 are independent of the phase θ_1, while d_3 and d_4 are given by sinusoidal functions of the phase θ_1. In order to find the optimal phase solution θ_1^{opt}, we can first obtain the phases assigned to the TAs by finding the intersections of the sinusoidal curves in Fig. 2, and then continue by computing the optimal PA matrix as $\mathbf{P} = \mathrm{diag}\{p_1^{opt}, p_2^{opt}\}$.

[1] Compared to the PRP method of [34], [35], the power of the SM symbols may indeed fluctuate due to the TPC algorithm. However, during the time when the channel envelope remains constant within its coherence-interval, the power values of the transmit symbols are selected from a finite discrete set. In practice, the constraint P_{T} should be carefully selected according to the system requirements, such as the peak to average power ratio (PAPR) and the BER metrics.

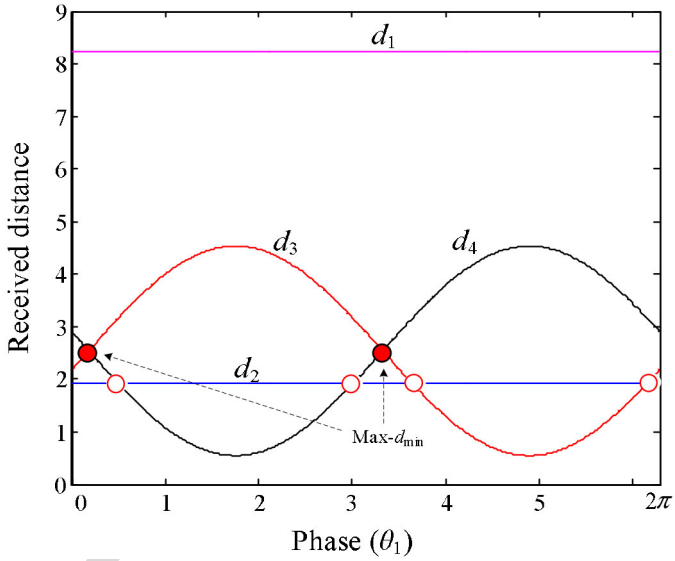

Fig. 2. The phase solutions of the BPSK-modulated $(2 \times N_r)$-element TPC based SM for a fixed PA.

To be specific, as shown in Fig. 2, regardless of the specific PA matrix $\mathbf{P}$, the optimal phase θ_1^{opt} that maximizes $d_{\min}$ should satisfy the constraint of $d_3 = d_4$ which from (11):

$$\left\|p_1\mathbf{h}_1 - p_2 e^{j\theta_1^{opt}}\mathbf{h}_2\right\|^2 = \left\|p_1\mathbf{h}_1 + p_2 e^{j\theta_1^{opt}}\mathbf{h}_2\right\|^2. \tag{13}$$

Eq. (13) can be further simplified to $\mathrm{Re}\{\mathbf{h}_1^H\mathbf{h}_2 e^{j\theta_1^{opt}}\} = 0$. Upon introducing the shorthands $a = \|\mathbf{h}_1\|^2$, $b = \|\mathbf{h}_2\|^2$, $c_1 = 2 \cdot \mathrm{Re}\{\mathbf{h}_1^H\mathbf{h}_2\}$ and $c_2 = 2 \cdot \mathrm{Im}\{\mathbf{h}_1^H\mathbf{h}_2\}$ for a given channel matrix $\mathbf{H}$, Eq. (13) can be solved as

$$c_1 \cos\theta_1^{opt} - c_2 \sin\theta_1^{opt} = 0 \Leftrightarrow \theta_1^{opt} = k\pi + \tan^{-1}\left(\frac{c_1}{c_2}\right), k \in \mathbb{Z}, 0 \le \theta_1^{opt} \le 2\pi. \tag{14}$$

Given the phase solution of Eq. (14), the distances d_3 and d_4 of Eq. (11) are simplified as follows

$$d_3 = d_4 = \|p_1\mathbf{h}_1\|^2 + \|p_2\mathbf{h}_2\|^2 = ap_1^2 + bp_2^2. \tag{15}$$

To compute the optimal PA parameters as p_1^{opt} and p_2^{opt}, since we have $d_3 = d_4$ in Eq. (15), the optimization problem of Eq. (12) can be further simplified to:

$$\begin{aligned} \mathbf{U}_{\mathrm{opt}} &= \arg\max_{\mathbf{U}} \{\min\{d_1, d_2, d_3\}\} \\ &= \arg\max_{\mathbf{U}} \left\{\min\left\{4ap_1^2, 4b\left(P_{\mathrm{T}} - p_1^2\right), ap_1^2 + b\left(P_{\mathrm{T}} - p_1^2\right)\right\}\right\}. \end{aligned} \tag{16}$$

As indicated in Eq. (16), d_1, d_2 and d_3 are linear functions of the parameter $\mu_1 = p_1^2$. Hence, the max-$d_{\min}$ solution given

μ_1 is one of the intersections between these distances $d_i (i = 1, 2, 3)$, which are given by

$$\begin{cases} p_1^{(1)} = \sqrt{b/(a+b)P_{\mathrm{T}}} \\ p_1^{(2)} = \sqrt{b/(3a+b)P_{\mathrm{T}}} \\ p_1^{(3)} = \sqrt{3b/(3b+a)P_{\mathrm{T}}} \end{cases}, \tag{17}$$

where $p_1^{(i)}, i = 1, 2, 3$ are the power assigned to the first TA for the ith intersections. Then, based on the fixed total power constraint P_{T}, the corresponding power assigned to the second TA is given by

$$\begin{cases} p_2^{(1)} = \sqrt{a/(a+b)P_{\mathrm{T}}} \\ p_2^{(2)} = \sqrt{3a/(3a+b)P_{\mathrm{T}}} \\ p_2^{(3)} = \sqrt{a/(3b+a)P_{\mathrm{T}}} \end{cases}. \tag{18}$$

Based on Eqs. (17) and (18), we select the one providing the maximum $d_{\min}$ as the final solution. Finally, the optimal TPC matrix $\mathbf{U}_{\mathrm{opt}}$ and the corresponding maximized $d_{\min}$, namely $d_{\min}^{\max}$, are given by

$$\begin{cases} \text{if } a \geq b, \quad \mathbf{U}_{\mathrm{opt}} = \mathrm{diag}\left\{p_1^{(2)}, p_2^{(2)} e^{j\theta_1^{opt}}\right\}, \quad d_{\min}^{\max} = \frac{4ab}{3a+b} \\ \text{if } a < b, \quad \mathbf{U}_{\mathrm{opt}} = \mathrm{diag}\left\{p_1^{(3)}, p_2^{(3)} e^{j\theta_1^{opt}}\right\}, \quad d_{\min}^{\max} = \frac{4ab}{3b+a} \end{cases} \tag{19}$$

It is worth noting that since the Euclidean distance $d_{\min}^{\max}$ of Eq. (19) has two independent channel gains, a transmit diversity order of two may be achieved [40].

C. Optimal TPC Matrix for M-PSK-Modulated $(2 \times N_r)$-Element SM

In this subsection, the approach proposed in Section III-B is extended to M-PSK modulated SM schemes. Based on the method of Section III-B, the max-$d_{\min}$ based TPC algorithm can be summarized as follows:

In order to better illustrate the general algorithm described above, let us consider the specific example of constant-modulus M-PSK modulation, whose symbols belong to the set $s \sim \Im = e^{j\frac{2l\pi}{M}} (l \in \{1, \ldots, M\})$. The minimum distance between two symbols of the M-PSK constellation is $d_{M-\mathrm{PSK}} = 2\sin(\pi/M)$ [38]. Since the SM symbols $\mathbf{x}_i$ and $\mathbf{x}_j$ only have a single non-zero element, the error vectors $\mathbf{e}_{ij} = \mathbf{x}_i - \mathbf{x}_j, i \neq j$ can be classified into two types: the error vectors having only a single non-zero element, and those having two non-zero elements. The first type is generated by the transmit symbols $\mathbf{x}_i$ and $\mathbf{x}_j$ associated with the same TA activation position, while the second type is generated by the symbols having different active TAs. As a result, the distance d_{ij} ($\mathbf{H}$) of Eq. (7) can be divided into two sets: $\mathbb{D}_1$ and $\mathbb{D}_2$, which are given by

$$\begin{cases} \mathbb{D}_1 = \left\{p_i^2 \|\mathbf{h}_i\|^2 (s_l - s_{\hat{l}}), l \neq \hat{l}, i = 1, 2\right\} \\ \mathbb{D}_2 = \left\{\left\|p_1 \mathbf{h}_1 s_l - p_2 \mathbf{h}_2 s_{\hat{l}}\right\|^2, l, \hat{l} = 1, \ldots M\right\} \end{cases}, \tag{20}$$

where $s_l = e^{j\frac{2l\pi}{M}}$ and $s_{\hat{l}} = e^{j\frac{2\hat{l}\pi}{M}}$ are two M-PSK symbols. Since only the minimum distance is investigated in the max-$d_{\min}$ optimization problem of Eq. (10), only the minimum value of the set $\mathbb{D}_1$ has to be considered. To be specific, only the pair of elements $d_1 = \min_{l \neq \hat{l}} p_1^2 \|\mathbf{h}_1\|^2 (s_l - s_{\hat{l}}) = d_{M-\mathrm{PSK}} p_1^2 \|\mathbf{h}_1\|^2$ and $d_2 = \min_{l \neq \hat{l}} p_2^2 \|\mathbf{h}_2\|^2 (s_l - s_{\hat{l}}) = d_{M-\mathrm{PSK}} p_2^2 \|\mathbf{h}_2\|^2$ has to be considered in $\mathbb{D}_1$. Hence, the set $\mathbb{D}_1$ is simplified to

$$\mathbb{D}_1 = \left\{d_{M-\mathrm{PSK}}^2 p_1^2 \|\mathbf{h}_1\|^2, d_{M-\mathrm{PSK}}^2 p_2^2 \|\mathbf{h}_2\|^2\right\}. \tag{21}$$

Let us reduce the set $\mathbb{D}_2$. When only the phase difference of the PSK symbols $s_l = e^{j\frac{2l\pi}{M}}$ and $s_{\hat{l}} = e^{j\frac{2\hat{l}\pi}{M}}$ is considered, the set $\mathbb{D}_2$ can be modified to

$$\begin{aligned} \mathbb{D}_2 &= \left\{\left\|\mathbf{h}_1 p_1 s_l - \mathbf{h}_2 p_2 e^{j\theta_1} s_{\hat{l}}\right\|^2, s_l, s_{\hat{l}} \in \Im\right\} \\ &= \left\{\left\|p_1 \mathbf{h}_1 e^{j\frac{2(l-\hat{l})\pi}{M}} - p_2 e^{j\theta_1} \mathbf{h}_2\right\|^2, l, \hat{l} = 1, \ldots M\right\} \\ &= \left\{\left\|p_1 \mathbf{h}_1 e^{j\frac{2k\pi}{M}} - p_2 e^{j\theta_1} \mathbf{h}_2\right\|^2, k = 0, \ldots M-1\right\}, \end{aligned} \tag{22}$$

where the phase difference factor is $k = l - \hat{l}$. The reduction principle behind Eq. (22) is that if the error vectors in the set $\mathbb{D}_2$ having only a phase difference, they provide the same distance at the receiver. Based on this principle, the number of elements in $\mathbb{D}_2$ is reduced to M compared to $M(M-1)$.

Let $\lambda_k = \frac{2k\pi}{M}$ be the phase difference of the symbol s_l and $s_{\hat{l}}$. Since the distances in the set $\mathbb{D}_1$ are independent of the phase θ_1, similar to the BPSK case portrayed in Section III-B,

Algorithm 1. The max-$d_{\min}$ based TPC algorithm

Step 1: Compute all legitimate error vectors $\mathbf{e}_{ij} = \mathbf{x}_i - \mathbf{x}_j, i \neq j$ by eliminating all collinear elements. Calculate all legitimate received distances d_{ij} ($\mathbf{H}$) with the aid of the channel matrix $\mathbf{H}$ and $\mathbf{e}_{ij}$. Let $\mathbb{D}$ be the set of these distances, whose elements are denoted by $d_v (v = 1, \ldots, V)$, where V is the cardinality of the set $\mathbb{D}$. The set $\mathbb{D}$ is divided into two sub-sets $\mathbb{D}_1$ and $\mathbb{D}_2$, where $\mathbb{D}_1$ contains the error vectors, which have only a single non-zero element, and $\mathbb{D}_2$ contains the error vectors, which have two non-zero elements.[2]

Step 2: Find the optimal phase θ_1^{opt}, which maximizes the minimum received distance of the set $\mathbb{D}_2$. Note that there may be multiple optimal phase solutions, which are calculated based on shifted sinusoidal functions d_v in $\mathbb{D}_2$. Since these solutions provide the same $d_{\min}$, any one of them can be randomly selected.

Step 3: After finding the optimal phase θ_1^{opt}, compute all possible intersections between the received distances d_i and d_j $(d_i, d_j \in \mathbb{D})$ and compute the corresponding PA matrix $\mathbf{P}$. Select the one having the largest $d_{\min}$ as the final PA result, which can be formulated as $\mathbf{P} = \mathrm{diag}\{p_1^{opt}, p_2^{opt}\}$. Then, the final TPC solution is given by $\mathbf{U}_{\mathrm{opt}} = \mathrm{diag}\{p_1^{opt}, p_2^{opt} e^{j\theta_1^{opt}}\}$.

[2]Note that the transmit vector of SM has only a single non-zero element, hence the number of non-zero elements of the error vectors of SM is up to 2.

it is possible to first find the optimal phase θ_1^{opt}, which maximizes the minimum received distance of the set $\mathbb{D}_2$. To achieve this goal, the intersections between arbitrary received distances $\left\|\mathbf{h}_1 p_1 e^{j\lambda_a} - \mathbf{h}_2 p_2 e^{j\theta_1}\right\|^2$ and $\left\|\mathbf{h}_1 p_1 e^{j\lambda_b} - \mathbf{h}_2 p_2 e^{j\theta_1}\right\|^2$ in Eq. (22) are firstly calculated as

$$\begin{aligned}&\left\|\mathbf{h}_1 p_1 e^{j\lambda_a} - \mathbf{h}_2 p_2 e^{j\theta_1}\right\|^2 = \left\|\mathbf{h}_1 p_1 e^{j\lambda_b} - \mathbf{h}_2 p_2 e^{j\theta_1}\right\|^2 \\ &\Leftrightarrow (c_1\cos\lambda_a - c_2\sin\lambda_a - c_1\cos\lambda_b + c_2\sin\lambda_b)\cos\theta_1 \\ &= -(c_1\sin\lambda_a + c_2\cos\lambda_a - c_1\sin\lambda_b - c_2\cos\lambda_b)\sin\theta_1 \\ &\Leftrightarrow \tan\theta_1 = -\frac{c_1\cos\lambda_a - c_2\sin\lambda_a - c_1\cos\lambda_b + c_2\sin\lambda_b}{c_1\sin\lambda_a + c_2\cos\lambda_a - c_1\sin\lambda_b - c_2\cos\lambda_b}.\end{aligned} \tag{23}$$

After that, all possible optimal phase θ_1^{opt} can be obtained from Eq. (23) as

$$\begin{cases}\theta_1^{opt} = k\pi + \tan^{-1}\left(\frac{-c_1\cos\lambda_a + c_2\sin\lambda_a + c_1\cos\lambda_b - c_2\sin\lambda_b}{c_1\sin\lambda_a + c_2\cos\lambda_a - c_1\sin\lambda_b - c_2\cos\lambda_b}\right), \\ k\in\mathbb{Z}, 0\le\theta_1^{opt}\le 2\pi.\end{cases}. \tag{24}$$

Finally, the optimal phase is the candidate providing the maximum distance $d_{\min}$ in the set of Eq. (24). After computing the optimal phase, the the PA matrix can be optimized based on all possible intersections of $d_v (v = 1, \ldots, V)$, similar to processes of Eqs. (16)–(18). Following these calculation steps, the optimal TPC matrix, which combines the optimal phase and PA parameters, is obtained in closed-form.

D. Example for QPSK Modulation

Based on the algorithm in Section III-C, we calculate the optimal TPC solution for QPSK-modulated $(2 \times N_r)$-element SM, which will be used in our simulations. The symbols of QPSK modulation belong to the set $\Im = \{1, -1, j, -j\}$ and the value of $d_{4-\mathrm{PSK}}$ is equal to $\sqrt{2}$. Based on Eqs. (21) and (22), the corresponding sets $\mathbb{D}_1$ and $\mathbb{D}_2$ for QPSK modulation are

$$\begin{cases}\mathbb{D}_1 = \left\{2p_1^2\left\|\mathbf{h}_1\right\|^2, 2p_2^2\left\|\mathbf{h}_2\right\|^2\right\}. \\ \mathbb{D}_2 = \left\{\left\|p_1\mathbf{h}_1 e^{j\frac{2k\pi}{M}} - p_2 e^{j\theta_1}\mathbf{h}_2\right\|^2, k = 0, \ldots, 3\right\},\end{cases} \tag{25}$$

According to Eq. (24), there are two optimal phases θ_1^{opt} that maximizes the distance $d_{\min}$ for Eq. (25), namely $\theta_1^{opt,1}$ and $\theta_1^{opt,2}$, which are given by

$$\begin{cases}\theta_1^{opt,1} = k\pi + \tan^{-1}\left(\frac{-c_1-c_2}{c_1-c_2}\right), \\ k\in\mathbb{Z}, 0\le\theta_1^{opt,1}\le 2\pi.\end{cases} \tag{26}$$

and

$$\begin{cases}\theta_1^{opt,2} = k\pi + \tan^{-1}\left(\frac{c_1-c_2}{c_1+c_2}\right), \\ k\in\mathbb{Z}, 0\le\theta_1^{opt,2}\le 2\pi.\end{cases} \tag{27}$$

Since both solutions $\theta_1^{opt,1}$ and $\theta_1^{opt,2}$ have the same $d_{\min}$, we consider only the first case $\theta_1 = \theta_1^{opt,1}$. After finding the optimal phase $\theta_1^{opt,1}$, the received distance set $\mathbb{D}_2$ is further reduced to $\mathbb{D}_2 = \{\|p_1\mathbf{h}_1 e^{j\frac{2k\pi}{M}} - p_2 e^{j\theta_1}\mathbf{h}_2\|^2, k = 0, 1\}$. This reduction is due to the fact that $\theta_1^{opt,1}$ corresponds to the intersection of two elements of $\mathbb{D}_2$ and the elements having the same value are eliminated. After this reduction, the final received distance set has only 4 elements (both $\mathbb{D}_1$ and $\mathbb{D}_2$ have 2 elements), denoted by $\bar{d}_i (i = 1, 2, 3, 4)$.

Given the optimal phase as $\theta_1^{opt} = \theta_1^{opt,1}$, we have to further identify the optimal PA parameters p_1^{opt} and p_2^{opt} ($p_2^{opt} = \sqrt{P_{\mathrm{T}} - (p_1^{opt})^2}$). According to the step 3 of **Algorithm 1**, the max-$d_{\min}$ solution of p_1 is one of the intersections between these received distance $\bar{d}_i (i = 1, 2, 3, 4)$, which are given by

$$\begin{cases}p_1^{(1)} = \sqrt{b/(a+b)P_{\mathrm{T}}} \\ p_1^{(2)} = p_1^{(5)} = \sqrt{\frac{2c^2+4ab+2\tilde{C}\sqrt{\tilde{C}^2+4ab}}{4a^2+2c^2+4ab+2\tilde{C}\sqrt{\tilde{C}^2+4ab}}}P_{\mathrm{T}}. \\ p_1^{(3)} = p_1^{(4)} = \sqrt{\frac{2c^2+4ab-2\tilde{C}\sqrt{\tilde{C}^2+4ab}}{4a^2+2c^2+4ab-2\tilde{C}\sqrt{\tilde{C}^2+4ab}}}P_{\mathrm{T}}\end{cases} \tag{28}$$

Based on the power constraint, the power allocated on the second TA is obtained by $p_2^{(i)} = \sqrt{P_{\mathrm{T}} - (p_1^{(i)})^2}, i = 1, \ldots, 5$. Finally, the distances $d_{\min}$ of these TPC solutions $\mathbf{U} = \mathrm{diag}\{p_1^{(i)}, p_2^{(i)} e^{j\theta_1^{opt,1}}\}$ $(i = 1, 2, 3, 4, 5)$ are generated and that having the largest $d_{\min}$ is chosen as our final result $\mathbf{U}_{\mathrm{opt}}$.

E. A Low-Complexity Iterative Max-$d_{\min}$ for $N_t > 2$

It is worth mentioning that the restriction of considering $(2 \times N_r)$-element SM is imposed by the difficulty of the $d_{\min}$ optimization. The solution of the general problem remains an open challenge for two reasons. Firstly, the solution depends on both the channel matrix and on the symbol alphabet, and secondly, the solution space is large. Similar to the general method proposed in the PA aided SM of [33], some sub-optimal methods can be adopted for the case of $N_t > 2$ based on an iterative process relying on the above-mentioned optimal max-$d_{\min}$ solution provided for $N_t = 2$, where the TPC algorithm will only be used for the specific TA pair associated with $d_{\min}$, while the parameters of other TAs remain unchanged in each iteration.

IV. Minimum BER Based TPC

Although the max-$d_{\min}$ based TPC algorithm is simple, it may not achieve a significant BER improvement for some SM systems, because only one of the distances in the PEP expression of Eq. (6), namely $d_{\min}$, is optimized at the receiver. Moreover, we can only obtain closed-form solutions for this TPC algorithm for the case of $N_t = 2$. To deal with these problems, we propose a new min-BER based TPC algorithm, which is capable of jointly optimizing all the received distances for directly improving the BER for arbitrary value of N_t. By considering the bit-to-symbol mapping rule of our SM scheme, a more accurate conditional BER bound based on Eq. (6) can be obtained as [41]

$$\begin{aligned}P_e(\mathbf{H}) \le P_e^{\mathrm{up}}(\mathbf{H}) = \frac{1}{L}\sum_{\mathbf{x}_i\in\mathbb{X}}\sum_{\substack{\mathbf{x}_j\in\mathbb{X}\\ \mathbf{x}_i\ne\mathbf{x}_j}} D_H(\mathbf{x}_i\to\mathbf{x}_j) \\ \cdot\ Q\left(\sqrt{\frac{1}{2N_0}\left\|\mathbf{HU}(\mathbf{x}_i-\mathbf{x}_j)\right\|^2}\right),\end{aligned} \tag{29}$$

where $D_H(\mathbf{x}_i \to \mathbf{x}_j)$ is the Hamming distance between the SM signals $\mathbf{x}_i$ and $\mathbf{x}_j$. From Eq. (29), the min-BER-based TPC matrix is proposed by solving the optimization problem as follows

$$\begin{aligned} \mathbf{U}_{\text{opt}} &= \arg\min_{\mathbf{U}} P_e^{\text{up}}(\mathbf{H}) \\ \text{s.t. } & tr(\mathbf{U}\mathbf{U}^T) = P_{\text{T}} \end{aligned}. \tag{30}$$

Remark: Compared to Eq. (30), the max-$d_{\min}$ based TPC algorithm of Eq. (10) considers only a reduced summation over a subset of $\mathbb{X}$, which has the smallest Euclidean distance. Therefore, it can only minimize a much looser bound of BER than the bound of Eq. (29).

A. Precoder Design Based on Gradient Optimization

Since the direct solution of Eq. (30) is complex, we drive the theoretical gradient of the cost function with respect to the diagonal TPC matrix $\mathbf{U}$ and invoke the SCG algorithm of [36] for low-complexity TPC matrix optimization. More specifically, the cost function of the SCG algorithm is obtained from Eq. (29) and is defined as

$$\begin{aligned} Je(\mathbf{U}) = & \sum_{\mathbf{x}_i \in \mathbb{X}} \sum_{\substack{\mathbf{x}_j \in \mathbb{X} \\ \mathbf{x}_i \neq \mathbf{x}_j}} D_H(\mathbf{x}_i \to \mathbf{x}_j) \\ & \cdot Q\left(\sqrt{\frac{1}{2N_0}\left\|\mathbf{H}\mathbf{U}(\mathbf{x}_i - \mathbf{x}_j)\right\|^2}\right). \end{aligned} \tag{31}$$

The conjugate gradient of Eq. (31) with respect to $\mathbf{U}$ is given by

$$\begin{aligned} \nabla Je(\mathbf{U}) = & \frac{-\mathbf{H}^H\mathbf{H}\mathbf{U}}{4\sqrt{\pi}N_0} \times \sum_{\mathbf{x}_i \in \mathbb{X}} \sum_{\substack{\mathbf{x}_j \in \mathbb{X} \\ \mathbf{x}_i \neq \mathbf{x}_j}} \left\{ D_H(\mathbf{x}_i \to \mathbf{x}_j) \right. \\ & \left. \cdot \varphi(\mathbf{x}_i \to \mathbf{x}_j) \cdot \exp\left(-\frac{\varepsilon}{4N_0}\right)\left(\frac{\varepsilon}{4N_0}\right)^{-\frac{1}{2}} \right\}, \end{aligned} \tag{32}$$

where we have

$$\begin{aligned} &\varphi(\mathbf{x}_i \to \mathbf{x}_j) = (\mathbf{x}_i - \mathbf{x}_j)(\mathbf{x}_i - \mathbf{x}_j)^H = \mathbf{e}_{ij}\mathbf{e}_{ij}^H, \\ &\varepsilon = \left\|\mathbf{H}\mathbf{U}(\mathbf{x}_i - \mathbf{x}_j)\right\|^2. \end{aligned} \tag{33}$$

It is worth noting that the TPC matrix $\mathbf{U}$ is a diagonal matrix, hence the final diagonal conjugate gradient matrix is constituted by the diagonal elements of $\nabla Je(\mathbf{U})$. The derivation of Eq. (32) is given in Appendix A. Given the conjugate gradient of Eq. (32), the problem of Eq. (30) can be solved iteratively by commencing the iterations from an appropriate initial point using the SCG algorithm of [36]. In order to have an initial diagonal TPC matrix $\mathbf{U}^{(1)} \in \mathbb{C}^{N_t \times N_t}$, we use the max-$d_{\min}$ based TPC matrix solution for $(2 \times N_r)$-element SM systems and adopt the near-optimal max-$d_{\min}$ solution in Section IV for the other scenarios.[3] Then, we optimize the TPC matrix with the aid of the SCG algorithm as follows:

[3]Moreover, we can also use the equally weighted diagonal matrix or other optimized TPC matrix of [33]–[35] as initial TPC matrix.

Algorithm 2. The min-BER based TPC algorithm

1) **Initialization**: Set a step size of $\mu > 0$, a termination scalar of $\beta > 0$ and a maximum number of iterations N_{all}; given the conjugate gradient of the initial diagonal TPC matrix $\mathbf{U}^{(1)}$ as $\tau(1) = \nabla Je(\mathbf{U}^{(1)}) \in \mathbb{C}^{N_t \times N_t}$, set $n = 1$.
2) **Loop**: if $\left\|\nabla Je(\mathbf{U}^{(1)})\right\| < \beta$ or $n > N_{all}$, goto **Stop**.

$$\mathbf{U}^{(n+1)} = \mathbf{U}^{(n)} - \mu\tau(n)/\left\|\tau(n)\right\|, \tag{34}$$

$$\alpha = P_{\text{T}}/tr(\mathbf{U}^{(n+1)}(\mathbf{U}^{(n+1)})^H), \tag{35}$$

$$\mathbf{U}^{(n+1)} = \sqrt{\alpha}\mathbf{U}^{(n+1)}, \tag{36}$$

$$\varphi_l = \left\|\nabla Je(\mathbf{U}^{(n+1)})\right\|^2 / \left\|\nabla Je(\mathbf{U}^{(n)})\right\|^2, \tag{37}$$

$$\tau(n+1) = \varphi_l\tau(n) - \nabla Je(\mathbf{U}^{(n+1)}). \tag{38}$$

$n = n + 1$, goto Loop.
3) **Stop**: $\mathbf{U}^{(n+1)}$ is the solution.

As shown in [36] and [37], the convergence of the SCG algorithm is more rapid than that of the classic steepest gradient algorithm. For the sake of avoiding convergence to a local optimum, the values of φ_l in SCG can be periodically reset either to zero or to their negative counterparts [36].[4]

B. SCG Algorithm Based on the Simple Q-function Estimations

In the SCG algorithm, the computational complexity is dominated by the calculation of the conjugate gradient of Eq. (32). To reduce this complexity, two simple upper bounds of the Gaussian Q-function can be adopted. The first well-known estimate is given by the Chernoff bound as follows [39]

$$Q(x) \leq \frac{1}{2}\exp\left(-\frac{x^2}{2}\right). \tag{39}$$

Hence, the conjugate gradient of Eq. (32) with respect to $\mathbf{U}$ is simplified to

$$\begin{aligned} \nabla Je_{Cher}(\mathbf{U}) = & \frac{-\mathbf{H}^H\mathbf{H}\mathbf{U}}{4N_0} \times \sum_{\mathbf{x}_i \in \mathbb{X}} \sum_{\substack{\mathbf{x}_j \in \mathbb{X} \\ \mathbf{x}_i \neq \mathbf{x}_j}} \left\{ D_H(\mathbf{x}_i \to \mathbf{x}_j) \right. \\ & \left. \cdot \varphi\left(\mathbf{x}_i \to \mathbf{x}_j\right) \cdot \exp\left(-\frac{\varepsilon}{4N_0}\right) \right\}. \end{aligned} \tag{40}$$

A more accurate approximation of the Q-function than the Chernoff bound is formulated as a sum of weighted exponentials. By considering only two components, the following Chiani-bound has been proposed in [39]

$$Q(x) \leq \frac{1}{12}\exp\left(-\frac{x^2}{2}\right) + \frac{1}{4}\exp\left(-\frac{2x^2}{3}\right) \tag{41}$$

[4]Further information about the SCG algorithm is available in [37].

and the corresponding conjugate gradient $\nabla Je_{Chai}(\mathbf{U})$ is

$$\nabla Je_{Chai}(\mathbf{U}) = \frac{-\mathbf{H}^H\mathbf{H}\mathbf{U}}{4N_0} \cdot \sum_{\mathbf{x}_i\in\mathbb{X}} \sum_{\substack{\mathbf{x}_j\in\mathbb{X} \\ \mathbf{x}_i\neq\mathbf{x}_j}} \left\{ D_H(\mathbf{x}_i \to \mathbf{x}_j) \right.$$
$$\left. \varphi\left(\mathbf{x}_i \to \mathbf{x}_j\right) \cdot \left[\frac{1}{6}\exp\left(-\frac{\varepsilon}{4N_0}\right) + \frac{2}{3}\exp\left(-\frac{\varepsilon}{3N_0}\right) \right] \right\}. \tag{42}$$

Eqs. (40) and (42) provide two simple approximations of Eq. (32). It is worth noting that the transmit vectors of SM schemes are sparsely populated, since they have mostly zero values, hence the space of non-linear error vectors $\mathbf{e}_{ij} = \mathbf{x}_i - \mathbf{x}_j$ is small, as shown in Section III. For example, the number of non-linear error vectors $\mathbf{e}_{ij}$ for QPSK-modulated SM associated with $N_t = 2$ is as low as six. In the SCG-based TPC optimization, we may only have to consider these non-linear error vectors and hence the computational complexity of the SCG algorithm can be further reduced.

C. Min-BER Based TPC Matrix Design With Imperfect CSI

In practical applications, pilot symbols are commonly used for estimating the MIMO channel, but naturally the estimated MIMO channel matrix is inevitably imperfect. Hence, the TPC design algorithm should give cognizance to the estimated MIMO channel matrix $\hat{\mathbf{H}}$, which is given by [42], [43]

$$\hat{\mathbf{H}} = \mathbf{H} + \Delta\mathbf{H}, \tag{43}$$

where $\Delta\mathbf{H}$ is the channel estimation error matrix. Let us assume that $\Delta\mathbf{H}$ is uncorrelated with $\mathbf{H}$ and satisfies $\Delta\mathbf{H}^H\Delta\mathbf{H} = \sigma_{err}^2\mathbf{I}_{N_t}$. Then, the corresponding gradient for SCG algorithm is computed as

$$\nabla Je(\mathbf{U}) = \frac{-\hat{\mathbf{H}}^H\hat{\mathbf{H}}\mathbf{U}}{4\sqrt{\pi}} \cdot \sum_{\mathbf{x}_i\in\mathbb{X}} \frac{1}{\sigma_e^2} \sum_{\substack{\mathbf{x}_j\in\mathbb{X} \\ \mathbf{x}_i\neq\mathbf{x}_j}} \left\{ D_H(\mathbf{x}_i \to \mathbf{x}_j) \right.$$
$$\left. \varphi\left(\mathbf{x}_i \to \mathbf{x}_j\right) \exp\left(-\frac{\varepsilon_{\hat{\mathbf{H}}}}{4\sigma_e^2}\right)\left(\frac{\varepsilon_{\hat{\mathbf{H}}}}{4\sigma_e^2}\right)^{-\frac{1}{2}} \right\} + \frac{\sigma_{err}^2\mathbf{U}}{4\sqrt{\pi}} \sum_{\mathbf{x}_i\in\mathbb{X}} \frac{\mathbf{x}_i\mathbf{x}_i^H}{\sigma_e^4}$$
$$\cdot \sum_{\substack{\mathbf{x}_j\in\mathbb{X} \\ \mathbf{x}_i\neq\mathbf{x}_j}} D_H\left(\mathbf{x}_i \to \mathbf{x}_j\right) \cdot \exp\left(-\frac{\varepsilon_{\hat{\mathbf{H}}}}{4\sigma_e^2}\right)\left(\frac{\varepsilon_{\hat{\mathbf{H}}}}{4\sigma_e^2}\right)^{-\frac{1}{2}} \varepsilon, \tag{44}$$

where we have

$$\sigma_e^2 = N_0 + (\mathbf{U}\mathbf{x}_i)^H \Delta\mathbf{H}^H \Delta\mathbf{H}\mathbf{U}\mathbf{x}_i, \tag{45}$$

and

$$\varepsilon_{\hat{\mathbf{H}}} = \left\| \hat{\mathbf{H}}\mathbf{U}(\mathbf{x}_i - \mathbf{x}_j) \right\|^2. \tag{46}$$

The derivation details of Eq. (44) are given in Appendix. As shown in Eq. (44), the resultant gradient carefully takes the channel estimation errors into account, when constructing the diagonal TPC matrix. Hence, the BER performance becomes resilient to CSI errors.

TABLE I
COMPUTATIONAL COMPLEXITY IMPOSED BY THE GRADIENT $\nabla Je(\mathbf{U})$

	Complexity imposed
$\mathbf{H}^H\mathbf{H}$	$O_1 = N_t^2(2N_r - 1)$
$\bullet \times \mathbf{U}$	$O_2 = N_t N_r$
$\varphi(\mathbf{x}_i \to \mathbf{x}_j)$	$O_3 = N_t\binom{2}{M} + 4\binom{2}{N_t}M^2$
$\varepsilon = \left\|\mathbf{H}\mathbf{U}(\mathbf{x}_i - \mathbf{x}_j)\right\|^2$	$O_4 = N_t\binom{2}{M}(2N_r - 1) + 4\binom{2}{N_t}M^2(2N_r - 1)$

V. COMPLEXITY ANALYSIS OF THE PROPOSED TPC ALGORITHMS

In this section, we provide complexity evaluations of the proposed max-$d_{\min}$ based TPC and the min-BER based TPC algorithms, where only the multiplications of complex numbers are considered.

Based on a similar analysis method to that of [33], for the case of $N_t = 2$, the closed-form solution of the max-$d_{\min}$ based TPC can be found by using the **Algorithm 1**, which imposes a complexity of

$$O_{\max-d_{\min}} = \underbrace{4(2N_r - 1)}_{\text{calculate } \mathbf{H}^H\mathbf{H}} + \underbrace{15M(M-1)/2}_{\text{calculate optimal phase}} + \underbrace{(2M+1)(M+7)}_{\text{calculate optimal PA}}. \tag{47}$$

Moreover, for the case of $N_t > 2$, an iterative max-$d_{\min}$ based TPC can be adopted and the associated complexity (similar to Eq. (22) of [33]) is

$$O_{\max-d_{\min}} = \underbrace{4(2N_r - 1)}_{\text{calculate } \mathbf{H}^H\mathbf{H}} + \underbrace{\binom{2}{N_t}(2M-1)}_{\text{intial } d_{\min}} + \cdots$$
$$n_{\text{TPC}} \left[\underbrace{15M(M-1)/2}_{\text{calculate optimal phase}} + \underbrace{(2M+1)(M+7)}_{\text{calculate optimal PA}} \right.$$
$$\left. + \underbrace{2(N_t - 2)(2M-1)}_{\text{optimized } d_{\min}} \right], \tag{48}$$

where n_{TPC} is the number of iterations in the max-$d_{\min}$ based TPC algorithm, which is varied according to the channel matrix. In our simulations, we found that the average value of n_{TPC} is approximated to 5.

The complexity of the proposed min-BER based TPC algorithm can be estimated by considering: (a) the computational complexity of the SCG solution process in each iteration and (b) the number of iterations n_{SCG} required for approaching convergence. The first term can be estimated based on Eqs. (34)–(38). In Table I, we characterize the computational complexity imposed by the gradient $\nabla Je(\mathbf{U})$, where the sparse structure of the SM symbols $\mathbf{x}_i, \mathbf{x}_j$ and of the diagonal TPC matrix $\mathbf{U}$ are exploited. To be specific, the error vectors $\mathbf{e}_{ij} = \mathbf{x}_i - \mathbf{x}_j, i \neq j$ can be classified into two sets: $N_t\binom{2}{M}$ vectors having a single non-zero element and $\binom{2}{N_t}M^2$ vectors having two non-zero elements. They have different complexity for the calculation of $\varphi(\mathbf{x}_i \to \mathbf{x}_j)$ and ε, as shown in Table I. Note that

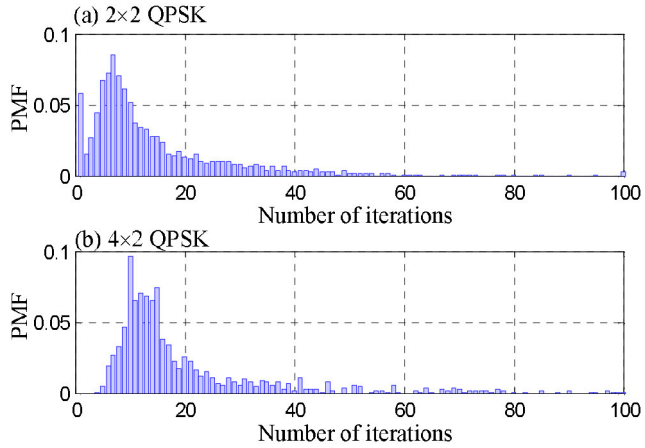

Fig. 3. Convergence behavior of the proposed min-BER based TPC in SM systems with QPSK modulation in i.i.d Rayleigh fading channels.

the bit-to-symbol mapping rule can be designed off-line, hence the complexity of $D_H(\mathbf{x}_i \rightarrow \mathbf{x}_j)$ is not considered in the calculation of $\nabla Je(\mathbf{U})$. Based on Table I and the SCG algorithm of Eqs. (34)–(38), the associated complexity of the proposed min-BER based TPC algorithm is approximately

$$O_{\min\text{-BER}} = O_1 + O_3 + n_{\text{SCG}}\Big[5(O_2+O_4) + \underbrace{N_t^2+N_t}_{\text{Eq.34}} + \cdots \underbrace{N_t^2-N_t+1}_{\text{Eq.35}} + \underbrace{N_t}_{\text{Eq.36}} + \underbrace{N_t^2-N_t+1}_{\text{Eq.37}} + \underbrace{2N_t}_{\text{Eq.38}}\Big]. \quad (49)$$

Moreover, similar to [30], in Fig. 3 we have portrayed the probability mass function (PMF) of the numbers of iterations for the min-BER based TPC algorithm in the QPSK-modulated (2×2) and (4×2) SM schemes. In the simulations, the threshold of SCG is given by $\beta = 10^{-5}$ and 25000 trails are considered to show the statistics of convergence. In Fig. 3 (a) and (b), more than 90% and 85% of the trials converged within 30 iterations. This is due to the rapid convergence of the SCG algorithm, as also verified in [37]. Note that although the approximation method of Section IV-B can reduce the complexity of calculating $\nabla Je(\mathbf{U})$, i.e. the complexity terms O_3 and O_4 in Table I, it has the same complexity order as (49). We will provide more detailed comparisons and discussions about the complexity issue in Section VI-C.

VI. Simulation Results

In this section, we provide simulation results (the distance $d_{\min}$ and the BER performance) for characterizing the max-$d_{\min}$ based TPC aided SM and the min-BER based TPC aided SM schemes for transmission over frequency-flat fading channels. For comparison, these performance results are compared to various adaptive SM schemes, such as the ASM arrangements of [21], the maximum minimum distance (MMD) aided SM schemes of [30], the PA-based SM schemes of [33], the TPC star-QAM SM schemes of [31], and the PRP aided SM schemes of [29] and [34], [35].

In the min-BER based TPC scheme, the step size μ is determined by Monte Carlo simulation methods, as suggested in [36] and we set $\mu = 0.01$, so that we achieve a rapid convergence, while maintaining excellent BER results. Moreover, for the BPSK case, we do not consider the ASM scheme because 'no-transmission' is assigned to one of the TAs and hence this TA is inactive [33].

A. $d_{\min}$ Performance for Different SM Schemes

In Fig. 4, we compare the complementary cumulative distribution functions (CCDF) of the distance $d_{\min}$ recorded for both for conventional SM and for the link adaptive SM schemes in (2×1) MIMO channels under different throughputs. First, we note that these adaptive SM schemes are capable of beneficially increasing the distance $d_{\min}$. As formally shown in Section III, we observe in Fig. 4 that the proposed max-$d_{\min}$ based TPC aided SM achieves the highest distance $d_{\min}$ compared to other link-adaptive SM schemes. Furthermore, we note that the min-BER based TPC schemes achieve lower $d_{\min}$ than the max-$d_{\min}$ based TPC schemes, and yet we will see in Figs. 5–7 that the min-BER based TPC outperforms the max-$d_{\min}$ based TPC in terms of its BER.

B. BER Comparisons of Different SM Schemes

In Fig. 5, we compare the BER performance of various SM systems for $L = 2$ bits/symbol in (2×1)- and (2×2)-element MIMO channels. We can see that the proposed min-BER based schemes provides gains of about 6 dB and 4 dB at the BER of 10^{-3} over the conventional SM schemes. We also confirm that the min-BER based schemes outperform the ASM of [21], the max-$d_{\min}$ based PA aided SM of [33] and the max-$d_{\min}$ based TPC aided SM proposed.

Note that, as shown in Fig. 4, although the optimal max-$d_{\min}$ based TPC aided SM is capable of achieving a higher distance $d_{\min}$ than the other adaptive SM schemes, it does not achieve a BER performance improvement over them. To expound a little further, in Fig. 5, when the proposed max-$d_{\min}$ based TPC-aided SM is compared to its special case, namely to the max-$d_{\min}$ based PA aided SM, we find that an increase of the distance $d_{\min}$ by TPC does not achieve any further BER improvement. Observe in Fig. 5 that at high SNRs, the max-$d_{\min}$ based TPC aided SM may even perform worse than the max-$d_{\min}$ based PA aided SM. This is mainly due to the fact that the maximum of $d_{\min}$ does not necessarily minimize the PEP bound of Eq. (29), which depends on all the received distances.

To be specific, the reason for the trends of Fig. 5 is that the max-$d_{\min}$ based TPC may achieve a lower Euclidean distance between the non-adjacent received constellation points than that of the PA schemes. Hence, based on the Q-function aided PEP upper bound of Eq. (29), which depends on all legitimate received distances $d_{ij}(\mathbf{H}) = \left\|\mathbf{HU}(\mathbf{x}_i - \mathbf{x}_j)\right\|$ $(i \neq j)$, the max-$d_{\min}$ based TPC fails to achieve the best BER performance. For example, let us consider the (2×1) SM scheme using BPSK. As shown in Section III, we only have four different distances

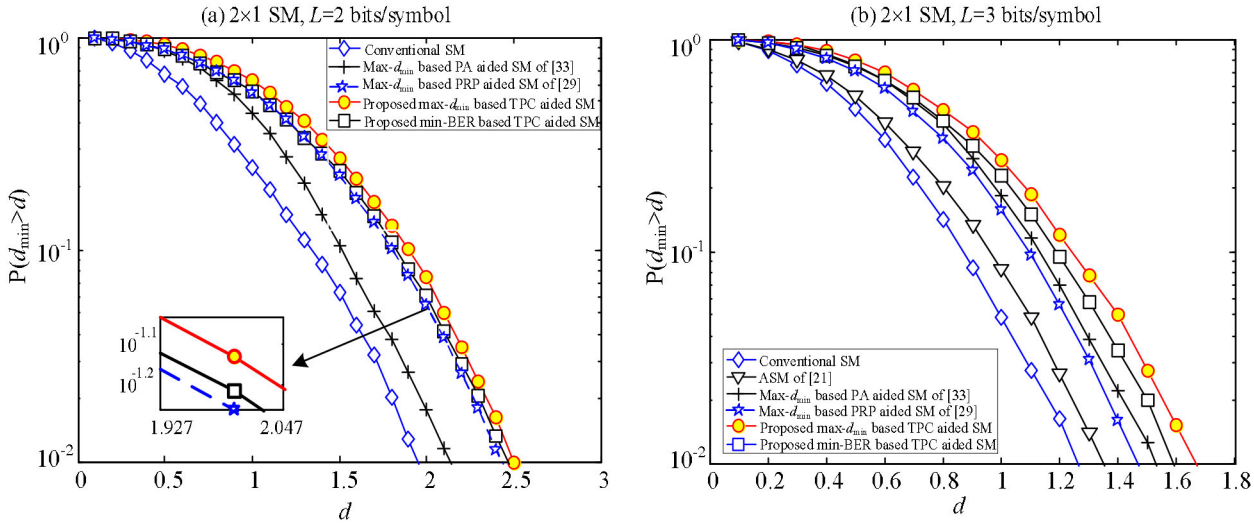

Fig. 4. The CCDF of the minimum distance $d_{\min}$ of conventional SM and of various link-adaptation aided SM schemes in (2×1)-element MIMO channels.

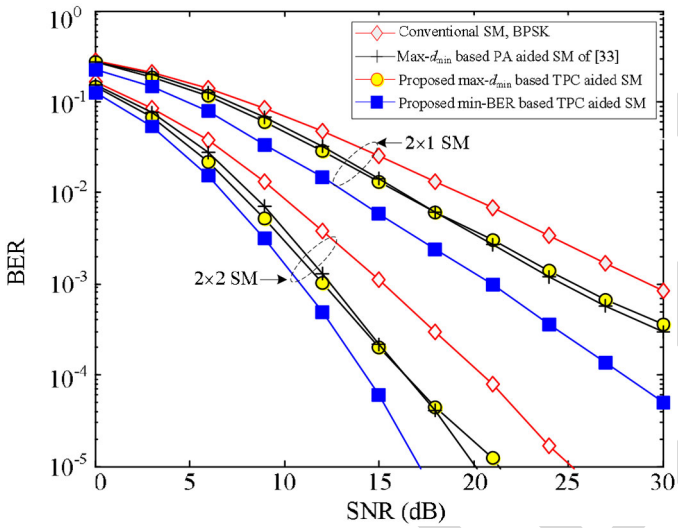

Fig. 5. BER comparison at $L = 2$ bits/symbol for the conventional SM, for the max-$d_{\min}$ based TPC aided SM and for the min-BER based TPC aided SM.

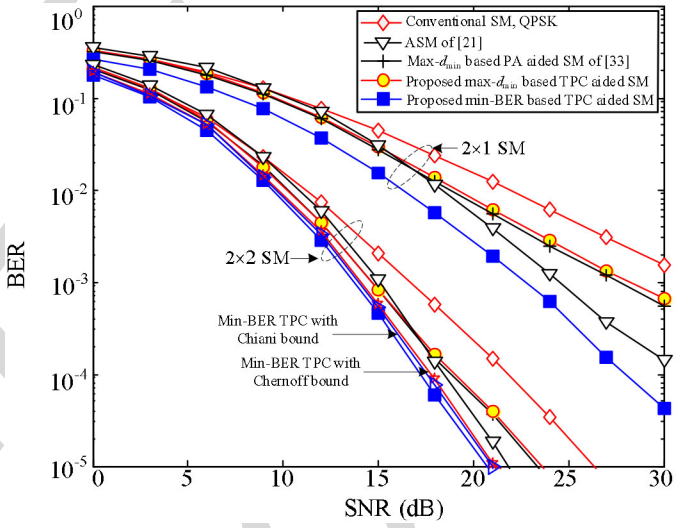

Fig. 6. BER comparison at $L = 3$ bits/symbol for various SM schemes. Here, the Q-function estimates of Section IV-B are only considered for the (2×2)-element MIMO channels.

at the receiver, namely d_1, d_2, d_3 and d_4. Assuming that the channel matrix is $\mathbf{H} = [0.056 - 0.069i, 0.414 + 1.267i]$ and the SNR is 25 dB, the resultant distance set for the max-$d_{\min}$ based TPC-aided SM is

$$\mathbb{D}_{TPC} = \{d_1 = 0.251, d_2 = 0.434, d_3 = 0.251, d_4 = 0.251\},$$

while the corresponding distance set for the max-$d_{\min}$ based PA aided SM is

$$\mathbb{D}_{PA} = \{d_1 = 0.248, d_2 = 0.718, d_3 = 0.476, d_4 = 0.248\}.$$

Then, the BER results of Eq. (29) calculated for the TPC-aided SM and the PA-aided SM schemes are $P_e(\mathbf{H}) = 0.7 \times 10^{-3}$ and $P_e(\mathbf{H}) = 0.5 \times 10^{-3}$, respectively. This result confirms that although the max-$d_{\min}$ based TPC algorithm achieves the highest distance of $d_{\min} = 0.251$, while the max-$d_{\min}$ based PA algorithm has $d_{\min} = 0.248$, the former has a worse PEP performance due to its lower values of d_2 and d_3. This result is consistent with the result seen in Fig. 5.

The above-mentioned trends of these proposed TPC algorithms are also visible in Fig. 6, where the throughput is $L = 3$ bits/symbol. It is shown in Fig. 6 that the proposed min-BER based TPC outperforms both ASM of [21] and the max-$d_{\min}$ based PA of [33]. Moreover, in Fig. 6, we demonstrate that the approximate Chernoff-based and Chiani-based optimizations perform almost the same as the exact Q-function based scheme. This is because these approximations do not change the direction of the gradient. We have also simulated the Chernoff-based and Chiani-based optimizations for the other MIMO setups considered, and obtained similar results, as evidenced by Fig. 6. Since the resultant curves approximately overlap with the optimal one, for clarity, these results are not included in other figures.

Due to the advantage of the proposed min-BER based TPC, in Fig. 7 we further investigate its performance for a higher number of TAs and modulation order. All the schemes are

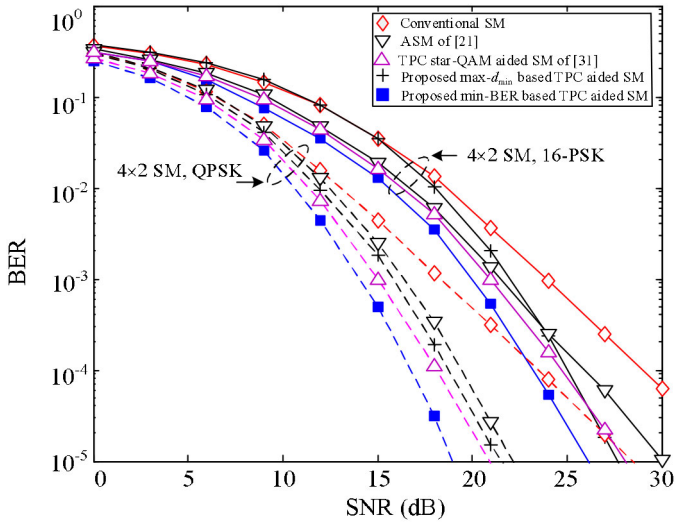

Fig. 7. BER comparison of the proposed min-BER-based TPC-aided SM schemes over the TPC star-QAM aided SM schemes.

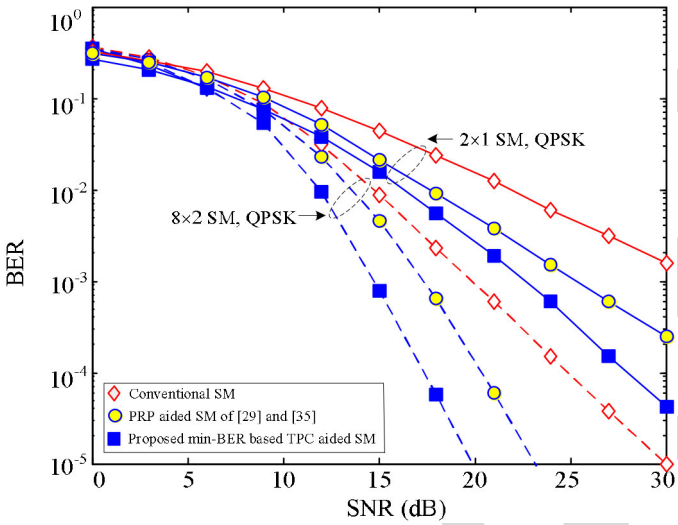

Fig. 8. BER comparison of the proposed min-BER-based TPC-aided SM schemes over the PRP-aided SM schemes.

assumed to have $N_t = 4$, $N_r = 2$ and the throughputs are $L = 4$ and $L = 6$ bits/symbol. In Fig. 7, the proposed schemes are also compared to the TPC star-QAM aided SM schemes of [31], which utilize a quantized search for optimizing the diagonal TPC matrix. In our simulation, the number of quantization levels for both amplitude and phase in TPC of [31] is 6. Observe in Fig. 7 that the proposed min-BER based TPC schemes achieve the best BER performance. The performance gain of the proposed scheme over the TPC star-QAM aided SM scheme is seen to be about 2.6 dB at BER= 10^{-5} for 4 bits/symbol transmissions in Fig. 7. This is due to the fact the TPC star-QAM based scheme of [31] also only optimizes a single received distance $d_{\min}$, which may limit the attainable BER performance.

In Fig. 8, we compared the proposed min-BER based TPC schemes to the max-$d_{\min}$ based PRP schemes of [29] and [35]. We observe in Fig. 8 that the proposed schemes outperform the PRP-aided schemes. To be specific, as seen in Fig. 8 the

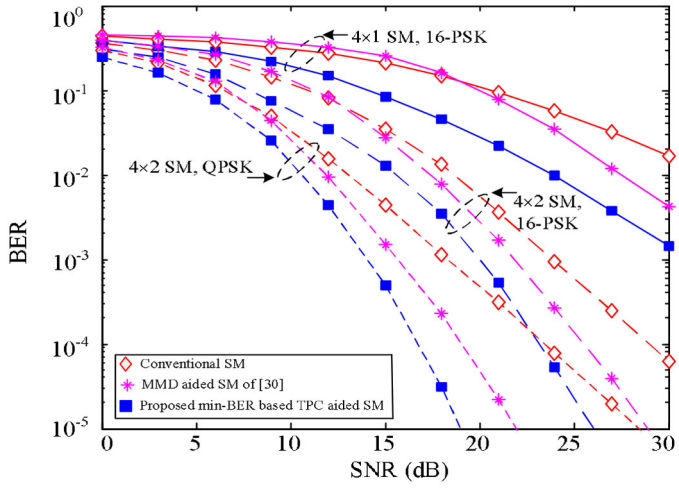

Fig. 9. BER comparison of the proposed min-BER based TPC aided SM schemes over the MMD aided SM schemes.

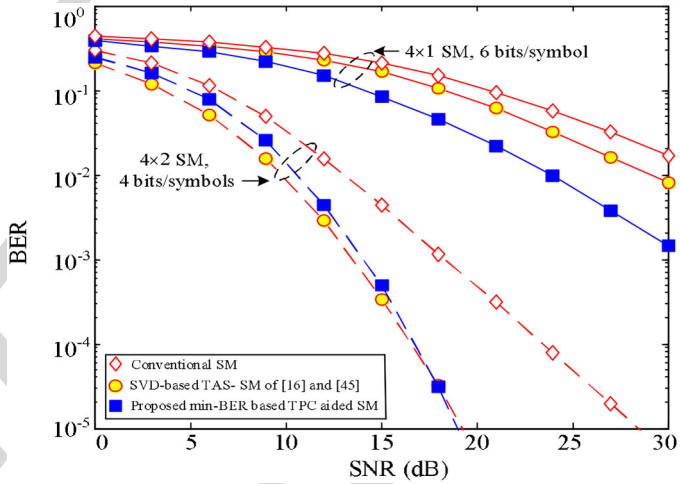

Fig. 10. BER performance of the proposed min-BER-based TPC-aided SM schemes and the SVD-based TAS-SM schemes.

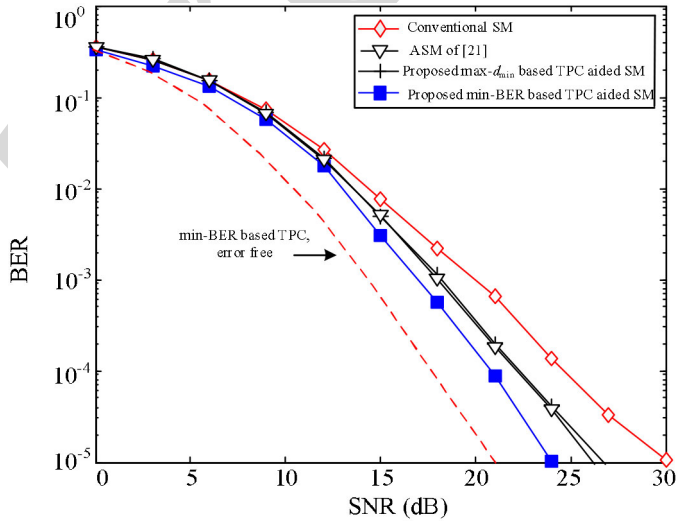

Fig. 11. BER performance of different adaptive SM schemes in the presence of CSI errors. Here, the error variance is $\sigma^2_{err} = 1/r$, where r is the average SNR at each receiver antenna.

TABLE II
COMPLEXITY ORDERS FOR DIFFERENT TPC DESIGNS. THE EXAMPLES ARE WITH PARAMETERS $n_{\mathrm{SCG}} = 30$, $n_{\mathrm{PA}} = 2$, $n_{\mathrm{PRP}} = 3$, $n_{\mathrm{TPC}} = 5$, $L_1 = 6$ AND $L_2 = 6$

Designs	Complexity order	Configuration 1 (4×2, QPSK)	Configuration 2 (4×2 16PSK)
ASM of [21]	$\mathcal{O}(N_t^2 M^2) + \mathcal{O}(N_t^2 N_r)$	320	4160
Max-$d_{\min}$ based PRP of [34]	$\mathcal{O}(N_t^2 M) + \mathcal{O}(n_{\mathrm{PRP}}(M^2 + N_t M))$	160	1216
Max-$d_{\min}$ based PA of [33]	$\mathcal{O}(N_t^2 M) + \mathcal{O}(n_{\mathrm{PA}}(M^2 + N_t M))$	128	896
Diagonal TPC method of [32]	$\mathcal{O}(L_1 L_2 N_t^2 M^2 N_r)$	18432	294912
MMD based TPC of [30]	$\mathcal{O}(N_t^2 M^2 N_r) + \mathcal{O}(N_t^4 M^4)$	66048	16785408
Proposed max-$d_{\min}$ based TPC	$\mathcal{O}(N_t^2 M) + \mathcal{O}(n_{\mathrm{TPC}}(M^2 + N_t M))$	224	1856
Proposed min-BER based TPC	$\mathcal{O}(n_{\mathrm{SCG}} N_t^2 M^2 N_r)$	15360	245760

proposed TPC scheme provides about 3.2 dB gain over the PRP scheme at BER $= 10^{-5}$ for (8×2)-element MIMO channels at a throughput of 5 bits/symbol. This benefit is due to the following two reasons: (1) the PRP schemes only adapt the phases of the SM symbols and hence the degrees of freedom utilized for TPC design are limited [35]; (2) similar to the methods of [31], [33], they are designed based on the max-$d_{\min}$ principle and hence may provide suboptimal BER.

In Fig. 9, the proposed min-BER based TPC schemes are compared to the MMD-aided SM schemes of [30]. Observe in Fig. 9 that the proposed TPC scheme provides an SNR gain of about 3 dB over the MMD-aided scheme at the BER of 10^{-5} for the (4×2) MIMO channels considered. Similar to the results in [30], the MMD-based TPC schemes provide minor performance improvements or even degrade the performance in low-SNR regimes. This is because the MMD criterion based TPC design may be ineffective in low SNR regimes, as discussed in [30].

Moreover, in Fig. 10, the proposed min-BER based TPC schemes are compared to the TAS-based SM schemes [16], [17], [44], [45] under different throughputs. In Fig. 10, the singular value decomposition (SVD)-based TAS algorithm of [16], [44], [45] is utilized due to its low-complexity and attractive performance. The number of TAs is $N_t = 4$ and 2 out of $N_t = 4$ TAs are selected by the TAS algorithm. Without loss of generality, we consider a PSK signal constellation diagram. As shown in Fig. 10, the TAS and the TPC schemes exhibit different BER advantages for different system setups. Specifically, the proposed TPC scheme outperforms the TAS scheme for (4×1) MIMO channels having a throughput of 6 bits/symbol, while they achieve a similar BER performance for (4×2) MIMO associated with 4 bits/symbol. This is not surprising, since the TAS and the TPC algorithms rely on different transmit parameters for the sake of achieving BER improvements. Note that TPC can be added on top of TAS to further improve performance. Hence they are complementary rather than competitive. It has been shown in [24], [30] that the joint design of TPC and TAS can further improve the system performance.

Fig. 11 shows the BER performance of various SM schemes in the presence of Gaussian-distributed CSI errors obeying $\mathcal{CN}\left(0, \sigma_{err}^2\right)$ [42], [43] for (2×2) MIMO channels and $L = 3$ bits/symbol. For the sake of simplification and clarity, we only consider the ASM and PA-aided SM schemes as benchmarks. In this paper, the variable σ_{err}^2, i.e. the value of the estimation error is adjusted according to the SNR. To be specific, $\sigma_{err}^2 = 1/r$ is adopted, where r is the average SNR at each receiver antenna. As expected, the BER performance of all SM schemes degrades upon imposing CSI estimation errors. However, Fig. 11 shows that the performance degradation of the proposed min-BER based TPC-aided SM is lower than that of the other schemes due to the fact that its BER upper bound was optimized bearing in mind the CSI error by using the SCG algorithm.

C. Complexity Comparison for Different TPC Designs

In Table II, the complexity orders of different TPC designs are compared. Specifically, in the randomly-selected diagonal TPC method of [31], [32], the quantization levels of amplitude and phase are L_1 and L_2, respectively. Its complexity order is provided in [30]. Moreover, the complexity orders of the max-$d_{\min}$ based PRP and of the max-$d_{\min}$ based PA algorithms can be found in [34] and [33], where their iteration numbers are n_{PA} and n_{PRP}, respectively. In Table II, we also provide the approximate quantified complexity for some specific configurations, where the QPSK- and 16PSK-modulated 4×2 SM schemes are considered. The number of iterations for the proposed SCG method is set to be $n_{\mathrm{SCG}} = 30$ due to it fast convergence.

As shown in Table II, the proposed max-$d_{\min}$ based TPC has a similar complexity order to that of the max-$d_{\min}$ based PRP of [34] and to that of the PA of [33], while exhibiting a lower complexity than the proposed min-BER design, since these max-$d_{\min}$ based designs only have to optimize a single distance $d_{\min}$. However, as shown in our simulation results of Figs 5–7 these max-$d_{\min}$ based designs suffer from a BER performance loss. The MMD-based TPC of [30] is a generalized max-$d_{\min}$ based TPC, which has to optimize $N_t M$ TPC weights for all legitimate SM symbols rather than relying on a diagonal TPC matrix having only N_t non-zero elements. Hence, the MMD-based TPC imposes a higher complexity than the proposed max-$d_{\min}$ and min-BER based TPC algorithms, as shown in Table II. For example, in configuration 2, the complexity of the proposed min-BER based design approximately achieves 68 times smaller than that of the MMD-based design.

Moreover, the diagonal TPC method of [32] requires an exhaustive search over a set of $L_1 L_2$ candidates, hence a higher complexity is imposed compared to the proposed min-BER based TPC for a high number of quantization levels. By taking into account both the BER versus complexity trends, we

conclude that the proposed min-BER based TPC provides an improved BER performance at a modest complexity cost. It should be noted that the extra complexity is imposed by the calculation of the gradient $\nabla Je(\mathbf{U})$ and by the convex problem solution algorithm, which may be further reduced by exploiting the spatial-domain sparsity of SM symbols and with the aid of reduced-complexity solution techniques. This issue will be investigated in our future studies.

VII. Conclusions

We have investigated two types of diagonal TPC design algorithms. For the max-$d_{\min}$ based TPC algorithm, closed-form solutions were derived for the case of two TAs and suboptimal solutions were achieved by using iterative method. For the min-BER based TPC algorithm, an iterative SCG algorithm was proposed for finding the specific TPC matrix solution. Finally, the proposed min-BER based TPC algorithm was further enhanced by taking into account the effects of imperfect CSI. It is shown from simulation results that the proposed max-$d_{\min}$ based TPC algorithm is optimal in terms of the minimum received distance, while the proposed min-BER based TPC algorithm is optimal in terms of the BER. Our further work will be focused on the integration of space-time coding, channel coding and TAS techniques into the proposed schemes.

Appendix

A. Gradient Derivation

In this appendix, we derive the theoretical gradient matrix of the cost function. Let us consider a general case associated with $\hat{\mathbf{H}} = \mathbf{H} + \Delta\mathbf{H}$. Then the cost function of Eq. (31) is reformulated as

$$Je_{\hat{\mathbf{H}}}(\mathbf{U}) = \sum_{\mathbf{x}_i \in \mathbb{X}} \sum_{\substack{\mathbf{x}_j \in \mathbb{X} \\ \mathbf{x}_i \neq \mathbf{x}_j}} D_H(\mathbf{x}_i \to \mathbf{x}_j) Q\left(\sqrt{\frac{\varepsilon_{\hat{\mathbf{H}}}}{2\sigma_e^2}}\right), \tag{50}$$

where we have

$$\sigma_e^2 = N_0 + \sigma_{err}^2 (\mathbf{U}\mathbf{x}_i)^H \mathbf{U}\mathbf{x}_i, \tag{51}$$

and

$$\varepsilon_{\hat{\mathbf{H}}} = \left\| \hat{\mathbf{H}}\mathbf{U}(\mathbf{x}_i - \mathbf{x}_j) \right\|^2. \tag{52}$$

Note that σ_e^2 and $\varepsilon_{\hat{\mathbf{H}}}$ are functions of the TPC matrix $\mathbf{U}$. Then the gradient of $Je_{\hat{\mathbf{H}}}(\mathbf{U})$ can be expressed as:

$$\begin{aligned} \nabla Je_{\hat{\mathbf{H}}}(\mathbf{U}) &= \frac{\partial Je_{\hat{\mathbf{H}}}(\mathbf{U})}{\partial \mathbf{U}^H} \\ &= \sum_{\mathbf{x}_i \in \mathbb{X}} \sum_{\substack{\mathbf{x}_j \in \mathbb{X} \\ \mathbf{x}_i \neq \mathbf{x}_j}} D_H(\mathbf{x}_i \to \mathbf{x}_j) \frac{\partial Q\left(\sqrt{\frac{\varepsilon_{\hat{\mathbf{H}}}}{2\sigma_e^2}}\right)}{\partial \mathbf{U}^H}. \end{aligned} \tag{53}$$

Here, $\partial Q\left(\sqrt{\frac{\varepsilon_{\hat{\mathbf{H}}}}{2\sigma_e^2}}\right) / \partial \mathbf{U}^H$ of Eq. (53) can be expressed as

$$\begin{aligned} \frac{\partial Q\left(\sqrt{\frac{\varepsilon_{\mathbf{H}}}{2\sigma_e^2}}\right)}{\partial \mathbf{U}^H} &= -\frac{1}{\sqrt{\pi}} e^{-\frac{\varepsilon_{\mathbf{H}}}{4\sigma_e^2}} \left(\frac{\varepsilon_{\hat{\mathbf{H}}}}{4\sigma_e^2}\right)^{-\frac{1}{2}} \frac{\partial\left(\sqrt{\frac{\varepsilon_{\hat{\mathbf{H}}}}{4\sigma_e^2}}\right)}{\partial \mathbf{U}^H} \\ &= -\frac{1}{\sqrt{\pi}} e^{-\frac{\varepsilon_{\hat{\mathbf{H}}}}{4\sigma_e^2}} \left(\frac{\varepsilon_{\hat{\mathbf{H}}}}{4\sigma_e^2}\right)^{-\frac{1}{2}} \left\{ \left(\frac{\partial(\varepsilon_{\hat{\mathbf{H}}})}{\partial \mathbf{U}^H} \frac{1}{4\sigma_e^2} \right) + \left(\frac{\partial\left(\frac{1}{4\sigma_e^2}\right)}{\partial \mathbf{U}^H} \varepsilon_{\hat{\mathbf{H}}} \right) \right\}, \end{aligned} \tag{54}$$

where we have the relationship of

$$\frac{\partial\left(\varepsilon_{\hat{\mathbf{H}}}\right)}{\partial \mathbf{U}^H} = \hat{\mathbf{H}}^H \hat{\mathbf{H}}\mathbf{U}\varphi(\mathbf{x}_i \to \mathbf{x}_j), \tag{55}$$

$$\frac{\partial\left(\frac{1}{4\sigma_e^2}\right)}{\partial \mathbf{U}^H} = -\frac{\sigma_{err}^2 \mathbf{U}\mathbf{x}_i \mathbf{x}_i^H}{4\sigma_e^4}. \tag{56}$$

Based on Eq. (56), we can arrive at the gradient matrix of Eq. (44). Moreover, assuming that the CSI is perfectly known, we have $\Delta\mathbf{H} = 0$, $\hat{\mathbf{H}} = \mathbf{H}$ and $\varepsilon_{\hat{\mathbf{H}}} = \varepsilon = \left\|\mathbf{H}\mathbf{U}(\mathbf{x}_i - \mathbf{x}_j)\right\|^2$. Then, the gradient matrix of Eq. (32) is readily obtained.

References

[1] R. Y. Mesleh, H. Haas, S. Sinanovic, C. W. Ahn, and S. Yun, "Spatial modulation," *IEEE Trans. Veh. Technol.*, vol. 57, no. 4, pp. 2228–2241, Jul. 2008.

[2] M. Di Renzo, H. Haas, A. Ghrayeb, S. Sugiura, and L. Hanzo, "Spatial modulation for generalized MIMO: Challenges, opportunities and implementation," *Proc. IEEE*, vol. 102, no. 1, pp. 56–103, Jan. 2014.

[3] S. Sugiura, S. Chen, and L. Hanzo, "A universal space-time architecture for multiple-antenna aided systems," *IEEE Commun. Surveys & Tuts.*, vol. 14, no. 2, pp. 401–420, May 2012.

[4] E. Başar, Ü. Aygölü, E. Panayırcı, and H. V. Poor, "Space-time block coded spatial modulation," *IEEE Trans. Commun.*, vol. 59, no. 3, pp. 823–832, Mar. 2011.

[5] M. Di Renzo, H. Haas, and P. M. Grant, "Spatial modulation for multiple-antenna wireless systems: A survey," *IEEE Commun. Mag.*, vol. 49, no. 12, pp. 182–191, Dec. 2011.

[6] M. Di Renzo and H. Haas, "Bit error probability of SM-MIMO over generalized fading channels," *IEEE Trans. Veh. Technol.*, vol. 61, no. 3, pp. 1124–1144, Mar. 2012.

[7] A. Stavridis, S. Sinanovic, M. Di Renzo, and H. Haas, "Energy evaluation of spatial modulation at a multi-antenna base station," in *Proc. IEEE Veh. Technol. Conf.*, Barcelona, Spain, Sep. 2013, pp. 1–5.

[8] N. Serafimovski *et al.*, "Practical implementation of spatial modulation," *IEEE Trans. Veh. Technol.*, vol. 62, no. 9, pp. 511–523, Nov. 2013.

[9] J. Jeganathan, A. Ghrayeb, and L. Szczecinski, "Spatial modulation: Optimal detection and performance analysis," *IEEE Commun. Lett.*, vol. 12, no. 8, pp. 545–547, Aug. 2008.

[10] S. Sugiura, C. Xu, S. X. Ng, and L. Hanzo, "Reduced complexity coherent versus non-coherent QAM-aided space time shift keying," *IEEE Trans. Commun.*, vol. 59, no. 11, pp. 3090–3101, Nov. 2011.

[11] N. R. Naidoo, H. Xu, and T. Quazi, "Spatial modulation: Optimal detector asymptotic performance and multiple-stage detection," *IET Commun.*, vol. 5, no. 10, pp. 1368–1376, Jul. 2011.

[12] A. Younis, S. Sinanovic, M. Di Renzo, R. Y. Mesleh, and H. Haas, "Generalised sphere decoding for spatial modulation," *IEEE Trans. Commun*, vol. 61, no. 7, pp. 2805–2815, Jul. 2013.

[13] R. Y. Chang, S.-J. Lin, and W.-H. Chung, "Energy efficient transmission over space shift keying modulated MIMO channels," *IEEE Trans. Commun.*, vol. 60, no. 10, pp. 2950–2959, Oct. 2012.

[14] S. Sanayei and A. Nosratinia, "Antenna selection in MIMO systems," *IEEE Commun. Mag.*, vol. 42, no. 10, pp. 68–73, Oct. 2004.

[15] D. J. Love, R. W. Heath Jr., U. K. N. Lau, D. Gesbert, B. D. Rao, and M. Andrews, "An overview of limited feedback in wireless communication systems," *IEEE J. Sel. Areas Commun.*, vol. 26, no. 8, pp. 1341–1365, Oct. 2008.

[16] K. Ntontin, M. Di Renzo, A. Perez-Neira, and C. Verikoukis, "A low-complexity method for antenna selection in spatial modulation systems," *IEEE Commun. Lett.*, vol. 17, no. 12, pp. 2312–2315, Aug. 2013.

[17] R. Rajashekar, K. V. S. Hari, and L. Hanzo, "Antenna selection in spatial modulation systems," *IEEE Commun. Lett.*, vol. 17, no. 3, pp. 521–524, Mar. 2013.

[18] N. Pillay and H. Xu, "Comments on 'Antenna selection in spatial modulation systems'," *IEEE Commun. Lett.*, vol. 17, no. 9, pp. 1681–1683, Sep. 2013.

[19] P. Yang, Y. Xiao, Y. Yi, and S. Li, "Adaptive spatial modulation for wireless MIMO transmission systems," *IEEE Commun. Lett.*, vol. 15, no. 6, pp. 602–604, Jun. 2011.

[20] P. Yang, Y. Xiao, L. Li, Q. Tang, Y. Yu, and S. Li, "Link adaptation for spatial modulation with limited feedback," *IEEE Trans. Veh. Technol.*, vol. 61, no. 8, pp. 3808–3813, Oct. 2012.

[21] P. Yang, Y. Xiao, Y. Yi, L. Li, Q. Tang, and S. Q. Li, "Simplified adaptive spatial modulation for limited-feedback MIMO," *IEEE Trans. Veh. Technol.*, vol. 62, no. 2, pp. 2656–2666, Jul. 2013.

[22] R. Rajashekar, K. V. S. Hari, and L. Hanzo, "Reduced-complexity ML detection and capacity-optimized training for spatial modulation," *IEEE Trans. Commun.*, vol. 62, no. 1, pp. 112–125, Jan. 2014.

[23] K. Ntontin, M. Di Renzo, A. I. Perez-Neira, and C. Verikoukis, "Adaptive generalized space shift keying," *EURASIP J. Wireless Commun. Netw.*, vol. 43, Feb. 2013.

[24] M. Maleki, H. R. Bahrami, S. Beygi, M. Kafashan, and N. H. Tran, "Space modulation with CSI: Constellation design and performance evaluation," *IEEE Trans. Veh. Technol.*, vol. 64, no. 4, pp. 1623–1634, May 2013.

[25] M. Maleki, H. R. Bahrami, M. Kafashan, and N. H. Tran, "On the performance of spatial modulation: Optimal constellation breakdown," *IEEE Trans. Commun.*, vol. 62, no. 1, pp. 144–157, Jan. 2014.

[26] C. B. Chae, A. Forenza, R. W. Heath Jr., M. R. Mckay, and I. B. Collings, "Adaptive MIMO transmission techniques for broadband wireless communication systems," *IEEE Commun. Mag.*, vol. 48, no. 5, pp. 112–118, May 2010.

[27] L. Collin, O. Berder, P. Rostaing, and G. Burel, "Optimal minimum distance-based precoder for MIMO spatial multiplexing systems," *IEEE Trans. Signal Process.*, vol. 52, no. 5, pp. 617–627, Mar. 2004.

[28] M. Di Renzo and H. Haas, "Improving the performance of space shift keying (SSK) modulation via opportunistic power allocation," *IEEE Commun. Lett.*, vol. 14, no. 6, pp. 500–502, Jun. 2010.

[29] C. Masouros, "Improving the diversity of spatial modulation in MISO channels by phase alignment," *IEEE Commun. Lett.*, vol. 18, no. 5, pp. 729–732, May 2014.

[30] M. Lee, W. Chung, and T. Lee, "Generalized precoder design formulation and iterative algorithm for spatial modulation in MIMO systems with CSIT," *IEEE Trans. Wireless Commun.*, vol. 63, no. 4, pp. 1230–1244, Apr. 2015.

[31] P. Yang, Y. Xiao, B. Zhang, S. Li, M. El-Hajjar, and L. Hanzo, "Star-QAM signaling constellations for spatial modulation," *IEEE Trans. Veh. Technol.*, vol. 63, no. 8, pp. 3741–3749, Oct. 2014.

[32] P. Yang, M. Di Renzo, Y. Xiao, S. Li, and L. Hanzo, "Design guidelines for spatial modulation," *IEEE Commun. Surveys Tuts.*, vol. 17, no. 1, pp. 6–26, Mar. 2015.

[33] P. Yang, Y. Xiao, S. Li, and L. Hanzo, "A low-complexity power allocation algorithm for multiple-input multiple-output spatial modulation systems," *IEEE Trans. Veh. Technol.*, 2015, to be published, doi: 10.1109/TVT.2015.2410252.

[34] C. Masouros and L. Hanzo, "Constellation-randomization achieves transmit diversity for single-RF spatial modulation," *IEEE Trans. Veh. Technol.*, 2015, to be published.

[35] P. Yang, Y. Xiao, S. Li, and L. Hanzo, "Phase rotation based transmit precoding improves the minimum Euclidean distance of single-RF-chain aided spatial modulation," *IET Commun.*, 2015, to be published.

[36] M. Bazaraa, H. Sherali, and C. Shetty, *Nonlinear Programming: Theory and Algorithms*. Hoboken, NJ, USA: Wiley, 1993.

[37] S. Chen, N. Ahmad, and L. Hanzo, "Adaptive minimum bit-error rate beamforming," *IEEE Trans. Wireless Commun.*, vol. 4, no. 2, pp. 341–348, Mar. 2005.

[38] J. Proakis, *Digital Communications*. New York, NY, USA: McGraw-Hill, 2001.

[39] A. Goldsmith, *Wireless Communications*. Cambridge, U.K.: Cambridge Univ. Press, 2005.

[40] D. Yang, C. Xu, L.-L. Yang, and L. Hanzo, "Transmit diversity-assisted space-shift keying for collocated and distributed/cooperative MIMO elements," *IEEE Trans. Veh. Technol.*, vol. 60, no. 6, pp. 2864–2869, Jul. 2011.

[41] T. Handte, A. Muller, and J. Speidel, "BER analysis and optimization of generalized spatial modulation in correlated fading channels," in *Proc. IEEE Veh. Technol. Conf.*, Anchorage, AK, USA, Sep. 2009, pp. 1–5.

[42] E. Başar, Ü. Aygölü, E. Panayırcı, and H. V. Poor, "Performance of spatial modulation in the presence of channel estimation errors," *IEEE Commun. Lett.*, vol. 16, no. 2, pp. 176–179, Feb. 2012.

[43] S. S. Ikki and R. Mesleh, "A general framework for performance analysis of space shift keying (SSK) modulation in the presence of Gaussian imperfect estimations," *IEEE Commun. Lett.*, vol. 16, no. 2, pp. 228–230, Feb. 2012.

[44] N. Wang, W. Liu, H. Men, M. Jin, and H. Xu. "Further complexity reduction using rotational symmetry for EDAS in spatial modulation," *IEEE Commun. Lett.*, vol. 18, no. 10, pp. 1835–1838, Oct. 2014.

[45] J. Zheng and J. Chen, "Further complexity reduction for antenna selection in spatial modulation systems," *IEEE Commun. Lett.*, vol. 19, no. 6, pp. 937–940, Jun. 2015, doi: 10.1109/LCOMM.2015.2417884.

Ping Yang received the B.E. and M.E. degrees from the University of Electronic Science and Technology of China (UESTC), Chengdu, China, in 2006 and 2009, respectively. From September 2012 to September 2013, he was a Visiting Student at the School of Electronics and Computer Science, University of Southampton, Southampton, U.K. From May 2014, he is a Research Fellow with EEE, NTU, Singapore. Also, he is an Assistant Professor with UESTC. His research interests include MIMO/OFDM, machine learning, life science, and communication signal processing.

Yong Liang Guan (S'94–AM'97–M'99) received the Ph.D. degree from the Imperial College of Science, Technology and Medicine, University of London, London, U.K., and the B.Eng. degree (with first class Hons.) from the National University of Singapore, Singapore, in 1997 and 1991, respectively. He is now an Associate Professor with the School of Electrical and Electronic Engineering, Nanyang Technological University, Singapore. His research interests include modulation, coding and signal processing for communication, information security, and storage systems.

Yue Xiao received the Ph.D. degree in communication and information systems from the University of Electronic Science and Technology of China, Chengdu, China, in 2007. He is now a Full Professor with the University of Electronic Science and Technology of China. He has authored more than 30 international journals and been involved in several projects in the Chinese Beyond 3G Communication R&D Program. His research interests include wireless and mobile communications.

Marco Di Renzo (S'05–AM'07–M'09–SM'14) was born in L'Aquila, Italy, in 1978. He received the Laurea (*cum laude*) and Ph.D. degrees in electrical and information engineering from the University of L'Aquila, L'Aquila, Italy, in April 2003 and January 2007, respectively. Since January 2010, he has been a Tenured Academic Researcher ("Chargé de Recherche Titulaire") with the French National Center for Scientific Research (CNRS), as well as a Faculty Member of the Laboratory of Signals and Systems (L2S), a joint Research Laboratory of the CNRS, the École Supérieure d'Électricité (SUPÉLEC) and the University of Paris–Sud XI, Paris, France. His research interests include wireless communications theory. Currently, he serves an Editor of the IEEE COMMUNICATIONS LETTERS and the IEEE TRANSACTIONS ON COMMUNICATIONS. He is the recipient of a special mention for the 2012 IEEE CAMAD Best Paper Award; the 2013 Network of Excellence NEWCOM# Best Paper Award; the 2013 IEEE–COMSOC Best Young Researcher Award for Europe, Middle East and Africa (EMEA Region); and the 2014 IEEE ICNC Single Best Paper Award Nomination (Wireless Communications Symposium).

Shaoqian Li (AM'04–SM'12) received the B.S.E. degree in communication technology from Northwest Institute of Telecommunication, Xidian University, Xidian, China, and the M.S.E. degree in communication system from the University of Electronic Science and Technology of China (UESTC), Chengdu, China, in 1982 and 1984, respectively. He is a Professor, Ph.D Supervisor, Director of the National Key Laboratory of Communication, UESTC, and Member of the National High Technology R&D Program (863 Program) Communications Group. His research interests include wireless communication theory, antiinterference technology for wireless communications, spread-spectrum and frequency-hopping technology, mobile, and personal communications.

Lajos Hanzo (M'91–SM'92–F'04) received the D.Sc. degree in electronics and the doctorate degree, in 1976 and 1983, respectively. During his 37-year career in telecommunications, he has held various research and academic posts in Hungary, Germany, and the U.K. Since 1986, he has been with the School of Electronics and Computer Science, University of Southampton, Southampton, U.K, where he holds the Chair in Telecommunications. He has successfully supervised 80+ Ph.D. students, coauthored 20 Wiley/IEEE Press books on mobile radio communications totaling in excess of 10 000 pages, authored 1400+ research entries at IEEE Xplore, acted both as TPC and General Chair of the IEEE conferences, presented keynote lectures and has been awarded a number of distinctions. Currently, he is directing a 100-strong academic research team, working on a range of research projects in the field of wireless multimedia communications sponsored by industry, the Engineering and Physical Sciences Research Council (EPSRC) U.K., the European Research Council's Advanced Fellow Grant and the Royal Society's Wolfson Research Merit Award. He is also a Governor of the IEEE VTS. From 2008 to 2012, he was the Editor-in-Chief of the IEEE Press and a Chaired Professor also at Tsinghua University, Beijing. His research is funded by the European Research Council's Senior Research Fellow Grant. He served as FREng, FIEEE, FIET, a Fellow of EURASIP. In 2009, he was the recipient of the honorary doctorate "Doctor Honoris Causa" by the Technical University of Budapest, Budapest, Hungary.

QUERIES

Q1: Please be advised that per instructions from the Communications Society this proof was formatted in Times Roman font and therefore some of the fonts will appear different from the fonts in your originally submitted manuscript. For instance, the math calligraphy font may appear different due to usage of the usepackage[mathcal]euscript. We are no longer permitted to use Computer Modern fonts.

Q2: Please provide page range for Ref. [23].

Q3: Please provide volume number, issue number, and page range for Refs. [33], [34], and [35].

Transmit Precoded Spatial Modulation: Maximizing the Minimum Euclidean Distance Versus Minimizing the Bit Error Ratio

Ping Yang, Yong Liang Guan, *Member, IEEE*, Yue Xiao, Marco Di Renzo, *Senior Member, IEEE*, Shaoqian Li, *Senior Member, IEEE*, and Lajos Hanzo, *Fellow, IEEE*

***Abstract*—In this paper, we investigate a pair of transmit precoding (TPC) algorithms conceived for spatial modulation (SM) systems communicating over flat-fading multiple-input multiple-output (MIMO) channels. In order to retain all the benefits of conventional SM, we design the TPC matrix to be diagonal and introduce two design criteria for optimizing the elements of the TPC matrix. Specifically, we first investigate a TPC design based on maximizing the minimum Euclidean distance $d_{\min}$ (max-$d_{\min}$) between the SM signal points at the receiver side. A closed-form solution of the optimal max-$d_{\min}$-based TPC matrix is derived. Then, another TPC design algorithm is proposed for directly minimizing the bit error ratio (BER) upper bound of SM, which is capable of jointly optimizing the overall Euclidean distance between all received signal points. In the minimum BER (min-BER)-based TPC algorithm, the theoretical gradient of the BER with respect to the diagonal TPC matrix is derived and a simplified iterative conjugate gradient (SCG) algorithm is invoked for TPC optimization. Our simulation results demonstrate that the proposed max-$d_{\min}$-based TPC algorithm is optimal in terms of the minimum distance. However, increasing $d_{\min}$ does not achieve a further BER improvement. We also confirm that the min-BER-based TPC outperforms the max-$d_{\min}$-based TPC schemes in terms of the achievable BER performance.**

Manuscript received March 23, 2015; revised November 2, 2015; accepted November 2, 2015. This work was supported in part by the National Science Foundation of China under Grant 61471090, in part by the National Basic Research Program of China under Grant 2013CB329001, in part by the National High-Tech R&D Program of China ("863" Project under Grant 2014AA01A707), in part by the Foundation Project of National Key Laboratory of Science and Technology on Communications under Grant 9140C020108140C02005, and in part by the European Research Council's Advanced Fellow Grant are gratefully acknowledged. The work of M. D. Renzo was supported by the European Commission under the auspices of the FP7-PEOPLE MITN-CROSSFIRE project (grant 317126). The associate editor coordinating the review of this paper and approving it for publication was Z. Wang.

P. Yang is with the National Key Laboratory of Science and Technology on Communications, University of Electronic Science and Technology of China, Sichuan 611731, China, and also with the School of Electrical and Electronic Engineering, Nanyang Technological University, Singapore (e-mail: yang.ping@uestc.edu.cn).

Y. L. Guan is with the School of Electrical and Electronic Engineering, Nanyang Technological University, Singapore (e-mail: eylguan@ntu.edu.sg).

Y. Xiao and S. Li are with the National Key Laboratory of Science and Technology on Communications, University of Electronic Science and Technology of China, Sichuan 611731, China (e-mail: xiaoyue@uestc.edu.cn; lsq@yeste.edu.cn).

M. D. Renzo is with the Laboratory of Signals and Systems (L2S), University of Paris-Sud XI, Orsay, France (e-mail: marco.direnzo@lss.supelec.fr).

L. Hanzo is with the School of Electronics and Computer Science, University of Southampton, Southampton SO17 1BJ, U.K. (e-mail: lh@ecs.soton.ac.uk).

Color versions of one or more of the figures in this paper are available online at http://ieeexplore.ieee.org.

Digital Object Identifier 10.1109/TWC.2015.2497692

***Index Terms*—Minimum Euclidean distance, minimum BER, multiple-input multiple-output, pre-coding technique, spatial modulation.**

I. Introduction

RECENTLY, spatial modulation (SM) has been proposed as a new class of low-complexity energy-efficient multiple-input multiple-output (MIMO) approach, whilst relying on a single-radio frequency (RF) chain [1]–[3]. SM scheme relies on the unique encoding philosophy of activating one out of N_t transmit antennas (TAs) during each transmission slot [4]. The activated TA then transmits classic complex-valued symbols of amplitude and phase modulation (APM). The potential benefits of SM over the conventional MIMO techniques have been validated not only via numerical simulations [5], [6] but also by laboratory experiments [7], [8].

Early work has been focused on low-complexity receiver designs conceived for minimizing the bit error ratio (BER) of SM [9]–[12]. It was shown in [9] that a low-complexity single-stream maximum likelihood (ML) detector or an even lower-complexity near-ML detector [10]–[12] is capable of striking a beneficial trade-off amongst the potentially conflicting factors of energy-efficiency, multiplexing gain and diversity gain compared to other MIMO transmission techniques [13]. In addition to a plethora of receivers, preprocessing at the transmitter has also been conceived for achieving a further performance improvement. Specifically, several antenna selection (AS) methods [14], [15] originally designed for conventional MIMO systems have also been generalized for employment in SM systems with the goal of enhancing its capacity or BER performance [16]–[18]. In [19]–[21], an adaptive SM (ASM) scheme was proposed for improving the achievable BER, while maintaining the target throughput with the aid of adaptive modulation (AM) techniques. In [22], the power allocation between the pilot and data was optimized for maximizing the capacity of SM transmission. In [23] and [24], a specific constellation design was proposed for space shift keying (SSK) systems in order to improve their BER. The constellation design was further developed in [25] for SM by finding the optimal combination of the number of TAs and the APM size that minimizes the BER.

Among the promising design alternatives, linear transmit pre-coding (TPC) techniques constitute an attractive transmit preprocessing regime, since they use a simple matrix $\mathbf{U}$ for

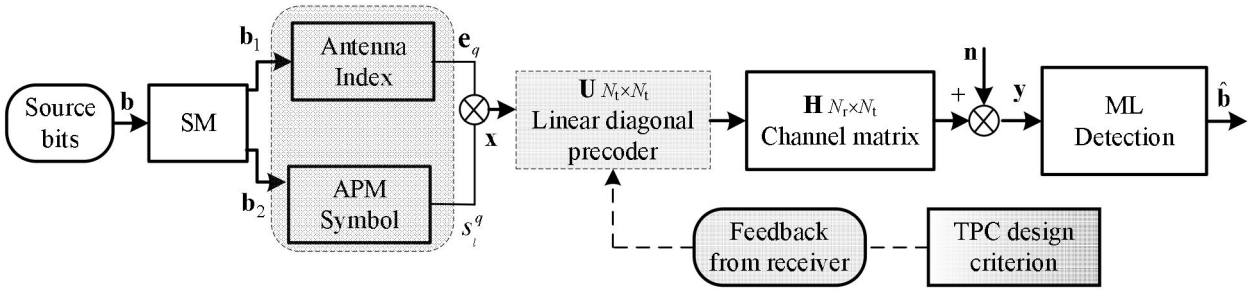

Fig. 1. The diagonal TPC based SM transmission system.

weighting the channel matrix in order to enhance the attainable performance [26]. Indeed, TPC has been widely researched in the context of classic spatial multiplexing systems [27]. However, since only a single TA is activated in each time slot in SM, these TPC approaches are not directly suitable for SM systems.

In [28] the effect of power imbalance has been researched in the context of SSK associated with TPC algorithms. More recently, the research efforts have been focused on the TPC design of SM based on maximizing the minimum Euclidean distance $d_{\min}$ (max-$d_{\min}$) in the received SM constellation. In [29], the phase alignment technique has also been extended to SM systems for constellation shaping in order to provide BER benefit in multiple-input single-output (MISO) channels. In [30], the max-$d_{\min}$ based TPC is designed by using an iterative concave-convex process, where the TPC parameters are calculated for each transmit constellation points. In [31], [32], a diagonal TPC was proposed for maximizing $d_{\min}$ in SM systems. However, an exhaustive numerical search method was used for identifying the specific TPC parameters. On the other hand, in [33], a special case of the diagonal TPC, namely an adaptive power allocation (PA) method, was investigated, where a simple real-valued diagonal TPC matrix was considered. As shown in [33], closed-form solutions of the optimal max-$d_{\min}$ aided PA were derived in the case of two TAs. In [34], another diagonal TPC method, namely phase rotation precoding (PRP), was proposed for energy-efficient transmission, where only the phases of the SM symbols were optimized based on the max-$d_{\min}$ criterion. The corresponding closed-form solutions were derived for two TAs and for PSK-modulated SM schemes in [35].

Against this background, the novel contributions of this paper are as follows.

1) We first investigate a general TPC matrix design algorithm based on the max-$d_{\min}$ criterion, where a complex-valued TPC matrix is considered instead of the real-valued PA matrix of [33] and the constant-modulus PRP matrix of [34], [35]. Compared to the heuristic method of computing the TPC matrix of [31], in this paper we derive closed-form solutions of the max-$d_{\min}$ TPC for a $(2 \times N_r)$-element BPSK-modulated SM scheme as well as for the more general cases of M-PSK modulated $(2 \times N_r)$-element SM. Moreover, we extend this method to the case of $N_t > 2$.
2) It is shown that the max-$d_{\min}$ based TPC-aided SM scheme is capable of achieving a larger $d_{\min}$ than other max-$d_{\min}$ aided adaptive SM schemes, such as the PA based TPC-aided SM scheme of [33] and the ASM scheme of [21]. However an increase of $d_{\min}$ does not achieve a further BER improvement. We find the reason that the max-$d_{\min}$ TPC only has a higher the minimum received distance $d_{\min}$ and may result in reduced Euclidean distances between the non-adjacent received constellation points.
3) To alleviate this shortcoming, we propose a new minimum-BER (min-BER) based TPC method, which is capable of jointly optimizing the overall Euclidean distance between the received signal points. Specifically, the theoretical gradient of the BER upper bound of SM with respect to the diagonal TPC matrix $\mathbf{U}$ is derived, and the simplified conjugate gradient (SCG) algorithm [36], [37] is invoked for efficient TPC optimization. We demonstrate that the overall BER gain of the proposed method is significantly improved compared to both that of conventional SM and to the other existing TPC schemes of [29]–[35]. We also extend the proposed algorithm to cope with channel state information (CSI) inaccuracies.

The organization of the paper is as follows. Section II introduces the concept as well as the system model of the TPC-based SM. In Section III and Section IV, we present a pair of TPC designs conceived for enhancing the BER performance of SM. The complexity analysis results are provided in Section V. Our Simulation results and performance comparisons are presented in Section VI. Finally, Section VII concludes the paper.

Notation: $(\cdot)^*$, $(\cdot)^T$ and $(\cdot)^H$ denote conjugate, transpose, and Hermitian transpose, respectively. The probability of an event is represented by $P(\cdot)$. Furthermore, $\|\cdot\|$ stands for the Frobenius norm and all logarithms are base of 2. $Tr(\cdot)$ denotes the trace of a square matrix, $E(\cdot)$ represents expectation, while $Re\{\mathbf{x}\}$ and $Im\{\mathbf{x}\}$ represent the real and imaginary parts of $\mathbf{x}$, respectively. $\mathbf{I}_b$ denotes a $(b \times b)$-element identity matrix and the operator diag$\{\cdot\}$ to be applied to a length i vector returns an $i \times i$ square matrix with the vector elements along the diagonal.

II. System Model

A. Signal Model of the Diagonal TPC Aided SM-MIMO

Consider a MIMO system having N_t transmit and N_r receive antennas. In this paper, N_t is assumed to be a power of two. Let $\mathbf{b} = [b_1, \ldots, b_L]$ be the transmit bit vector of each time slot, which contains $L = \log_2(N_t M)$ bits. As shown in Fig. 1, the input vector $\mathbf{b}$ is divided into two sub-vectors of $\log_2(N_t)$

and $\log_2(M)$ bits, denoted as $\mathbf{b}_1$ and $\mathbf{b}_2$, respectively. The bits in the sub-vector $\mathbf{b}_1$ are used for selecting a unique TA index q for activation, which is mapped to a N_t-dimensional standard basis vector $\mathbf{e}_q$ $(1 \le q \le N_t)$. The bits in the sub-vector $\mathbf{b}_2$ are mapped to a Gray-coded APM symbol $s_m^q \in \Im$ $(m \in \{1, \ldots, M\})$ [38]. Then, the resultant SM symbol $\mathbf{x} \in \mathbb{C}^{N_t \times 1}$ can be formulated as [1]

$$\mathbf{x} = s_m^q \mathbf{e}_q = [0, \ldots, \underset{\downarrow\, qth \text{ term}}{s_m^q}, \ldots, 0]^{\cdot}. \tag{1}$$

As shown in Fig. 1, after TPC relying on the linear diagonal matrix $\mathbf{U}$, the signal observed at the N_r receive antennas is given by

$$\mathbf{y} = \mathbf{HUx} + \mathbf{n}, \tag{2}$$

where $\mathbf{H}$ is the $(N_r \times N_t)$-element channel matrix, $\mathbf{U}$ is the $(N_t \times N_t)$-element TPC matrix, and $\mathbf{n}$ is the $(N_r \times 1)$-element noise vector. We assume $E[\mathbf{nn}^H] = N_0 \mathbf{I}_{N_r}$ and $E[\mathbf{xn}^H] = \mathbf{0}_{N_t \times N_t}$. The elements of the noise vector $\mathbf{n}$ are complex Gaussian random variables obeying $\mathcal{CN}(0, N_0)$. Furthermore, the diagonal TPC matrix $\mathbf{U}$ is given by

$$\mathbf{U} = \text{diag}\{u_1, \ldots, u_q, \ldots, u_{N_t}\}, \tag{3}$$

where u_q is a complex-valued TPC parameter, which controls the channel gain associated with x_q. We enforce the constraint $\sum_{q=1}^{N_t} |u_q|^2 = P_T$ for the sake of normalizing the transmit power. The diagonal structure of $\mathbf{U}$ guarantees that the transmit vector $\mathbf{Ux}$ has a single non-zero component, hence the single-RF-chain benefits (such as the avoidance of both the inter antenna interference (IAI) and of the multiple RFs) of SM are preserved. The matrix $\mathbf{U}$ can be decomposed as follows [31]

$$\mathbf{U} = \mathbf{P\Theta} = \text{diag}\{p_1, p_2 e^{j\theta_1}, \ldots, p_q e^{j\theta_{q-1}}, \ldots, p_{N_t} e^{j\theta_{N_t-1}}\}, \tag{4}$$

where $u_q = p_q e^{j\theta_{q-1}}$ and p_q represents the complex modulus of u_q, while θ_{q-1} represents the phase angle of u_q. In (4), the TPC matrix $\mathbf{U}$ is decomposed into two matrices related to the modulus and phase, which correspond to the real-valued PA matrix $\mathbf{P} = \text{diag}\{p_1, p_2, \ldots, p_q, \ldots, p_{N_t}\}$ and to the complex-valued PRP matrix $\mathbf{\Theta} = \text{diag}\{1, e^{j\theta_1}, \ldots, e^{j\theta_{q-1}}, \ldots, e^{j\theta_{N_t-1}}\}$, respectively.

Remark: The max-$d_{\min}$ based PA-aided SM schemes of [33] and the PRP-aided SM schemes of [34], [35] constitute special cases of the proposed TPC schemes, which can be obtained by setting $\mathbf{\Theta} = \mathbf{I}_{N_t}$ and $\mathbf{P} = \mathbf{I}_{N_t}$, respectively.

B. Maximum Likelihood Receiver

The receiver performs ML detection over all possible SM symbols $\mathbf{x} \in \mathbb{C}^{N_t \times 1}$ for retrieving the transmit symbols, which can be formulated as [9], [10]:

$$\begin{aligned}\hat{\mathbf{x}} &= \arg\min_{\mathbf{x}\in\mathbb{X}} \|\mathbf{y} - \mathbf{HUx}\|^2 \\ &= \arg\min_{\mathbf{x}\in\mathbb{X}} \left\|\mathbf{y} - \tilde{\mathbf{H}}\mathbf{x}\right\|^2 = \arg\min_{q\in\{1,\ldots,N_t\}} \left\|\mathbf{y} - \tilde{\mathbf{h}}_q s_m^q\right\|^2 \\ &\Leftrightarrow \arg\min_{q\in\{1,\ldots,N_t\}} \left\|\tilde{\mathbf{h}}_q^H \mathbf{y}/\left\|\tilde{\mathbf{h}}_q\right\|^2 - s_m^q\right\|^2,\end{aligned} \tag{5}$$

where $\mathbb{X}$ is the set of all legitimate transmit symbols and $\tilde{\mathbf{h}}_q$ is the $q-th$ column of the equivalent channel matrix $\tilde{\mathbf{H}} = \mathbf{HU}$. As shown in Eq. (5), a low-complexity single-stream ML detector is obtained [10], [22]. Moreover, it is shown in Proposition 1 of [22] that for a square- or for a rectangular-QAM constellation, the complexity imposed is independent of the constellation size, and that it increases only with N_t.

The conditional error performance of a ML receiver for a given channel $\mathbf{H}$ can be approximated by the sum of the pairwise error probability (PEP) [39], which is given by

$$P(\mathbf{H}) \le \frac{1}{L} \sum_{i=1}^{L} \sum_{\substack{j=1,\\ i\neq j}}^{L} Q\left(\sqrt{\frac{1}{2N_0} d_{ij}(\mathbf{H})}\right), \tag{6}$$

where $Q(x) = (1/\sqrt{2\pi}) \int_x^\infty e^{-y^2/2} dy$ denotes the Gaussian tail probability, while the distance $d_{ij}(\mathbf{H})$ at the receiver is defined as

$$\begin{aligned} d_{ij}(\mathbf{H}) &= \left\|\mathbf{HU}(\mathbf{x}_i - \mathbf{x}_j)\right\|^2 \\ &= \left\|\mathbf{HUe}_{ij}\right\|^2, \end{aligned} \tag{7}$$

where $\mathbf{e}_{ij} = \mathbf{x}_i - \mathbf{x}_j$, $i \neq j$ denotes the error vector. The PEP depends on the specific SM symbol pair $(\mathbf{x}_i, \mathbf{x}_j)$, on the instantaneous channel realization $\mathbf{H}$ and the TPC matrix $\mathbf{U}$.

III. Minimum Euclidean Distance Based TPC

It follows by direct inspection of the PEP expression of Eq. (6) that the performance of the ML receiver is predominantly affected by the distances $d_{ij}(\mathbf{H})$. Motivated by this observation, TPC design methods based on maximizing the minimum value of $d_{ij}(\mathbf{H})$ (the distance $d_{\min}$) have been introduced in [31] and [32]. However, only a high-complexity numerical approach was proposed for optimizing the TPC matrix. In this section, we first briefly introduce the max-$d_{\min}$ based TPC method. Then, we derive the related solutions.

A. Design Criterion

At high SNR, Eq. (6) can be further simplified as follows [39]

$$P(\mathbf{H}) \le \lambda \cdot Q\left(\sqrt{\frac{1}{2N_0} d_{\min}}\right), \tag{8}$$

where λ is the number of neighbor points [39] and $d_{\min}$ is defined as

$$d_{\min} = \min_{\substack{i,j\\ i\neq j}} d_{ij}(\mathbf{H}) = \min_{\mathbf{e}_{ij}\in\mathbb{E}} \left\|\mathbf{HUe}_{ij}\right\|^2. \tag{9}$$

In Eq. (8), $P(\mathbf{H})$ is a monotonically decreasing function of $d_{\min}$. Hence, the system's BER performance may be improved by maximizing the distance $d_{\min}$ of the received constellation upon carefully adapting the TPC matrix $\mathbf{U}$ under the power

constraint P_{T}.[1] Based on this principle, the max-$d_{\min}$ based TPC matrix $\mathbf{U}$ design rule can be formulated as follows

$$\mathbf{U}_{\mathrm{opt}} = \arg\max_{\mathbf{U}} d_{\min} \quad \text{s.t.} \quad tr\left(\mathbf{U}\mathbf{U}^T\right) \leq P_{\mathrm{T}}. \tag{10}$$

Note that in [33] and [35] the closed-form solutions for two special cases of Eq. (10), namely for the max-$d_{\min}$ based PA matrix and for the max-$d_{\min}$ based PRP matrix, have been derived. However, to the best of our knowledge, the closed-form solution for the joint design of the PA and PRP of Eq. (10) has not been reported in the existing literature. In the following subsections, we derive a closed-form solution for the TPC matrix of the BPSK-modulated $(2 \times N_r)$-element SM and extend the method to the more general M-PSK modulated $(2 \times N_r)$-element SM arrangements. Additionally, as shown in [2] and [6], PSK schemes are preferred over QAM schemes in SM. Hence, PSK is adopted in this paper.

B. Optimal TPC Matrix for BPSK-modulated $2 \times N_r$ SM

Let us consider a BPSK-modulated SM systems associated with $N_t = 2$, where the BPSK symbols belong to the set $\Im = \{1, -1\}$, and all possible error vectors $\mathbf{e}_{ij} = \mathbf{x}_i - \mathbf{x}_j$, $i \neq j$ are listed as follows: $\{[-2, 0]^T, [2, 0]^T, [0, -2]^T, [0, 2]^T, [-1, 1]^T, [-1, -1]^T, [1, -1]^T, [1, 1]^T\}$. Similar to the method of [33], since some vectors are collinear, the set to be studied is reduced to $\tilde{\mathbb{E}}_{BPSK} = \{\mathbf{e}_1, \mathbf{e}_2, \mathbf{e}_3, \mathbf{e}_4\} = \{[2, 0]^T, [0, 2]^T, [1, -1]^T, [1, 1]^T\}$. Given the channel matrix $\mathbf{H} = [\mathbf{h}_1, \mathbf{h}_2]$ and the corresponding TPC matrix $\mathbf{U} = \mathrm{diag}\{p_1, p_2 e^{j\theta_1}\}$, the distances at the receiver based on Eq. (7) are given by

$$\begin{cases} d_1 = \|\mathbf{H}\mathbf{U}\mathbf{e}_1\|^2 = 4\,\|p_1\mathbf{h}_1\|^2 \\ d_2 = \|\mathbf{H}\mathbf{U}\mathbf{e}_2\|^2 = 4\,\|p_2\mathbf{h}_2\|^2 \\ d_3 = \|\mathbf{H}\mathbf{U}\mathbf{e}_3\|^2 = \left\|p_1\mathbf{h}_1 - p_2 e^{j\theta_1}\mathbf{h}_2\right\|^2 \\ d_4 = \|\mathbf{H}\mathbf{U}\mathbf{e}_4\|^2 = \left\|p_1\mathbf{h}_1 + p_2 e^{j\theta_1}\mathbf{h}_2\right\|^2 \end{cases}. \tag{11}$$

Based on the distances in Eq. (11), the optimization problem of Eq. (10) can be modified as follows

$$\mathbf{U}_{\mathrm{opt}} = \arg\max_{\mathbf{U}} \{\min\{d_1, d_2, d_3, d_4\}\} \quad \text{s.t.} \quad tr(\mathbf{U}\mathbf{U}^T) \leq P_{\mathrm{T}}. \tag{12}$$

To obtain the specific TPC matrix $\mathbf{U}_{\mathrm{opt}}$, which maximizes the distance $d_{\min}$, the parameters p_1, p_2 and θ_1 in Eq. (12) have to be computed. As indicated in Eq. (11) and shown in Fig. 2, for a fixed PA matrix $\mathbf{P} = \mathrm{diag}\{p_1, p_2\}$, d_1 and d_2 are independent of the phase θ_1, while d_3 and d_4 are given by sinusoidal functions of the phase θ_1. In order to find the optimal phase solution θ_1^{opt}, we can first obtain the phases assigned to the TAs by finding the intersections of the sinusoidal curves in Fig. 2, and then continue by computing the optimal PA matrix as $\mathbf{P} = \mathrm{diag}\{p_1^{opt}, p_2^{opt}\}$.

[1] Compared to the PRP method of [34], [35], the power of the SM symbols may indeed fluctuate due to the TPC algorithm. However, during the time when the channel envelope remains constant within its coherence-interval, the power values of the transmit symbols are selected from a finite discrete set. In practice, the constraint P_{T} should be carefully selected according to the system requirements, such as the peak to average power ratio (PAPR) and the BER metrics.

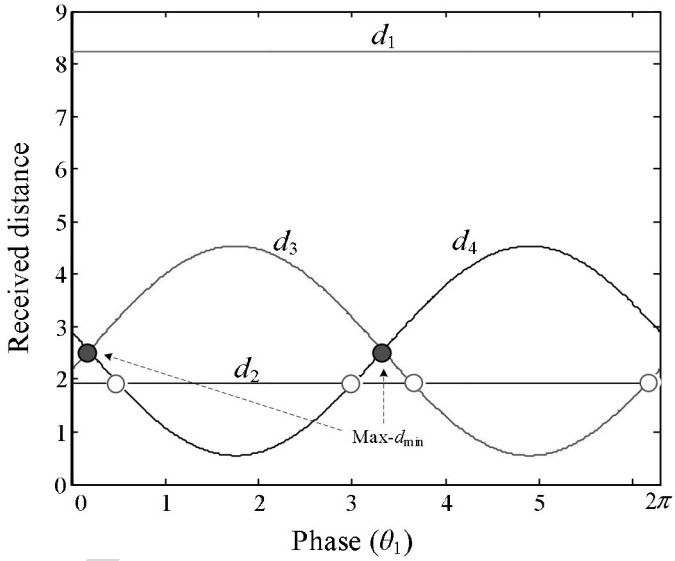

Fig. 2. The phase solutions of the BPSK-modulated $(2 \times N_r)$-element TPC based SM for a fixed PA.

To be specific, as shown in Fig. 2, regardless of the specific PA matrix $\mathbf{P}$, the optimal phase θ_1^{opt} that maximizes $d_{\min}$ should satisfy the constraint of $d_3 = d_4$ which from (11):

$$\left\|p_1\mathbf{h}_1 - p_2 e^{j\theta_1^{opt}}\mathbf{h}_2\right\|^2 = \left\|p_1\mathbf{h}_1 + p_2 e^{j\theta_1^{opt}}\mathbf{h}_2\right\|^2. \tag{13}$$

Eq. (13) can be further simplified to $\mathrm{Re}\{\mathbf{h}_1^H\mathbf{h}_2 e^{j\theta_1^{opt}}\} = 0$. Upon introducing the shorthands $a = \|\mathbf{h}_1\|^2$, $b = \|\mathbf{h}_2\|^2$, $c_1 = 2 \cdot \mathrm{Re}\{\mathbf{h}_1^H\mathbf{h}_2\}$ and $c_2 = 2 \cdot \mathrm{Im}\{\mathbf{h}_1^H\mathbf{h}_2\}$ for a given channel matrix $\mathbf{H}$, Eq. (13) can be solved as

$$c_1 \cos\theta_1^{opt} - c_2 \sin\theta_1^{opt} = 0 \Leftrightarrow \theta_1^{opt} = k\pi + \tan^{-1}\left(\frac{c_1}{c_2}\right), k \in \mathbb{Z}, 0 \leq \theta_1^{opt} \leq 2\pi. \tag{14}$$

Given the phase solution of Eq. (14), the distances d_3 and d_4 of Eq. (11) are simplified as follows

$$d_3 = d_4 = \|p_1\mathbf{h}_1\|^2 + \|p_2\mathbf{h}_2\|^2 = ap_1^2 + bp_2^2. \tag{15}$$

To compute the optimal PA parameters as p_1^{opt} and p_2^{opt}, since we have $d_3 = d_4$ in Eq. (15), the optimization problem of Eq. (12) can be further simplified to:

$$\begin{aligned} \mathbf{U}_{\mathrm{opt}} &= \arg\max_{\mathbf{U}} \{\min\{d_1, d_2, d_3\}\} \\ &= \arg\max_{\mathbf{U}} \left\{\min\left\{4ap_1^2, 4b\left(P_{\mathrm{T}} - p_1^2\right), ap_1^2 + b\left(P_{\mathrm{T}} - p_1^2\right)\right\}\right\}. \end{aligned} \tag{16}$$

As indicated in Eq. (16), d_1, d_2 and d_3 are linear functions of the parameter $\mu_1 = p_1^2$. Hence, the max-$d_{\min}$ solution given

μ_1 is one of the intersections between these distances $d_i (i = 1, 2, 3)$, which are given by

$$\begin{cases} p_1^{(1)} = \sqrt{b/(a+b)P_{\mathrm{T}}} \\ p_1^{(2)} = \sqrt{b/(3a+b)P_{\mathrm{T}}} \\ p_1^{(3)} = \sqrt{3b/(3b+a)P_{\mathrm{T}}} \end{cases}, \tag{17}$$

where $p_1^{(i)}, i = 1, 2, 3$ are the power assigned to the first TA for the ith intersections. Then, based on the fixed total power constraint P_{T}, the corresponding power assigned to the second TA is given by

$$\begin{cases} p_2^{(1)} = \sqrt{a/(a+b)P_{\mathrm{T}}} \\ p_2^{(2)} = \sqrt{3a/(3a+b)P_{\mathrm{T}}} \\ p_2^{(3)} = \sqrt{a/(3b+a)P_{\mathrm{T}}} \end{cases}. \tag{18}$$

Based on Eqs. (17) and (18), we select the one providing the maximum $d_{\min}$ as the final solution. Finally, the optimal TPC matrix $\mathbf{U}_{\mathrm{opt}}$ and the corresponding maximized $d_{\min}$, namely $d_{\min}^{\max}$, are given by

$$\begin{cases} \text{if } a \geq b, \quad \mathbf{U}_{\mathrm{opt}} = \mathrm{diag}\left\{p_1^{(2)}, p_2^{(2)} e^{j\theta_1^{opt}}\right\}, \quad d_{\min}^{\max} = \frac{4ab}{3a+b} \\ \text{if } a < b, \quad \mathbf{U}_{\mathrm{opt}} = \mathrm{diag}\left\{p_1^{(3)}, p_2^{(3)} e^{j\theta_1^{opt}}\right\}, \quad d_{\min}^{\max} = \frac{4ab}{3b+a} \end{cases} \tag{19}$$

It is worth noting that since the Euclidean distance $d_{\min}^{\max}$ of Eq. (19) has two independent channel gains, a transmit diversity order of two may be achieved [40].

C. Optimal TPC Matrix for M-PSK-Modulated $(2 \times N_r)$-Element SM

In this subsection, the approach proposed in Section III-B is extended to M-PSK modulated SM schemes. Based on the method of Section III-B, the max-$d_{\min}$ based TPC algorithm can be summarized as follows:

In order to better illustrate the general algorithm described above, let us consider the specific example of constant-modulus M-PSK modulation, whose symbols belong to the set $s \sim \Im = e^{j\frac{2l\pi}{M}} (l \in \{1, \ldots, M\})$. The minimum distance between two symbols of the M-PSK constellation is $d_{M-\mathrm{PSK}} = 2\sin(\pi/M)$ [38]. Since the SM symbols $\mathbf{x}_i$ and $\mathbf{x}_j$ only have a single non-zero element, the error vectors $\mathbf{e}_{ij} = \mathbf{x}_i - \mathbf{x}_j, i \neq j$ can be classified into two types: the error vectors having only a single non-zero element, and those having two non-zero elements. The first type is generated by the transmit symbols $\mathbf{x}_i$ and $\mathbf{x}_j$ associated with the same TA activation position, while the second type is generated by the symbols having different active TAs. As a result, the distance d_{ij} ($\mathbf{H}$) of Eq. (7) can be divided into two sets: $\mathbb{D}_1$ and $\mathbb{D}_2$, which are given by

$$\begin{cases} \mathbb{D}_1 = \left\{p_i^2 \|\mathbf{h}_i\|^2 (s_l - s_{\hat{l}}), l \neq \hat{l}, i = 1, 2\right\} \\ \mathbb{D}_2 = \left\{\left\|p_1 \mathbf{h}_1 s_l - p_2 \mathbf{h}_2 s_{\hat{l}}\right\|^2, l, \hat{l} = 1, \ldots M\right\} \end{cases}, \tag{20}$$

where $s_l = e^{j\frac{2l\pi}{M}}$ and $s_{\hat{l}} = e^{j\frac{2\hat{l}\pi}{M}}$ are two M-PSK symbols. Since only the minimum distance is investigated in the max-$d_{\min}$ optimization problem of Eq. (10), only the minimum value of the set $\mathbb{D}_1$ has to be considered. To be specific, only the pair of elements $d_1 = \min_{l \neq \hat{l}} p_1^2 \|\mathbf{h}_1\|^2 (s_l - s_{\hat{l}}) = d_{M-\mathrm{PSK}} p_1^2 \|\mathbf{h}_1\|^2$ and $d_2 = \min_{l \neq \hat{l}} p_2^2 \|\mathbf{h}_2\|^2 (s_l - s_{\hat{l}}) = d_{M-\mathrm{PSK}} p_2^2 \|\mathbf{h}_2\|^2$ has to be considered in $\mathbb{D}_1$. Hence, the set $\mathbb{D}_1$ is simplified to

$$\mathbb{D}_1 = \left\{d_{M-\mathrm{PSK}}^2 p_1^2 \|\mathbf{h}_1\|^2, d_{M-\mathrm{PSK}}^2 p_2^2 \|\mathbf{h}_2\|^2\right\}. \tag{21}$$

Let us reduce the set $\mathbb{D}_2$. When only the phase difference of the PSK symbols $s_l = e^{j\frac{2l\pi}{M}}$ and $s_{\hat{l}} = e^{j\frac{2\hat{l}\pi}{M}}$ is considered, the set $\mathbb{D}_2$ can be modified to

$$\begin{aligned} \mathbb{D}_2 &= \left\{\left\|\mathbf{h}_1 p_1 s_l - \mathbf{h}_2 p_2 e^{j\theta_1} s_{\hat{l}}\right\|^2, s_l, s_{\hat{l}} \in \Im\right\} \\ &= \left\{\left\|p_1 \mathbf{h}_1 e^{j\frac{2(l-\hat{l})\pi}{M}} - p_2 e^{j\theta_1} \mathbf{h}_2\right\|^2, l, \hat{l} = 1, \ldots M\right\} \\ &= \left\{\left\|p_1 \mathbf{h}_1 e^{j\frac{2k\pi}{M}} - p_2 e^{j\theta_1} \mathbf{h}_2\right\|^2, k = 0, \ldots M-1\right\}, \end{aligned} \tag{22}$$

where the phase difference factor is $k = l - \hat{l}$. The reduction principle behind Eq. (22) is that if the error vectors in the set $\mathbb{D}_2$ having only a phase difference, they provide the same distance at the receiver. Based on this principle, the number of elements in $\mathbb{D}_2$ is reduced to M compared to $M(M-1)$.

Let $\lambda_k = \frac{2k\pi}{M}$ be the phase difference of the symbol s_l and $s_{\hat{l}}$. Since the distances in the set $\mathbb{D}_1$ are independent of the phase θ_1, similar to the BPSK case portrayed in Section III-B,

Algorithm 1. The max-$d_{\min}$ based TPC algorithm

Step 1: Compute all legitimate error vectors $\mathbf{e}_{ij} = \mathbf{x}_i - \mathbf{x}_j, i \neq j$ by eliminating all collinear elements. Calculate all legitimate received distances d_{ij} ($\mathbf{H}$) with the aid of the channel matrix $\mathbf{H}$ and $\mathbf{e}_{ij}$. Let $\mathbb{D}$ be the set of these distances, whose elements are denoted by $d_v (v = 1, \ldots, V)$, where V is the cardinality of the set $\mathbb{D}$. The set $\mathbb{D}$ is divided into two sub-sets $\mathbb{D}_1$ and $\mathbb{D}_2$, where $\mathbb{D}_1$ contains the error vectors, which have only a single non-zero element, and $\mathbb{D}_2$ contains the error vectors, which have two non-zero elements.[2]

Step 2: Find the optimal phase θ_1^{opt}, which maximizes the minimum received distance of the set $\mathbb{D}_2$. Note that there may be multiple optimal phase solutions, which are calculated based on shifted sinusoidal functions d_v in $\mathbb{D}_2$. Since these solutions provide the same $d_{\min}$, any one of them can be randomly selected.

Step 3: After finding the optimal phase θ_1^{opt}, compute all possible intersections between the received distances d_i and d_j $(d_i, d_j \in \mathbb{D})$ and compute the corresponding PA matrix $\mathbf{P}$. Select the one having the largest $d_{\min}$ as the final PA result, which can be formulated as $\mathbf{P} = \mathrm{diag}\{p_1^{opt}, p_2^{opt}\}$. Then, the final TPC solution is given by $\mathbf{U}_{\mathrm{opt}} = \mathrm{diag}\{p_1^{opt}, p_2^{opt} e^{j\theta_1^{opt}}\}$.

[2]Note that the transmit vector of SM has only a single non-zero element, hence the number of non-zero elements of the error vectors of SM is up to 2.

it is possible to first find the optimal phase θ_1^{opt}, which maximizes the minimum received distance of the set $\mathbb{D}_2$. To achieve this goal, the intersections between arbitrary received distances $\left\|\mathbf{h}_1 p_1 e^{j\lambda_a} - \mathbf{h}_2 p_2 e^{j\theta_1}\right\|^2$ and $\left\|\mathbf{h}_1 p_1 e^{j\lambda_b} - \mathbf{h}_2 p_2 e^{j\theta_1}\right\|^2$ in Eq. (22) are firstly calculated as

$$\begin{aligned}&\left\|\mathbf{h}_1 p_1 e^{j\lambda_a} - \mathbf{h}_2 p_2 e^{j\theta_1}\right\|^2 = \left\|\mathbf{h}_1 p_1 e^{j\lambda_b} - \mathbf{h}_2 p_2 e^{j\theta_1}\right\|^2 \\ &\Leftrightarrow (c_1\cos\lambda_a - c_2\sin\lambda_a - c_1\cos\lambda_b + c_2\sin\lambda_b)\cos\theta_1 \\ &= -(c_1\sin\lambda_a + c_2\cos\lambda_a - c_1\sin\lambda_b - c_2\cos\lambda_b)\sin\theta_1 \\ &\Leftrightarrow \tan\theta_1 = -\frac{c_1\cos\lambda_a - c_2\sin\lambda_a - c_1\cos\lambda_b + c_2\sin\lambda_b}{c_1\sin\lambda_a + c_2\cos\lambda_a - c_1\sin\lambda_b - c_2\cos\lambda_b}.\end{aligned} \tag{23}$$

After that, all possible optimal phase θ_1^{opt} can be obtained from Eq. (23) as

$$\begin{cases}\theta_1^{opt} = k\pi + \tan^{-1}\left(\frac{-c_1\cos\lambda_a + c_2\sin\lambda_a + c_1\cos\lambda_b - c_2\sin\lambda_b}{c_1\sin\lambda_a + c_2\cos\lambda_a - c_1\sin\lambda_b - c_2\cos\lambda_b}\right), \\ k\in\mathbb{Z}, 0\le\theta_1^{opt}\le 2\pi.\end{cases} \tag{24}$$

Finally, the optimal phase is the candidate providing the maximum distance $d_{\min}$ in the set of Eq. (24). After computing the optimal phase, the the PA matrix can be optimized based on all possible intersections of $d_v (v = 1, \ldots, V)$, similar to processes of Eqs. (16)–(18). Following these calculation steps, the optimal TPC matrix, which combines the optimal phase and PA parameters, is obtained in closed-form.

D. Example for QPSK Modulation

Based on the algorithm in Section III-C, we calculate the optimal TPC solution for QPSK-modulated $(2 \times N_r)$-element SM, which will be used in our simulations. The symbols of QPSK modulation belong to the set $\Im = \{1, -1, j, -j\}$ and the value of $d_{4-\mathrm{PSK}}$ is equal to $\sqrt{2}$. Based on Eqs. (21) and (22), the corresponding sets $\mathbb{D}_1$ and $\mathbb{D}_2$ for QPSK modulation are

$$\begin{cases}\mathbb{D}_1 = \left\{2p_1^2\left\|\mathbf{h}_1\right\|^2, 2p_2^2\left\|\mathbf{h}_2\right\|^2\right\}. \\ \mathbb{D}_2 = \left\{\left\|p_1\mathbf{h}_1 e^{j\frac{2k\pi}{M}} - p_2 e^{j\theta_1}\mathbf{h}_2\right\|^2, k = 0, \ldots, 3\right\},\end{cases} \tag{25}$$

According to Eq. (24), there are two optimal phases θ_1^{opt} that maximizes the distance $d_{\min}$ for Eq. (25), namely $\theta_1^{opt,1}$ and $\theta_1^{opt,2}$, which are given by

$$\begin{cases}\theta_1^{opt,1} = k\pi + \tan^{-1}\left(\frac{-c_1-c_2}{c_1-c_2}\right), \\ k\in\mathbb{Z}, 0\le\theta_1^{opt,1}\le 2\pi.\end{cases} \tag{26}$$

and

$$\begin{cases}\theta_1^{opt,2} = k\pi + \tan^{-1}\left(\frac{c_1-c_2}{c_1+c_2}\right), \\ k\in\mathbb{Z}, 0\le\theta_1^{opt,2}\le 2\pi.\end{cases} \tag{27}$$

Since both solutions $\theta_1^{opt,1}$ and $\theta_1^{opt,2}$ have the same $d_{\min}$, we consider only the first case $\theta_1 = \theta_1^{opt,1}$. After finding the optimal phase $\theta_1^{opt,1}$, the received distance set $\mathbb{D}_2$ is further reduced to $\mathbb{D}_2 = \{\|p_1\mathbf{h}_1 e^{j\frac{2k\pi}{M}} - p_2 e^{j\theta_1}\mathbf{h}_2\|^2, k = 0, 1\}$. This reduction is due to the fact that $\theta_1^{opt,1}$ corresponds to the intersection of two elements of $\mathbb{D}_2$ and the elements having the same value are eliminated. After this reduction, the final received distance set has only 4 elements (both $\mathbb{D}_1$ and $\mathbb{D}_2$ have 2 elements), denoted by $\bar{d}_i (i = 1, 2, 3, 4)$.

Given the optimal phase as $\theta_1^{opt} = \theta_1^{opt,1}$, we have to further identify the optimal PA parameters p_1^{opt} and p_2^{opt} ($p_2^{opt} = \sqrt{P_{\mathrm{T}} - (p_1^{opt})^2}$). According to the step 3 of **Algorithm 1**, the max-$d_{\min}$ solution of p_1 is one of the intersections between these received distance $\bar{d}_i (i = 1, 2, 3, 4)$, which are given by

$$\begin{cases}p_1^{(1)} = \sqrt{b/(a+b)P_{\mathrm{T}}} \\ p_1^{(2)} = p_1^{(5)} = \sqrt{\frac{2c^2+4ab+2\tilde{C}\sqrt{\tilde{C}^2+4ab}}{4a^2+2c^2+4ab+2\tilde{C}\sqrt{\tilde{C}^2+4ab}}P_{\mathrm{T}}}. \\ p_1^{(3)} = p_1^{(4)} = \sqrt{\frac{2c^2+4ab-2\tilde{C}\sqrt{\tilde{C}^2+4ab}}{4a^2+2c^2+4ab-2\tilde{C}\sqrt{\tilde{C}^2+4ab}}P_{\mathrm{T}}}\end{cases} \tag{28}$$

Based on the power constraint, the power allocated on the second TA is obtained by $p_2^{(i)} = \sqrt{P_{\mathrm{T}} - (p_1^{(i)})^2}, i = 1, \ldots, 5$. Finally, the distances $d_{\min}$ of these TPC solutions $\mathbf{U} = \mathrm{diag}\{p_1^{(i)}, p_2^{(i)} e^{j\theta_1^{opt,1}}\}$ $(i = 1, 2, 3, 4, 5)$ are generated and that having the largest $d_{\min}$ is chosen as our final result $\mathbf{U}_{\mathrm{opt}}$.

E. A Low-Complexity Iterative Max-$d_{\min}$ for $N_t > 2$

It is worth mentioning that the restriction of considering $(2 \times N_r)$-element SM is imposed by the difficulty of the $d_{\min}$ optimization. The solution of the general problem remains an open challenge for two reasons. Firstly, the solution depends on both the channel matrix and on the symbol alphabet, and secondly, the solution space is large. Similar to the general method proposed in the PA aided SM of [33], some sub-optimal methods can be adopted for the case of $N_t > 2$ based on an iterative process relying on the above-mentioned optimal max-$d_{\min}$ solution provided for $N_t = 2$, where the TPC algorithm will only be used for the specific TA pair associated with $d_{\min}$, while the parameters of other TAs remain unchanged in each iteration.

IV. Minimum BER Based TPC

Although the max-$d_{\min}$ based TPC algorithm is simple, it may not achieve a significant BER improvement for some SM systems, because only one of the distances in the PEP expression of Eq. (6), namely $d_{\min}$, is optimized at the receiver. Moreover, we can only obtain closed-form solutions for this TPC algorithm for the case of $N_t = 2$. To deal with these problems, we propose a new min-BER based TPC algorithm, which is capable of jointly optimizing all the received distances for directly improving the BER for arbitrary value of N_t. By considering the bit-to-symbol mapping rule of our SM scheme, a more accurate conditional BER bound based on Eq. (6) can be obtained as [41]

$$\begin{aligned}P_e(\mathbf{H}) \le P_e^{\mathrm{up}}(\mathbf{H}) = \frac{1}{L}\sum_{\mathbf{x}_i\in\mathbb{X}}\sum_{\substack{\mathbf{x}_j\in\mathbb{X}\\ \mathbf{x}_i\ne\mathbf{x}_j}} D_H(\mathbf{x}_i\to\mathbf{x}_j) \\ \cdot\ Q\left(\sqrt{\frac{1}{2N_0}\left\|\mathbf{HU}(\mathbf{x}_i - \mathbf{x}_j)\right\|^2}\right),\end{aligned} \tag{29}$$

where $D_H(\mathbf{x}_i \to \mathbf{x}_j)$ is the Hamming distance between the SM signals $\mathbf{x}_i$ and $\mathbf{x}_j$. From Eq. (29), the min-BER-based TPC matrix is proposed by solving the optimization problem as follows

$$\begin{aligned} \mathbf{U}_{\text{opt}} &= \arg\min_{\mathbf{U}} P_e^{\text{up}}(\mathbf{H}) \\ \text{s.t. } & tr(\mathbf{U}\mathbf{U}^T) = P_{\text{T}} \end{aligned}. \tag{30}$$

Remark: Compared to Eq. (30), the max-$d_{\min}$ based TPC algorithm of Eq. (10) considers only a reduced summation over a subset of $\mathbb{X}$, which has the smallest Euclidean distance. Therefore, it can only minimize a much looser bound of BER than the bound of Eq. (29).

A. Precoder Design Based on Gradient Optimization

Since the direct solution of Eq. (30) is complex, we drive the theoretical gradient of the cost function with respect to the diagonal TPC matrix $\mathbf{U}$ and invoke the SCG algorithm of [36] for low-complexity TPC matrix optimization. More specifically, the cost function of the SCG algorithm is obtained from Eq. (29) and is defined as

$$\begin{aligned} Je(\mathbf{U}) = &\sum_{\mathbf{x}_i \in \mathbb{X}} \sum_{\substack{\mathbf{x}_j \in \mathbb{X} \\ \mathbf{x}_i \neq \mathbf{x}_j}} D_H(\mathbf{x}_i \to \mathbf{x}_j) \\ &\cdot Q\left(\sqrt{\frac{1}{2N_0}\left\|\mathbf{H}\mathbf{U}(\mathbf{x}_i - \mathbf{x}_j)\right\|^2}\right). \end{aligned} \tag{31}$$

The conjugate gradient of Eq. (31) with respect to $\mathbf{U}$ is given by

$$\begin{aligned} \nabla Je(\mathbf{U}) = &\frac{-\mathbf{H}^H\mathbf{H}\mathbf{U}}{4\sqrt{\pi}N_0} \times \sum_{\mathbf{x}_i \in \mathbb{X}} \sum_{\substack{\mathbf{x}_j \in \mathbb{X} \\ \mathbf{x}_i \neq \mathbf{x}_j}} \left\{ D_H(\mathbf{x}_i \to \mathbf{x}_j) \right. \\ &\left. \cdot \varphi(\mathbf{x}_i \to \mathbf{x}_j) \cdot \exp\left(-\frac{\varepsilon}{4N_0}\right)\left(\frac{\varepsilon}{4N_0}\right)^{-\frac{1}{2}} \right\}, \end{aligned} \tag{32}$$

where we have

$$\begin{aligned} &\varphi(\mathbf{x}_i \to \mathbf{x}_j) = (\mathbf{x}_i - \mathbf{x}_j)(\mathbf{x}_i - \mathbf{x}_j)^H = \mathbf{e}_{ij}\mathbf{e}_{ij}^H, \\ &\varepsilon = \left\|\mathbf{H}\mathbf{U}(\mathbf{x}_i - \mathbf{x}_j)\right\|^2. \end{aligned} \tag{33}$$

It is worth noting that the TPC matrix $\mathbf{U}$ is a diagonal matrix, hence the final diagonal conjugate gradient matrix is constituted by the diagonal elements of $\nabla Je(\mathbf{U})$. The derivation of Eq. (32) is given in Appendix A. Given the conjugate gradient of Eq. (32), the problem of Eq. (30) can be solved iteratively by commencing the iterations from an appropriate initial point using the SCG algorithm of [36]. In order to have an initial diagonal TPC matrix $\mathbf{U}^{(1)} \in \mathbb{C}^{N_t \times N_t}$, we use the max-$d_{\min}$ based TPC matrix solution for $(2 \times N_r)$-element SM systems and adopt the near-optimal max-$d_{\min}$ solution in Section IV for the other scenarios.[3] Then, we optimize the TPC matrix with the aid of the SCG algorithm as follows:

[3]Moreover, we can also use the equally weighted diagonal matrix or other optimized TPC matrix of [33]–[35] as initial TPC matrix.

Algorithm 2. The min-BER based TPC algorithm

1) **Initialization**: Set a step size of $\mu > 0$, a termination scalar of $\beta > 0$ and a maximum number of iterations N_{all}; given the conjugate gradient of the initial diagonal TPC matrix $\mathbf{U}^{(1)}$ as $\tau(1) = \nabla Je(\mathbf{U}^{(1)}) \in \mathbb{C}^{N_t \times N_t}$, set $n = 1$.
2) **Loop**: if $\left\|\nabla Je(\mathbf{U}^{(1)})\right\| < \beta$ or $n > N_{all}$, goto **Stop**.

$$\mathbf{U}^{(n+1)} = \mathbf{U}^{(n)} - \mu\tau(n)/\left\|\tau(n)\right\|, \tag{34}$$

$$\alpha = P_{\text{T}}/tr(\mathbf{U}^{(n+1)}(\mathbf{U}^{(n+1)})^H), \tag{35}$$

$$\mathbf{U}^{(n+1)} = \sqrt{\alpha}\mathbf{U}^{(n+1)}, \tag{36}$$

$$\varphi_l = \left\|\nabla Je(\mathbf{U}^{(n+1)})\right\|^2 / \left\|\nabla Je(\mathbf{U}^{(n)})\right\|^2, \tag{37}$$

$$\tau(n+1) = \varphi_l\tau(n) - \nabla Je(\mathbf{U}^{(n+1)}). \tag{38}$$

$n = n + 1$, goto Loop.
3) **Stop**: $\mathbf{U}^{(n+1)}$ is the solution.

As shown in [36] and [37], the convergence of the SCG algorithm is more rapid than that of the classic steepest gradient algorithm. For the sake of avoiding convergence to a local optimum, the values of φ_l in SCG can be periodically reset either to zero or to their negative counterparts [36].[4]

B. SCG Algorithm Based on the Simple Q-function Estimations

In the SCG algorithm, the computational complexity is dominated by the calculation of the conjugate gradient of Eq. (32). To reduce this complexity, two simple upper bounds of the Gaussian Q-function can be adopted. The first well-known estimate is given by the Chernoff bound as follows [39]

$$Q(x) \leq \frac{1}{2}\exp\left(-\frac{x^2}{2}\right). \tag{39}$$

Hence, the conjugate gradient of Eq. (32) with respect to $\mathbf{U}$ is simplified to

$$\begin{aligned} \nabla Je_{Cher}(\mathbf{U}) = &\frac{-\mathbf{H}^H\mathbf{H}\mathbf{U}}{4N_0} \times \sum_{\mathbf{x}_i \in \mathbb{X}} \sum_{\substack{\mathbf{x}_j \in \mathbb{X} \\ \mathbf{x}_i \neq \mathbf{x}_j}} \left\{ D_H(\mathbf{x}_i \to \mathbf{x}_j) \right. \\ &\left. \cdot \varphi\left(\mathbf{x}_i \to \mathbf{x}_j\right) \cdot \exp\left(-\frac{\varepsilon}{4N_0}\right) \right\}. \end{aligned} \tag{40}$$

A more accurate approximation of the Q-function than the Chernoff bound is formulated as a sum of weighted exponentials. By considering only two components, the following Chiani-bound has been proposed in [39]

$$Q(x) \leq \frac{1}{12}\exp\left(-\frac{x^2}{2}\right) + \frac{1}{4}\exp\left(-\frac{2x^2}{3}\right) \tag{41}$$

[4]Further information about the SCG algorithm is available in [37].

and the corresponding conjugate gradient $\nabla Je_{Chai}(\mathbf{U})$ is

$$\nabla Je_{Chai}(\mathbf{U}) = \frac{-\mathbf{H}^H\mathbf{H}\mathbf{U}}{4N_0} \cdot \sum_{\mathbf{x}_i\in\mathbb{X}} \sum_{\substack{\mathbf{x}_j\in\mathbb{X} \\ \mathbf{x}_i\neq\mathbf{x}_j}} \left\{ D_H(\mathbf{x}_i \to \mathbf{x}_j) \right.$$
$$\left. \varphi\left(\mathbf{x}_i \to \mathbf{x}_j\right) \cdot \left[\frac{1}{6}\exp\left(-\frac{\varepsilon}{4N_0}\right) + \frac{2}{3}\exp\left(-\frac{\varepsilon}{3N_0}\right) \right] \right\}. \tag{42}$$

Eqs. (40) and (42) provide two simple approximations of Eq. (32). It is worth noting that the transmit vectors of SM schemes are sparsely populated, since they have mostly zero values, hence the space of non-linear error vectors $\mathbf{e}_{ij} = \mathbf{x}_i - \mathbf{x}_j$ is small, as shown in Section III. For example, the number of non-linear error vectors $\mathbf{e}_{ij}$ for QPSK-modulated SM associated with $N_t = 2$ is as low as six. In the SCG-based TPC optimization, we may only have to consider these non-linear error vectors and hence the computational complexity of the SCG algorithm can be further reduced.

C. Min-BER Based TPC Matrix Design With Imperfect CSI

In practical applications, pilot symbols are commonly used for estimating the MIMO channel, but naturally the estimated MIMO channel matrix is inevitably imperfect. Hence, the TPC design algorithm should give cognizance to the estimated MIMO channel matrix $\hat{\mathbf{H}}$, which is given by [42], [43]

$$\hat{\mathbf{H}} = \mathbf{H} + \Delta\mathbf{H}, \tag{43}$$

where $\Delta\mathbf{H}$ is the channel estimation error matrix. Let us assume that $\Delta\mathbf{H}$ is uncorrelated with $\mathbf{H}$ and satisfies $\Delta\mathbf{H}^H\Delta\mathbf{H} = \sigma_{err}^2\mathbf{I}_{N_t}$. Then, the corresponding gradient for SCG algorithm is computed as

$$\nabla Je(\mathbf{U}) = \frac{-\hat{\mathbf{H}}^H\hat{\mathbf{H}}\mathbf{U}}{4\sqrt{\pi}} \cdot \sum_{\mathbf{x}_i\in\mathbb{X}} \frac{1}{\sigma_e^2} \sum_{\substack{\mathbf{x}_j\in\mathbb{X} \\ \mathbf{x}_i\neq\mathbf{x}_j}} \left\{ D_H(\mathbf{x}_i \to \mathbf{x}_j) \right.$$
$$\left. \varphi\left(\mathbf{x}_i \to \mathbf{x}_j\right) \exp\left(-\frac{\varepsilon_{\hat{\mathbf{H}}}}{4\sigma_e^2}\right)\left(\frac{\varepsilon_{\hat{\mathbf{H}}}}{4\sigma_e^2}\right)^{-\frac{1}{2}} \right\} + \frac{\sigma_{err}^2\mathbf{U}}{4\sqrt{\pi}} \sum_{\mathbf{x}_i\in\mathbb{X}} \frac{\mathbf{x}_i\mathbf{x}_i^H}{\sigma_e^4}$$
$$\cdot \sum_{\substack{\mathbf{x}_j\in\mathbb{X} \\ \mathbf{x}_i\neq\mathbf{x}_j}} D_H\left(\mathbf{x}_i \to \mathbf{x}_j\right) \cdot \exp\left(-\frac{\varepsilon_{\hat{\mathbf{H}}}}{4\sigma_e^2}\right)\left(\frac{\varepsilon_{\hat{\mathbf{H}}}}{4\sigma_e^2}\right)^{-\frac{1}{2}} \varepsilon, \tag{44}$$

where we have

$$\sigma_e^2 = N_0 + (\mathbf{U}\mathbf{x}_i)^H\Delta\mathbf{H}^H\Delta\mathbf{H}\mathbf{U}\mathbf{x}_i, \tag{45}$$

and

$$\varepsilon_{\hat{\mathbf{H}}} = \left\|\hat{\mathbf{H}}\mathbf{U}(\mathbf{x}_i - \mathbf{x}_j)\right\|^2. \tag{46}$$

The derivation details of Eq. (44) are given in Appendix. As shown in Eq. (44), the resultant gradient carefully takes the channel estimation errors into account, when constructing the diagonal TPC matrix. Hence, the BER performance becomes resilient to CSI errors.

TABLE I
COMPUTATIONAL COMPLEXITY IMPOSED BY THE GRADIENT $\nabla Je(\mathbf{U})$

	Complexity imposed
$\mathbf{H}^H\mathbf{H}$	$O_1 = N_t^2(2N_r - 1)$
$\bullet \times \mathbf{U}$	$O_2 = N_t N_r$
$\varphi(\mathbf{x}_i \to \mathbf{x}_j)$	$O_3 = N_t\binom{2}{M}+4\binom{2}{N_t}M^2$
$\varepsilon = \left\|\mathbf{H}\mathbf{U}(\mathbf{x}_i - \mathbf{x}_j)\right\|^2$	$O_4 = N_t\binom{2}{M}(2N_r - 1) + 4\binom{2}{N_t}M^2(2N_r - 1)$

V. COMPLEXITY ANALYSIS OF THE PROPOSED TPC ALGORITHMS

In this section, we provide complexity evaluations of the proposed max-$d_{\min}$ based TPC and the min-BER based TPC algorithms, where only the multiplications of complex numbers are considered.

Based on a similar analysis method to that of [33], for the case of $N_t = 2$, the closed-form solution of the max-$d_{\min}$ based TPC can be found by using the **Algorithm 1**, which imposes a complexity of

$$O_{\max-d_{\min}} = \underbrace{4(2N_r - 1)}_{\text{calculate } \mathbf{H}^H\mathbf{H}} + \underbrace{15M(M-1)/2}_{\text{calculate optimal phase}} + \underbrace{(2M+1)(M+7)}_{\text{calculate optimal PA}}. \tag{47}$$

Moreover, for the case of $N_t > 2$, an iterative max-$d_{\min}$ based TPC can be adopted and the associated complexity (similar to Eq. (22) of [33]) is

$$O_{\max-d_{\min}} = \underbrace{4(2N_r - 1)}_{\text{calculate } \mathbf{H}^H\mathbf{H}} + \underbrace{\binom{2}{N_t}(2M-1)}_{\text{intial } d_{\min}} + \cdots$$
$$n_{\text{TPC}}\left[\underbrace{15M(M-1)/2}_{\text{calculate optimal phase}} + \underbrace{(2M+1)(M+7)}_{\text{calculate optimal PA}} \right.$$
$$\left. + \underbrace{2(N_t - 2)(2M-1)}_{\text{optimized } d_{\min}} \right], \tag{48}$$

where n_{TPC} is the number of iterations in the max-$d_{\min}$ based TPC algorithm, which is varied according to the channel matrix. In our simulations, we found that the average value of n_{TPC} is approximated to 5.

The complexity of the proposed min-BER based TPC algorithm can be estimated by considering: (a) the computational complexity of the SCG solution process in each iteration and (b) the number of iterations n_{SCG} required for approaching convergence. The first term can be estimated based on Eqs. (34)–(38). In Table I, we characterize the computational complexity imposed by the gradient $\nabla Je(\mathbf{U})$, where the sparse structure of the SM symbols $\mathbf{x}_i, \mathbf{x}_j$ and of the diagonal TPC matrix $\mathbf{U}$ are exploited. To be specific, the error vectors $\mathbf{e}_{ij} = \mathbf{x}_i - \mathbf{x}_j, i \neq j$ can be classified into two sets: $N_t\binom{2}{M}$ vectors having a single non-zero element and $\binom{2}{N_t}M^2$ vectors having two non-zero elements. They have different complexity for the calculation of $\varphi(\mathbf{x}_i \to \mathbf{x}_j)$ and ε, as shown in Table I. Note that

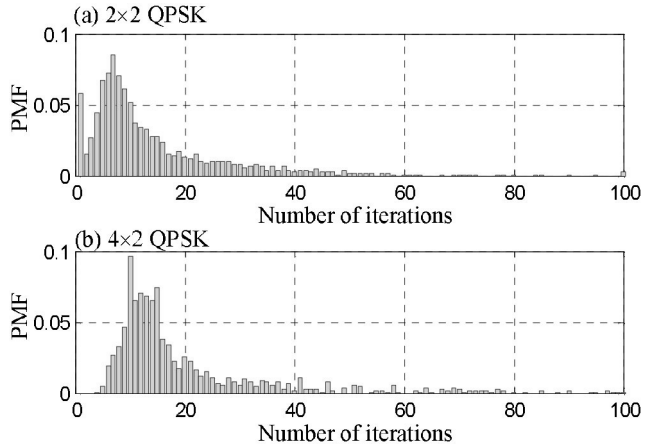

Fig. 3. Convergence behavior of the proposed min-BER based TPC in SM systems with QPSK modulation in i.i.d Rayleigh fading channels.

the bit-to-symbol mapping rule can be designed off-line, hence the complexity of $D_H(\mathbf{x}_i \to \mathbf{x}_j)$ is not considered in the calculation of $\nabla Je(\mathbf{U})$. Based on Table I and the SCG algorithm of Eqs. (34)–(38), the associated complexity of the proposed min-BER based TPC algorithm is approximately

$$O_{\min-\mathrm{BER}} = O_1 + O_3 + n_{\mathrm{SCG}}\Bigg[5(O_2+O_4) + \underbrace{N_t^2+N_t}_{\text{Eq.34}} + \cdots \underbrace{N_t^2-N_t+1}_{\text{Eq.35}} + \underbrace{N_t}_{\text{Eq.36}} + \underbrace{N_t^2-N_t+1}_{\text{Eq.37}} + \underbrace{2N_t}_{\text{Eq.38}}\Bigg]. \quad (49)$$

Moreover, similar to [30], in Fig. 3 we have portrayed the probability mass function (PMF) of the numbers of iterations for the min-BER based TPC algorithm in the QPSK-modulated (2×2) and (4×2) SM schemes. In the simulations, the threshold of SCG is given by $\beta = 10^{-5}$ and 25000 trails are considered to show the statistics of convergence. In Fig. 3 (a) and (b), more than 90% and 85% of the trials converged within 30 iterations. This is due to the rapid convergence of the SCG algorithm, as also verified in [37]. Note that although the approximation method of Section IV-B can reduce the complexity of calculating $\nabla Je(\mathbf{U})$, i.e. the complexity terms O_3 and O_4 in Table I, it has the same complexity order as (49). We will provide more detailed comparisons and discussions about the complexity issue in Section VI-C.

VI. Simulation Results

In this section, we provide simulation results (the distance $d_{\min}$ and the BER performance) for characterizing the max-$d_{\min}$ based TPC aided SM and the min-BER based TPC aided SM schemes for transmission over frequency-flat fading channels. For comparison, these performance results are compared to various adaptive SM schemes, such as the ASM arrangements of [21], the maximum minimum distance (MMD) aided SM schemes of [30], the PA-based SM schemes of [33], the TPC star-QAM SM schemes of [31], and the PRP aided SM schemes of [29] and [34], [35].

In the min-BER based TPC scheme, the step size μ is determined by Monte Carlo simulation methods, as suggested in [36] and we set $\mu = 0.01$, so that we achieve a rapid convergence, while maintaining excellent BER results. Moreover, for the BPSK case, we do not consider the ASM scheme because 'no-transmission' is assigned to one of the TAs and hence this TA is inactive [33].

A. $d_{\min}$ Performance for Different SM Schemes

In Fig. 4, we compare the complementary cumulative distribution functions (CCDF) of the distance $d_{\min}$ recorded for both for conventional SM and for the link adaptive SM schemes in (2×1) MIMO channels under different throughputs. First, we note that these adaptive SM schemes are capable of beneficially increasing the distance $d_{\min}$. As formally shown in Section III, we observe in Fig. 4 that the proposed max-$d_{\min}$ based TPC aided SM achieves the highest distance $d_{\min}$ compared to other link-adaptive SM schemes. Furthermore, we note that the min-BER based TPC schemes achieve lower $d_{\min}$ than the max-$d_{\min}$ based TPC schemes, and yet we will see in Figs. 5–7 that the min-BER based TPC outperforms the max-$d_{\min}$ based TPC in terms of its BER.

B. BER Comparisons of Different SM Schemes

In Fig. 5, we compare the BER performance of various SM systems for $L = 2$ bits/symbol in (2×1)- and (2×2)-element MIMO channels. We can see that the proposed min-BER based schemes provides gains of about 6 dB and 4 dB at the BER of 10^{-3} over the conventional SM schemes. We also confirm that the min-BER based schemes outperform the ASM of [21], the max-$d_{\min}$ based PA aided SM of [33] and the max-$d_{\min}$ based TPC aided SM proposed.

Note that, as shown in Fig. 4, although the optimal max-$d_{\min}$ based TPC aided SM is capable of achieving a higher distance $d_{\min}$ than the other adaptive SM schemes, it does not achieve a BER performance improvement over them. To expound a little further, in Fig. 5, when the proposed max-$d_{\min}$ based TPC-aided SM is compared to its special case, namely to the max-$d_{\min}$ based PA aided SM, we find that an increase of the distance $d_{\min}$ by TPC does not achieve any further BER improvement. Observe in Fig. 5 that at high SNRs, the max-$d_{\min}$ based TPC aided SM may even perform worse than the max-$d_{\min}$ based PA aided SM. This is mainly due to the fact that the maximum of $d_{\min}$ does not necessarily minimize the PEP bound of Eq. (29), which depends on all the received distances.

To be specific, the reason for the trends of Fig. 5 is that the max-$d_{\min}$ based TPC may achieve a lower Euclidean distance between the non-adjacent received constellation points than that of the PA schemes. Hence, based on the Q-function aided PEP upper bound of Eq. (29), which depends on all legitimate received distances $d_{ij}(\mathbf{H}) = \left\|\mathbf{HU}(\mathbf{x}_i - \mathbf{x}_j)\right\|$ $(i \neq j)$, the max-$d_{\min}$ based TPC fails to achieve the best BER performance. For example, let us consider the (2×1) SM scheme using BPSK. As shown in Section III, we only have four different distances

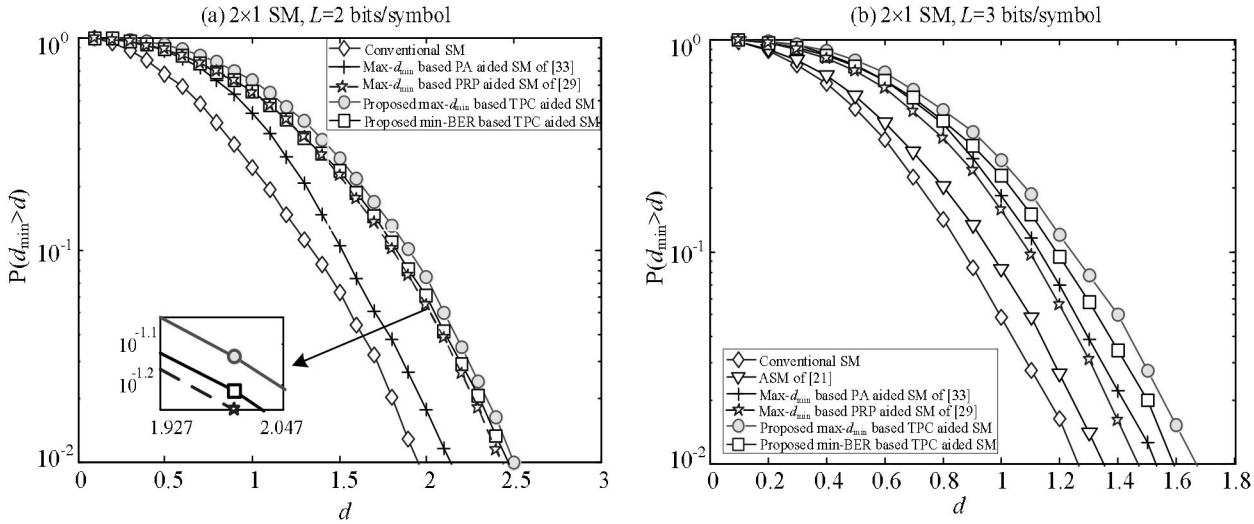

Fig. 4. The CCDF of the minimum distance $d_{\min}$ of conventional SM and of various link-adaptation aided SM schemes in (2×1)-element MIMO channels.

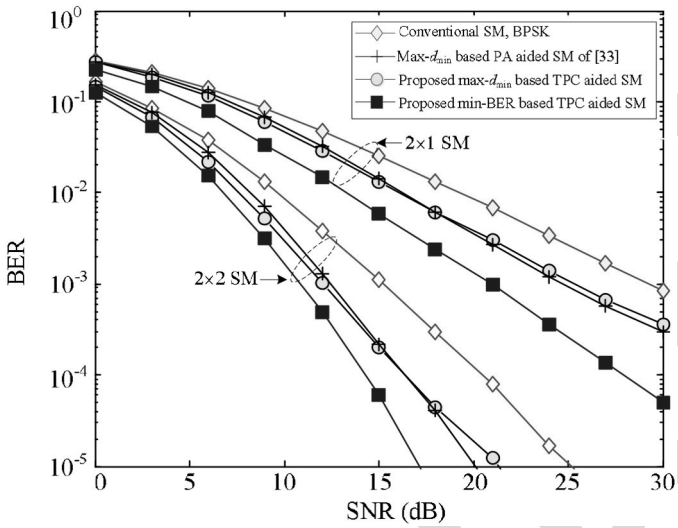

Fig. 5. BER comparison at $L = 2$ bits/symbol for the conventional SM, for the max-$d_{\min}$ based TPC aided SM and for the min-BER based TPC aided SM.

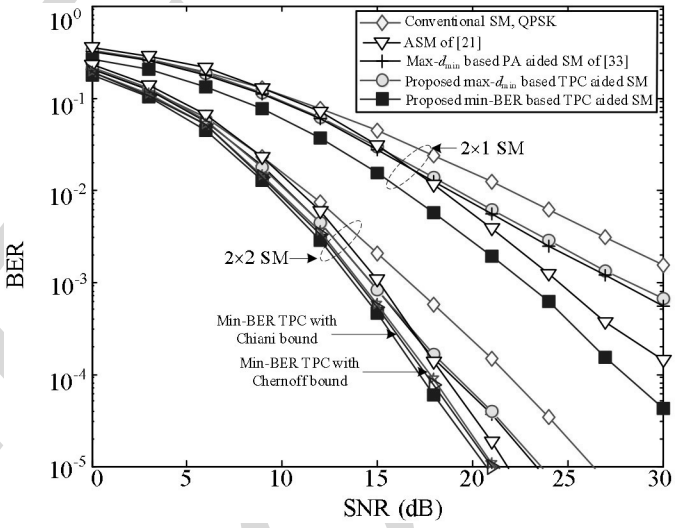

Fig. 6. BER comparison at $L = 3$ bits/symbol for various SM schemes. Here, the Q-function estimates of Section IV-B are only considered for the (2×2)-element MIMO channels.

at the receiver, namely d_1, d_2, d_3 and d_4. Assuming that the channel matrix is $\mathbf{H} = [0.056 - 0.069i, 0.414 + 1.267i]$ and the SNR is 25 dB, the resultant distance set for the max-$d_{\min}$ based TPC-aided SM is

$$\mathbb{D}_{TPC} = \{d_1 = 0.251, d_2 = 0.434, d_3 = 0.251, d_4 = 0.251\},$$

while the corresponding distance set for the max-$d_{\min}$ based PA aided SM is

$$\mathbb{D}_{PA} = \{d_1 = 0.248, d_2 = 0.718, d_3 = 0.476, d_4 = 0.248\}.$$

Then, the BER results of Eq. (29) calculated for the TPC-aided SM and the PA-aided SM schemes are $P_e(\mathbf{H}) = 0.7 \times 10^{-3}$ and $P_e(\mathbf{H}) = 0.5 \times 10^{-3}$, respectively. This result confirms that although the max-$d_{\min}$ based TPC algorithm achieves the highest distance of $d_{\min} = 0.251$, while the max-$d_{\min}$ based PA algorithm has $d_{\min} = 0.248$, the former has a worse PEP performance due to its lower values of d_2 and d_3. This result is consistent with the result seen in Fig. 5.

The above-mentioned trends of these proposed TPC algorithms are also visible in Fig. 6, where the throughput is $L = 3$ bits/symbol. It is shown in Fig. 6 that the proposed min-BER based TPC outperforms both ASM of [21] and the max-$d_{\min}$ based PA of [33]. Moreover, in Fig. 6, we demonstrate that the approximate Chernoff-based and Chiani-based optimizations perform almost the same as the exact Q-function based scheme. This is because these approximations do not change the direction of the gradient. We have also simulated the Chernoff-based and Chiani-based optimizations for the other MIMO setups considered, and obtained similar results, as evidenced by Fig. 6. Since the resultant curves approximately overlap with the optimal one, for clarity, these results are not included in other figures.

Due to the advantage of the proposed min-BER based TPC, in Fig. 7 we further investigate its performance for a higher number of TAs and modulation order. All the schemes are

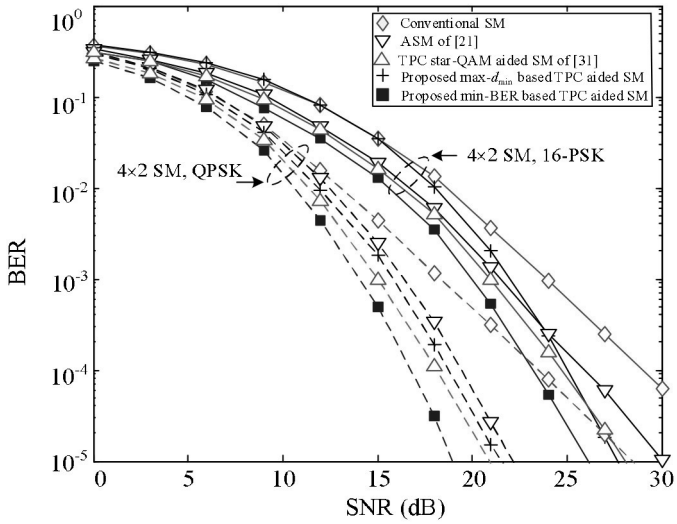

Fig. 7. BER comparison of the proposed min-BER-based TPC-aided SM schemes over the TPC star-QAM aided SM schemes.

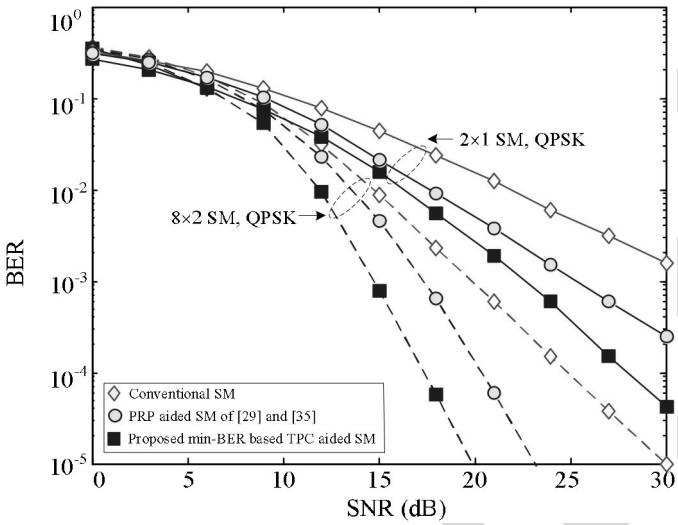

Fig. 8. BER comparison of the proposed min-BER-based TPC-aided SM schemes over the PRP-aided SM schemes.

assumed to have $N_t = 4$, $N_r = 2$ and the throughputs are $L = 4$ and $L = 6$ bits/symbol. In Fig. 7, the proposed schemes are also compared to the TPC star-QAM aided SM schemes of [31], which utilize a quantized search for optimizing the diagonal TPC matrix. In our simulation, the number of quantization levels for both amplitude and phase in TPC of [31] is 6. Observe in Fig. 7 that the proposed min-BER based TPC schemes achieve the best BER performance. The performance gain of the proposed scheme over the TPC star-QAM aided SM scheme is seen to be about 2.6 dB at BER= 10^{-5} for 4 bits/symbol transmissions in Fig. 7. This is due to the fact the TPC star-QAM based scheme of [31] also only optimizes a single received distance $d_{\min}$, which may limit the attainable BER performance.

In Fig. 8, we compared the proposed min-BER based TPC schemes to the max-$d_{\min}$ based PRP schemes of [29] and [35]. We observe in Fig. 8 that the proposed schemes outperform the PRP-aided schemes. To be specific, as seen in Fig. 8 the

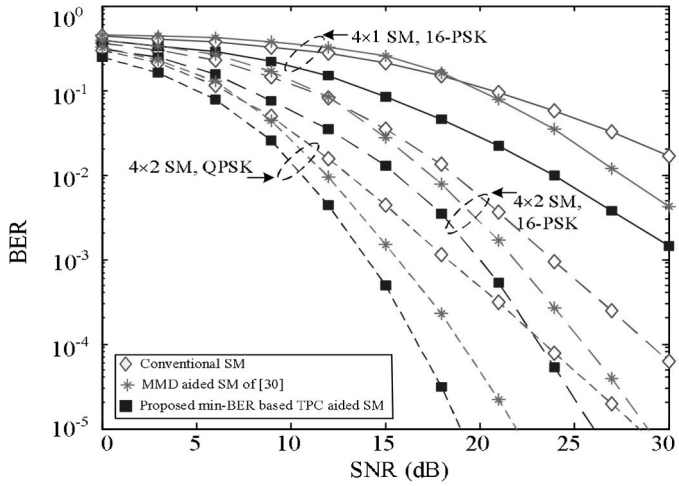

Fig. 9. BER comparison of the proposed min-BER based TPC aided SM schemes over the MMD aided SM schemes.

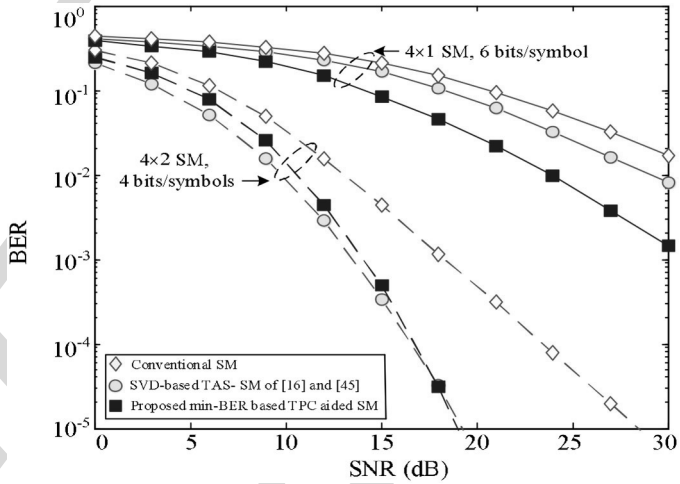

Fig. 10. BER performance of the proposed min-BER-based TPC-aided SM schemes and the SVD-based TAS-SM schemes.

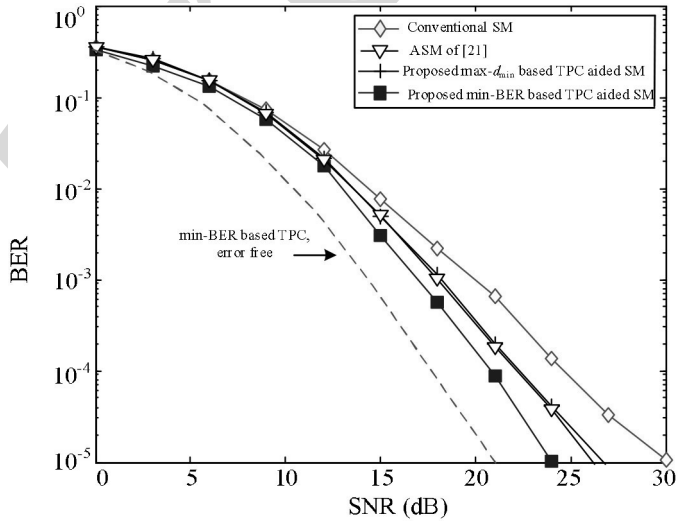

Fig. 11. BER performance of different adaptive SM schemes in the presence of CSI errors. Here, the error variance is $\sigma^2_{err} = 1/r$, where r is the average SNR at each receiver antenna.

TABLE II
COMPLEXITY ORDERS FOR DIFFERENT TPC DESIGNS. THE EXAMPLES ARE WITH PARAMETERS $n_{\mathrm{SCG}} = 30$, $n_{\mathrm{PA}} = 2$, $n_{\mathrm{PRP}} = 3$, $n_{\mathrm{TPC}} = 5$, $L_1 = 6$ AND $L_2 = 6$

Designs	Complexity order	Configuration 1 (4×2, QPSK)	Configuration 2 (4×2 16PSK)
ASM of [21]	$\mathcal{O}(N_t^2 M^2) + \mathcal{O}(N_t^2 N_r)$	320	4160
Max-$d_{\min}$ based PRP of [34]	$\mathcal{O}(N_t^2 M) + \mathcal{O}(n_{\mathrm{PRP}}(M^2 + N_t M))$	160	1216
Max-$d_{\min}$ based PA of [33]	$\mathcal{O}(N_t^2 M) + \mathcal{O}(n_{\mathrm{PA}}(M^2 + N_t M))$	128	896
Diagonal TPC method of [32]	$\mathcal{O}(L_1 L_2 N_t^2 M^2 N_r)$	18432	294912
MMD based TPC of [30]	$\mathcal{O}(N_t^2 M^2 N_r) + \mathcal{O}(N_t^4 M^4)$	66048	16785408
Proposed max-$d_{\min}$ based TPC	$\mathcal{O}(N_t^2 M) + \mathcal{O}(n_{\mathrm{TPC}}(M^2 + N_t M))$	224	1856
Proposed min-BER based TPC	$\mathcal{O}(n_{\mathrm{SCG}} N_t^2 M^2 N_r)$	15360	245760

proposed TPC scheme provides about 3.2 dB gain over the PRP scheme at BER $= 10^{-5}$ for (8×2)-element MIMO channels at a throughput of 5 bits/symbol. This benefit is due to the following two reasons: (1) the PRP schemes only adapt the phases of the SM symbols and hence the degrees of freedom utilized for TPC design are limited [35]; (2) similar to the methods of [31], [33], they are designed based on the max-$d_{\min}$ principle and hence may provide suboptimal BER.

In Fig. 9, the proposed min-BER based TPC schemes are compared to the MMD-aided SM schemes of [30]. Observe in Fig. 9 that the proposed TPC scheme provides an SNR gain of about 3 dB over the MMD-aided scheme at the BER of 10^{-5} for the (4×2) MIMO channels considered. Similar to the results in [30], the MMD-based TPC schemes provide minor performance improvements or even degrade the performance in low-SNR regimes. This is because the MMD criterion based TPC design may be ineffective in low SNR regimes, as discussed in [30].

Moreover, in Fig. 10, the proposed min-BER based TPC schemes are compared to the TAS-based SM schemes [16], [17], [44], [45] under different throughputs. In Fig. 10, the singular value decomposition (SVD)-based TAS algorithm of [16], [44], [45] is utilized due to its low-complexity and attractive performance. The number of TAs is $N_t = 4$ and 2 out of $N_t = 4$ TAs are selected by the TAS algorithm. Without loss of generality, we consider a PSK signal constellation diagram. As shown in Fig. 10, the TAS and the TPC schemes exhibit different BER advantages for different system setups. Specifically, the proposed TPC scheme outperforms the TAS scheme for (4×1) MIMO channels having a throughput of 6 bits/symbol, while they achieve a similar BER performance for (4×2) MIMO associated with 4 bits/symbol. This is not surprising, since the TAS and the TPC algorithms rely on different transmit parameters for the sake of achieving BER improvements. Note that TPC can be added on top of TAS to further improve performance. Hence they are complementary rather than competitive. It has been shown in [24], [30] that the joint design of TPC and TAS can further improve the system performance.

Fig. 11 shows the BER performance of various SM schemes in the presence of Gaussian-distributed CSI errors obeying $\mathcal{CN}\left(0, \sigma_{err}^2\right)$ [42], [43] for (2×2) MIMO channels and $L = 3$ bits/symbol. For the sake of simplification and clarity, we only consider the ASM and PA-aided SM schemes as benchmarks. In this paper, the variable σ_{err}^2, i.e. the value of the estimation error is adjusted according to the SNR. To be specific, $\sigma_{err}^2 = 1/r$ is adopted, where r is the average SNR at each receiver antenna. As expected, the BER performance of all SM schemes degrades upon imposing CSI estimation errors. However, Fig. 11 shows that the performance degradation of the proposed min-BER based TPC-aided SM is lower than that of the other schemes due to the fact that its BER upper bound was optimized bearing in mind the CSI error by using the SCG algorithm.

C. Complexity Comparison for Different TPC Designs

In Table II, the complexity orders of different TPC designs are compared. Specifically, in the randomly-selected diagonal TPC method of [31], [32], the quantization levels of amplitude and phase are L_1 and L_2, respectively. Its complexity order is provided in [30]. Moreover, the complexity orders of the max-$d_{\min}$ based PRP and of the max-$d_{\min}$ based PA algorithms can be found in [34] and [33], where their iteration numbers are n_{PA} and n_{PRP}, respectively. In Table II, we also provide the approximate quantified complexity for some specific configurations, where the QPSK- and 16PSK-modulated 4×2 SM schemes are considered. The number of iterations for the proposed SCG method is set to be $n_{\mathrm{SCG}} = 30$ due to it fast convergence.

As shown in Table II, the proposed max-$d_{\min}$ based TPC has a similar complexity order to that of the max-$d_{\min}$ based PRP of [34] and to that of the PA of [33], while exhibiting a lower complexity than the proposed min-BER design, since these max-$d_{\min}$ based designs only have to optimize a single distance $d_{\min}$. However, as shown in our simulation results of Figs 5–7 these max-$d_{\min}$ based designs suffer from a BER performance loss. The MMD-based TPC of [30] is a generalized max-$d_{\min}$ based TPC, which has to optimize $N_t M$ TPC weights for all legitimate SM symbols rather than relying on a diagonal TPC matrix having only N_t non-zero elements. Hence, the MMD-based TPC imposes a higher complexity than the proposed max-$d_{\min}$ and min-BER based TPC algorithms, as shown in Table II. For example, in configuration 2, the complexity of the proposed min-BER based design approximately achieves 68 times smaller than that of the MMD-based design.

Moreover, the diagonal TPC method of [32] requires an exhaustive search over a set of $L_1 L_2$ candidates, hence a higher complexity is imposed compared to the proposed min-BER based TPC for a high number of quantization levels. By taking into account both the BER versus complexity trends, we

conclude that the proposed min-BER based TPC provides an improved BER performance at a modest complexity cost. It should be noted that the extra complexity is imposed by the calculation of the gradient $\nabla Je(\mathbf{U})$ and by the convex problem solution algorithm, which may be further reduced by exploiting the spatial-domain sparsity of SM symbols and with the aid of reduced-complexity solution techniques. This issue will be investigated in our future studies.

VII. Conclusions

We have investigated two types of diagonal TPC design algorithms. For the max-$d_{\min}$ based TPC algorithm, closed-form solutions were derived for the case of two TAs and suboptimal solutions were achieved by using iterative method. For the min-BER based TPC algorithm, an iterative SCG algorithm was proposed for finding the specific TPC matrix solution. Finally, the proposed min-BER based TPC algorithm was further enhanced by taking into account the effects of imperfect CSI. It is shown from simulation results that the proposed max-$d_{\min}$ based TPC algorithm is optimal in terms of the minimum received distance, while the proposed min-BER based TPC algorithm is optimal in terms of the BER. Our further work will be focused on the integration of space-time coding, channel coding and TAS techniques into the proposed schemes.

Appendix

A. Gradient Derivation

In this appendix, we derive the theoretical gradient matrix of the cost function. Let us consider a general case associated with $\hat{\mathbf{H}} = \mathbf{H} + \Delta\mathbf{H}$. Then the cost function of Eq. (31) is reformulated as

$$Je_{\hat{\mathbf{H}}}(\mathbf{U}) = \sum_{\mathbf{x}_i \in \mathbb{X}} \sum_{\substack{\mathbf{x}_j \in \mathbb{X} \\ \mathbf{x}_i \neq \mathbf{x}_j}} D_H(\mathbf{x}_i \to \mathbf{x}_j) Q\left(\sqrt{\frac{\varepsilon_{\hat{\mathbf{H}}}}{2\sigma_e^2}}\right), \tag{50}$$

where we have

$$\sigma_e^2 = N_0 + \sigma_{err}^2 (\mathbf{U}\mathbf{x}_i)^H \mathbf{U}\mathbf{x}_i, \tag{51}$$

and

$$\varepsilon_{\hat{\mathbf{H}}} = \left\| \hat{\mathbf{H}}\mathbf{U}(\mathbf{x}_i - \mathbf{x}_j) \right\|^2. \tag{52}$$

Note that σ_e^2 and $\varepsilon_{\hat{\mathbf{H}}}$ are functions of the TPC matrix $\mathbf{U}$. Then the gradient of $Je_{\hat{\mathbf{H}}}(\mathbf{U})$ can be expressed as:

$$\begin{aligned} \nabla Je_{\hat{\mathbf{H}}}(\mathbf{U}) &= \frac{\partial Je_{\hat{\mathbf{H}}}(\mathbf{U})}{\partial \mathbf{U}^H} \\ &= \sum_{\mathbf{x}_i \in \mathbb{X}} \sum_{\substack{\mathbf{x}_j \in \mathbb{X} \\ \mathbf{x}_i \neq \mathbf{x}_j}} D_H(\mathbf{x}_i \to \mathbf{x}_j) \frac{\partial Q\left(\sqrt{\frac{\varepsilon_{\hat{\mathbf{H}}}}{2\sigma_e^2}}\right)}{\partial \mathbf{U}^H}. \end{aligned} \tag{53}$$

Here, $\partial Q\left(\sqrt{\frac{\varepsilon_{\hat{\mathbf{H}}}}{2\sigma_e^2}}\right) / \partial \mathbf{U}^H$ of Eq. (53) can be expressed as

$$\begin{aligned} \frac{\partial Q\left(\sqrt{\frac{\varepsilon_{\mathbf{H}}}{2\sigma_e^2}}\right)}{\partial \mathbf{U}^H} &= -\frac{1}{\sqrt{\pi}} e^{-\frac{\varepsilon_{\mathbf{H}}}{4\sigma_e^2}} \left(\frac{\varepsilon_{\hat{\mathbf{H}}}}{4\sigma_e^2}\right)^{-\frac{1}{2}} \frac{\partial\left(\sqrt{\frac{\varepsilon_{\hat{\mathbf{H}}}}{4\sigma_e^2}}\right)}{\partial \mathbf{U}^H} \\ &= -\frac{1}{\sqrt{\pi}} e^{-\frac{\varepsilon_{\hat{\mathbf{H}}}}{4\sigma_e^2}} \left(\frac{\varepsilon_{\hat{\mathbf{H}}}}{4\sigma_e^2}\right)^{-\frac{1}{2}} \left\{ \left(\frac{\partial(\varepsilon_{\hat{\mathbf{H}}})}{\partial \mathbf{U}^H} \frac{1}{4\sigma_e^2} \right) + \left(\frac{\partial\left(\frac{1}{4\sigma_e^2}\right)}{\partial \mathbf{U}^H} \varepsilon_{\hat{\mathbf{H}}} \right) \right\}, \end{aligned} \tag{54}$$

where we have the relationship of

$$\frac{\partial\left(\varepsilon_{\hat{\mathbf{H}}}\right)}{\partial \mathbf{U}^H} = \hat{\mathbf{H}}^H \hat{\mathbf{H}}\mathbf{U}\varphi(\mathbf{x}_i \to \mathbf{x}_j), \tag{55}$$

$$\frac{\partial\left(\frac{1}{4\sigma_e^2}\right)}{\partial \mathbf{U}^H} = -\frac{\sigma_{err}^2 \mathbf{U}\mathbf{x}_i \mathbf{x}_i^H}{4\sigma_e^4}. \tag{56}$$

Based on Eq. (56), we can arrive at the gradient matrix of Eq. (44). Moreover, assuming that the CSI is perfectly known, we have $\Delta\mathbf{H} = 0$, $\hat{\mathbf{H}} = \mathbf{H}$ and $\varepsilon_{\hat{\mathbf{H}}} = \varepsilon = \left\|\mathbf{H}\mathbf{U}(\mathbf{x}_i - \mathbf{x}_j)\right\|^2$. Then, the gradient matrix of Eq. (32) is readily obtained.

References

[1] R. Y. Mesleh, H. Haas, S. Sinanovic, C. W. Ahn, and S. Yun, "Spatial modulation," *IEEE Trans. Veh. Technol.*, vol. 57, no. 4, pp. 2228–2241, Jul. 2008.

[2] M. Di Renzo, H. Haas, A. Ghrayeb, S. Sugiura, and L. Hanzo, "Spatial modulation for generalized MIMO: Challenges, opportunities and implementation," *Proc. IEEE*, vol. 102, no. 1, pp. 56–103, Jan. 2014.

[3] S. Sugiura, S. Chen, and L. Hanzo, "A universal space-time architecture for multiple-antenna aided systems," *IEEE Commun. Surveys & Tuts.*, vol. 14, no. 2, pp. 401–420, May 2012.

[4] E. Başar, Ü. Aygölü, E. Panayırcı, and H. V. Poor, "Space-time block coded spatial modulation," *IEEE Trans. Commun.*, vol. 59, no. 3, pp. 823–832, Mar. 2011.

[5] M. Di Renzo, H. Haas, and P. M. Grant, "Spatial modulation for multiple-antenna wireless systems: A survey," *IEEE Commun. Mag.*, vol. 49, no. 12, pp. 182–191, Dec. 2011.

[6] M. Di Renzo and H. Haas, "Bit error probability of SM-MIMO over generalized fading channels," *IEEE Trans. Veh. Technol.*, vol. 61, no. 3, pp. 1124–1144, Mar. 2012.

[7] A. Stavridis, S. Sinanovic, M. Di Renzo, and H. Haas, "Energy evaluation of spatial modulation at a multi-antenna base station," in *Proc. IEEE Veh. Technol. Conf.*, Barcelona, Spain, Sep. 2013, pp. 1–5.

[8] N. Serafimovski *et al.*, "Practical implementation of spatial modulation," *IEEE Trans. Veh. Technol.*, vol. 62, no. 9, pp. 511–523, Nov. 2013.

[9] J. Jeganathan, A. Ghrayeb, and L. Szczecinski, "Spatial modulation: Optimal detection and performance analysis," *IEEE Commun. Lett.*, vol. 12, no. 8, pp. 545–547, Aug. 2008.

[10] S. Sugiura, C. Xu, S. X. Ng, and L. Hanzo, "Reduced complexity coherent versus non-coherent QAM-aided space time shift keying," *IEEE Trans. Commun.*, vol. 59, no. 11, pp. 3090–3101, Nov. 2011.

[11] N. R. Naidoo, H. Xu, and T. Quazi, "Spatial modulation: Optimal detector asymptotic performance and multiple-stage detection," *IET Commun.*, vol. 5, no. 10, pp. 1368–1376, Jul. 2011.

[12] A. Younis, S. Sinanovic, M. Di Renzo, R. Y. Mesleh, and H. Haas, "Generalised sphere decoding for spatial modulation," *IEEE Trans. Commun*, vol. 61, no. 7, pp. 2805–2815, Jul. 2013.

[13] R. Y. Chang, S.-J. Lin, and W.-H. Chung, "Energy efficient transmission over space shift keying modulated MIMO channels," *IEEE Trans. Commun.*, vol. 60, no. 10, pp. 2950–2959, Oct. 2012.

[14] S. Sanayei and A. Nosratinia, "Antenna selection in MIMO systems," *IEEE Commun. Mag.*, vol. 42, no. 10, pp. 68–73, Oct. 2004.

[15] D. J. Love, R. W. Heath Jr., U. K. N. Lau, D. Gesbert, B. D. Rao, and M. Andrews, "An overview of limited feedback in wireless communication systems," *IEEE J. Sel. Areas Commun.*, vol. 26, no. 8, pp. 1341–1365, Oct. 2008.

[16] K. Ntontin, M. Di Renzo, A. Perez-Neira, and C. Verikoukis, "A low-complexity method for antenna selection in spatial modulation systems," *IEEE Commun. Lett.*, vol. 17, no. 12, pp. 2312–2315, Aug. 2013.

[17] R. Rajashekar, K. V. S. Hari, and L. Hanzo, "Antenna selection in spatial modulation systems," *IEEE Commun. Lett.*, vol. 17, no. 3, pp. 521–524, Mar. 2013.

[18] N. Pillay and H. Xu, "Comments on 'Antenna selection in spatial modulation systems'," *IEEE Commun. Lett.*, vol. 17, no. 9, pp. 1681–1683, Sep. 2013.

[19] P. Yang, Y. Xiao, Y. Yi, and S. Li, "Adaptive spatial modulation for wireless MIMO transmission systems," *IEEE Commun. Lett.*, vol. 15, no. 6, pp. 602–604, Jun. 2011.

[20] P. Yang, Y. Xiao, L. Li, Q. Tang, Y. Yu, and S. Li, "Link adaptation for spatial modulation with limited feedback," *IEEE Trans. Veh. Technol.*, vol. 61, no. 8, pp. 3808–3813, Oct. 2012.

[21] P. Yang, Y. Xiao, Y. Yi, L. Li, Q. Tang, and S. Q. Li, "Simplified adaptive spatial modulation for limited-feedback MIMO," *IEEE Trans. Veh. Technol.*, vol. 62, no. 2, pp. 2656–2666, Jul. 2013.

[22] R. Rajashekar, K. V. S. Hari, and L. Hanzo, "Reduced-complexity ML detection and capacity-optimized training for spatial modulation," *IEEE Trans. Commun.*, vol. 62, no. 1, pp. 112–125, Jan. 2014.

[23] K. Ntontin, M. Di Renzo, A. I. Perez-Neira, and C. Verikoukis, "Adaptive generalized space shift keying," *EURASIP J. Wireless Commun. Netw.*, vol. 43, Feb. 2013.

[24] M. Maleki, H. R. Bahrami, S. Beygi, M. Kafashan, and N. H. Tran, "Space modulation with CSI: Constellation design and performance evaluation," *IEEE Trans. Veh. Technol.*, vol. 64, no. 4, pp. 1623–1634, May 2013.

[25] M. Maleki, H. R. Bahrami, M. Kafashan, and N. H. Tran, "On the performance of spatial modulation: Optimal constellation breakdown," *IEEE Trans. Commun.*, vol. 62, no. 1, pp. 144–157, Jan. 2014.

[26] C. B. Chae, A. Forenza, R. W. Heath Jr., M. R. Mckay, and I. B. Collings, "Adaptive MIMO transmission techniques for broadband wireless communication systems," *IEEE Commun. Mag.*, vol. 48, no. 5, pp. 112–118, May 2010.

[27] L. Collin, O. Berder, P. Rostaing, and G. Burel, "Optimal minimum distance-based precoder for MIMO spatial multiplexing systems," *IEEE Trans. Signal Process.*, vol. 52, no. 5, pp. 617–627, Mar. 2004.

[28] M. Di Renzo and H. Haas, "Improving the performance of space shift keying (SSK) modulation via opportunistic power allocation," *IEEE Commun. Lett.*, vol. 14, no. 6, pp. 500–502, Jun. 2010.

[29] C. Masouros, "Improving the diversity of spatial modulation in MISO channels by phase alignment," *IEEE Commun. Lett.*, vol. 18, no. 5, pp. 729–732, May 2014.

[30] M. Lee, W. Chung, and T. Lee, "Generalized precoder design formulation and iterative algorithm for spatial modulation in MIMO systems with CSIT," *IEEE Trans. Wireless Commun.*, vol. 63, no. 4, pp. 1230–1244, Apr. 2015.

[31] P. Yang, Y. Xiao, B. Zhang, S. Li, M. El-Hajjar, and L. Hanzo, "Star-QAM signaling constellations for spatial modulation," *IEEE Trans. Veh. Technol.*, vol. 63, no. 8, pp. 3741–3749, Oct. 2014.

[32] P. Yang, M. Di Renzo, Y. Xiao, S. Li, and L. Hanzo, "Design guidelines for spatial modulation," *IEEE Commun. Surveys Tuts.*, vol. 17, no. 1, pp. 6–26, Mar. 2015.

[33] P. Yang, Y. Xiao, S. Li, and L. Hanzo, "A low-complexity power allocation algorithm for multiple-input multiple-output spatial modulation systems," *IEEE Trans. Veh. Technol.*, 2015, to be published, doi: 10.1109/TVT.2015.2410252.

[34] C. Masouros and L. Hanzo, "Constellation-randomization achieves transmit diversity for single-RF spatial modulation," *IEEE Trans. Veh. Technol.*, 2015, to be published.

[35] P. Yang, Y. Xiao, S. Li, and L. Hanzo, "Phase rotation based transmit precoding improves the minimum Euclidean distance of single-RF-chain aided spatial modulation," *IET Commun.*, 2015, to be published.

[36] M. Bazaraa, H. Sherali, and C. Shetty, *Nonlinear Programming: Theory and Algorithms*. Hoboken, NJ, USA: Wiley, 1993.

[37] S. Chen, N. Ahmad, and L. Hanzo, "Adaptive minimum bit-error rate beamforming," *IEEE Trans. Wireless Commun.*, vol. 4, no. 2, pp. 341–348, Mar. 2005.

[38] J. Proakis, *Digital Communications*. New York, NY, USA: McGraw-Hill, 2001.

[39] A. Goldsmith, *Wireless Communications*. Cambridge, U.K.: Cambridge Univ. Press, 2005.

[40] D. Yang, C. Xu, L.-L. Yang, and L. Hanzo, "Transmit diversity-assisted space-shift keying for collocated and distributed/cooperative MIMO elements," *IEEE Trans. Veh. Technol.*, vol. 60, no. 6, pp. 2864–2869, Jul. 2011.

[41] T. Handte, A. Muller, and J. Speidel, "BER analysis and optimization of generalized spatial modulation in correlated fading channels," in *Proc. IEEE Veh. Technol. Conf.*, Anchorage, AK, USA, Sep. 2009, pp. 1–5.

[42] E. Başar, Ü. Aygölü, E. Panayırcı, and H. V. Poor, "Performance of spatial modulation in the presence of channel estimation errors," *IEEE Commun. Lett.*, vol. 16, no. 2, pp. 176–179, Feb. 2012.

[43] S. S. Ikki and R. Mesleh, "A general framework for performance analysis of space shift keying (SSK) modulation in the presence of Gaussian imperfect estimations," *IEEE Commun. Lett.*, vol. 16, no. 2, pp. 228–230, Feb. 2012.

[44] N. Wang, W. Liu, H. Men, M. Jin, and H. Xu. "Further complexity reduction using rotational symmetry for EDAS in spatial modulation," *IEEE Commun. Lett.*, vol. 18, no. 10, pp. 1835–1838, Oct. 2014.

[45] J. Zheng and J. Chen, "Further complexity reduction for antenna selection in spatial modulation systems," *IEEE Commun. Lett.*, vol. 19, no. 6, pp. 937–940, Jun. 2015, doi: 10.1109/LCOMM.2015.2417884.

Ping Yang received the B.E. and M.E. degrees from the University of Electronic Science and Technology of China (UESTC), Chengdu, China, in 2006 and 2009, respectively. From September 2012 to September 2013, he was a Visiting Student at the School of Electronics and Computer Science, University of Southampton, Southampton, U.K. From May 2014, he is a Research Fellow with EEE, NTU, Singapore. Also, he is an Assistant Professor with UESTC. His research interests include MIMO/OFDM, machine learning, life science, and communication signal processing.

Yong Liang Guan (S'94–AM'97–M'99) received the Ph.D. degree from the Imperial College of Science, Technology and Medicine, University of London, London, U.K., and the B.Eng. degree (with first class Hons.) from the National University of Singapore, Singapore, in 1997 and 1991, respectively. He is now an Associate Professor with the School of Electrical and Electronic Engineering, Nanyang Technological University, Singapore. His research interests include modulation, coding and signal processing for communication, information security, and storage systems.

Yue Xiao received the Ph.D. degree in communication and information systems from the University of Electronic Science and Technology of China, Chengdu, China, in 2007. He is now a Full Professor with the University of Electronic Science and Technology of China. He has authored more than 30 international journals and been involved in several projects in the Chinese Beyond 3G Communication R&D Program. His research interests include wireless and mobile communications.

Marco Di Renzo (S'05–AM'07–M'09–SM'14) was born in L'Aquila, Italy, in 1978. He received the Laurea (*cum laude*) and Ph.D. degrees in electrical and information engineering from the University of L'Aquila, L'Aquila, Italy, in April 2003 and January 2007, respectively. Since January 2010, he has been a Tenured Academic Researcher ("Chargé de Recherche Titulaire") with the French National Center for Scientific Research (CNRS), as well as a Faculty Member of the Laboratory of Signals and Systems (L2S), a joint Research Laboratory of the CNRS, the École Supérieure d'Électricité (SUPÉLEC) and the University of Paris–Sud XI, Paris, France. His research interests include wireless communications theory. Currently, he serves an Editor of the IEEE COMMUNICATIONS LETTERS and the IEEE TRANSACTIONS ON COMMUNICATIONS. He is the recipient of a special mention for the 2012 IEEE CAMAD Best Paper Award; the 2013 Network of Excellence NEWCOM# Best Paper Award; the 2013 IEEE–COMSOC Best Young Researcher Award for Europe, Middle East and Africa (EMEA Region); and the 2014 IEEE ICNC Single Best Paper Award Nomination (Wireless Communications Symposium).

Shaoqian Li (AM'04–SM'12) received the B.S.E. degree in communication technology from Northwest Institute of Telecommunication, Xidian University, Xidian, China, and the M.S.E. degree in communication system from the University of Electronic Science and Technology of China (UESTC), Chengdu, China, in 1982 and 1984, respectively. He is a Professor, Ph.D Supervisor, Director of the National Key Laboratory of Communication, UESTC, and Member of the National High Technology R&D Program (863 Program) Communications Group. His research interests include wireless communication theory, antiinterference technology for wireless communications, spread-spectrum and frequency-hopping technology, mobile, and personal communications.

Lajos Hanzo (M'91–SM'92–F'04) received the D.Sc. degree in electronics and the doctorate degree, in 1976 and 1983, respectively. During his 37-year career in telecommunications, he has held various research and academic posts in Hungary, Germany, and the U.K. Since 1986, he has been with the School of Electronics and Computer Science, University of Southampton, Southampton, U.K, where he holds the Chair in Telecommunications. He has successfully supervised 80+ Ph.D. students, coauthored 20 Wiley/IEEE Press books on mobile radio communications totaling in excess of 10 000 pages, authored 1400+ research entries at IEEE Xplore, acted both as TPC and General Chair of the IEEE conferences, presented keynote lectures and has been awarded a number of distinctions. Currently, he is directing a 100-strong academic research team, working on a range of research projects in the field of wireless multimedia communications sponsored by industry, the Engineering and Physical Sciences Research Council (EPSRC) U.K., the European Research Council's Advanced Fellow Grant and the Royal Society's Wolfson Research Merit Award. He is also a Governor of the IEEE VTS. From 2008 to 2012, he was the Editor-in-Chief of the IEEE Press and a Chaired Professor also at Tsinghua University, Beijing. His research is funded by the European Research Council's Senior Research Fellow Grant. He served as FREng, FIEEE, FIET, a Fellow of EURASIP. In 2009, he was the recipient of the honorary doctorate "Doctor Honoris Causa" by the Technical University of Budapest, Budapest, Hungary.

QUERIES

Q1: Please be advised that per instructions from the Communications Society this proof was formatted in Times Roman font and therefore some of the fonts will appear different from the fonts in your originally submitted manuscript. For instance, the math calligraphy font may appear different due to usage of the usepackage[mathcal]euscript. We are no longer permitted to use Computer Modern fonts.

Q2: Please provide page range for Ref. [23].

Q3: Please provide volume number, issue number, and page range for Refs. [33], [34], and [35].